ACTA INNOVATIONS

CENTRUM
BADAŃ I INNOWACJI
PRO - AKADEMIA
RESEARCH AND INNOVATION CENTRE

no. 31

April 2019

Ministerstwo Nauki
i Szkolnictwa Wyższego

Contents

Jarosław Goszczak, Bartosz Radzymiński, Grzegorz Mitukiewicz

Lodz University of Technology, Faculty of Mechanical Engineering, Department of Vehicles and Fundamentals of Machine Design

116 Żeromskego street, 90-924, Łódź, Poland, jaroslaw.goszczak@p.lodz.pl, bartosz.radzyminski@p.lodz.pl, grzegorz.mitukiewicz@p.lodz.pl

CONTINUOUSLY VARIABLE TRANSMISSION LEAKAGE TEST RESULTS

Abstract
After a short introduction characterizing the general outline of the issue, this paper describes the test results of oil leakage measurements through CVT actuator seals. The research was done using Jatco company's CVT 7 model, the popular gearbox for small passenger cars. Several curves of leakage values are given for both actuators, concerning different conditions such as rotational speed, oil temperature or pressure.
In the summary several conclusions are formulated, based on presented test results. The determined maximal value of leakage is about 1 l/min. It emerged that the influence of centrifugal force is negligible. What is more, the observed phenomena are shortly described and projected for more detailed investigation.

Key words
passenger car's driveline, power loss, efficiency improvement, continuously variable transmission, hydraulic control system, leakage values

Introduction
The stepless transmissions in passenger cars called CVT (Continuously Variable Transmission) are becoming increasingly more popular [1]. This is because of their advantages and progress made during the last two or three decades concerning their design and control [2, 3]. They make it possible to accelerate a car at a constant value of an engine's rotational speed, which may be set to maximal efficiency, torque, power or minimal fuel consumption [4].

Unique feature of CVT is that it permits the KERS [5] system (Kinetic Energy Recovery System) to work in a car. With this system, it is possible to recover a car's energy during braking and use it later for accelerating. The idea of a hybrid system with CVT and mechanical energy accumulator is described in [6]. They are different methods of braking energy recuperation (e.g. popular electric storage [7], [8] or pneumatic storage [9], [10]) but the kinetic energy accumulator (which is actually a rotating mass) is much more ecofriendly than a set of batteries and their long-term effect on CO_2 balance, considering the manufacturing process, utilization, recycling, etc.

Minimization of energy consumption is one of a vehicles' essential requirements from the viewpoint of sustainable transport. The features of this type transmission lead to savings in fuel consumption [2, 11]. Nevertheless, the method of ratio control system remains problematic because of its high energy-consuming character [12, 13]. The Department of Vehicles and Fundamentals of Machine Design of Lodz University of Technology (TUL), has devised a new solution which has a good chance of solving this difficulty [14].

Currently, the most common CVT solution employs a pair of conical sheaves which are moved axially for changing the ratio. The axial movement is executed by hydraulic actuators. The characteristic feature of the actuators is they are located inside the conical pulleys (sheaves) and rotate. The phenomenon of leakage through their sealings can be noticed and of course contributes to the deterioration of the system's efficiency [15], [16]. Study on CVT's sealings is presented in [17]. Research is incessantly carried out around the world both to improve the efficiency of pump of hydraulic control system [18] and to elaborate more efficient way of controlling CVT ratio [19].

Maintaining value of leakage is vital for CVT control's operation, particularly when considering the new, TUL solution. In this design, there are two pumps driven electrically. The first pump, described as P1 is responsible for ratio changing and placed between the pulleys' actuators [14]. It can rotate in both directions and transmit

oil between the actuators. A second pump called P2 is accountable for the belt's tension and compensating leakages in the circuit.

If the value of leakage is negligible, there is a possibility to change the positions of actuators (and ratio) by controlling the volume of oil which is pumped between them. In this case, the P2 pump's delivery will be very small as well as its power consumption. In case of serious leakages (about 6[l/min]) it can turn out that pump P1 (responsible for ratio changing) might have only one direction of rotation. This is because when this pump is being stopped, the decrease of pressure due to the leakages will be so fast that the ratio's change speed will be sufficient.

Significant values of leakage deteriorate the mentioned conception of ratio control because this phenomenon changes the volumes of oil inside the actuators. This issue must take in account the algorithm of the control system. Designers of transmissions have to make a compromise between the leak tightness and the resistance caused by the sealings.

Because of the above mentioned triggers, the need of research of currently available CVT sealing systems becomes evident. For typical solutions with one pump, results of this investigation will contribute to improve the control algorithm and a slight improvement of fuel consumption. The results are much more significant for TUL's solution where not only algorithm tuning will be possible. Outcomes of the research enable the design of a proper hydraulic circuit with a new solution, e.g. fit all size pumps. It is crucial to equally optimize software as well as system hardware because it results in the best reduction of energy consumption. According to Bradley [20, 21], the results of vehicle testing show that a similar control system reduces the required control power by more than 83% and TUL's solution, after mentioned optimization, could be even more efficient.

Test stand description
The object chosen to be tested was the popular Jatco model CVT 7 [22] gearbox. It has a built-in pump which had to be disconnected from the actuators in order to measure the leakage values by using (external) flow-meters. After the analysis of the design, special plugs were made and put inside the gearbox's channels to block the oil flow from the internal pump.

The external oil flow was delivered to both actuators by technological holes which were unplugged, as presented in Fig. 1 on the gearbox's side view.

Fig. 1. Picture of the tested gearbox
Source: Author's

The next task was to devise a way to supply the actuators with the proper pressure values. First, it was pointed out that to determine the dependence of leakage from pressure value, both actuators can operate at equal pressures – therefore there is no need to control them independently.

The first idea was the use of a simple hydraulic pump and a PWM-controlled solenoid valve [23] to change the pressure. Unfortunately, severe disturbances in oil flow measurement were observed. It could be caused by the solenoid valve, which connects 200÷300 times per second the oil supply with the output line. When using a precise flow-meter with high resolution (circa 2200 samples per liter) the oscillations from the solenoid valve could have been transferred to its output.

After this misfortune, another solution to supply the actuators was selected and is presented in the scheme of the test bench in Fig. 2. The CVT transmission (No. 6) is driven by an electric motor (No. 5) characterized by its maximum rotational speed of 3000[rpm]. The needed pressure value is supplied from the hydraulic group (No. 3) (H-G). Hydraulic group contains an oil filter with 3 micron solid particulate filtration, a flow-meter and regulation of temperature of output oil. An oil filter in original gearbox's hydraulic circuit is employed as well to keep oil uncontaminated.

The oil is delivered to both pulley's actuators. The oil which enters each chamber is measured by flow-meters No. 1 and No. 2. One of them, has a small range of 1,6[l/min] with measurement tolerance 1[%] and values from this flow-meter were taken for all further analyzes because the expected maximal value of leakage was about 1[l/min]. After tests of the P1 pulley, the position of this flow-meter was changed from "1" to "2" in order to precisely measure the value of leakages on the second actuator. Oil which passed through the sealings dripped to the oil sump and when the amount exceeded a specified level was directed to the hydraulic group - Fig. 2.

Two oil temperature sensors were applied. The T_1 sensor (Fig. 2) measures the CVT's input oil temperature which delivers the H-G. This temperature is controlled by the cooling system of H-G and was always kept constant during particular test series. Because this is supply line for CVT, this value of temperature was selected as a reference during research. The T_2 sensor was employed to check the temperature of oil which quit the CVT gearbox. To achieve the best uniformity of temperature in the gearbox and most accurate results, both temperatures had to be similar at the beginning of the test. The fan (No. 4) was used to intensify the dissipation of heat from the gearbox during tests at high rotational speed. Temperature phenomena will be described further.
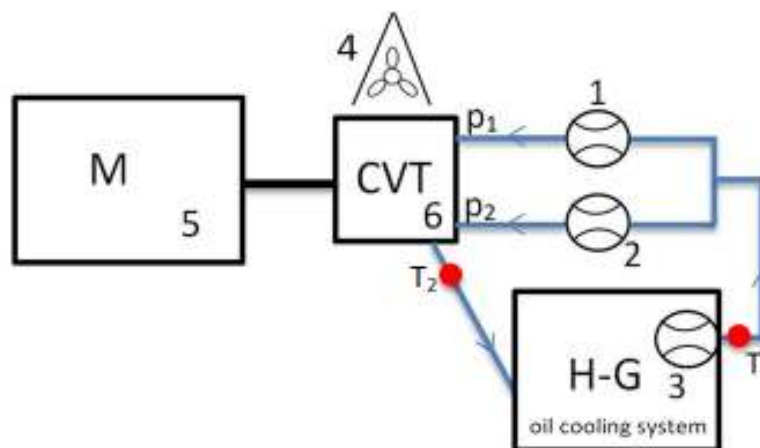

Fig. 2. Scheme of the test bench
Source: Author's

The test stand correspond to real conditions in a car because electric motor (No. 5) substitutes the engine. Additional fan (No. 4) simulates the air flow which occurs during driving and cools the gearbox. H-G (No. 3) replaces the original oil sump with integrated radiator.

Test results

Tests were conducted at three constant values of oil temperature: 30[°C], 60[°C] and 80[°C]. Temperature 80[°C] is the typical operational temperature of oil in vehicle's gearbox and that is why selected test results are presented only for this temperature. Research of lower values was conducted in order to check the influence of temperature and phenomena which occurs when gearbox gets warm.

Leakages were tested at the following pressures: 0,5[MPa], 1,5[MPa], 2,5[MPa], 3,5[MPa] and 4,5[MPa] in order to verify the suspected pressure influence.

Each pulley's leakages were tested at rotational speed of the pulley set to: 0[rpm], 500[rpm], 1000[rpm] and 3000[rpm].

In most cases, the leakages were checked twice in order to examine the reliability and repeatability of measurements. If both series gave similar results, averaged values are presented. After finishing all the measurements for the P1 pulley, a precise flow-meter was installed on the P2 pulley and all points were repeated - in this test series, the rotational speed was set on the P2 pulley.

It should be underlined, that the P1 pulley has a doubled actuator chamber (with a total area of 175[cm^2]) while the P2 actuator chamber is single and has 82[cm^2] area, as shown in Fig. 3. P_2 pressure is highest in the Jatco CVT 7 and it was necessary to double the P1 actuator to achieve greater axial force to the P1 actuator to enable the ratio change.
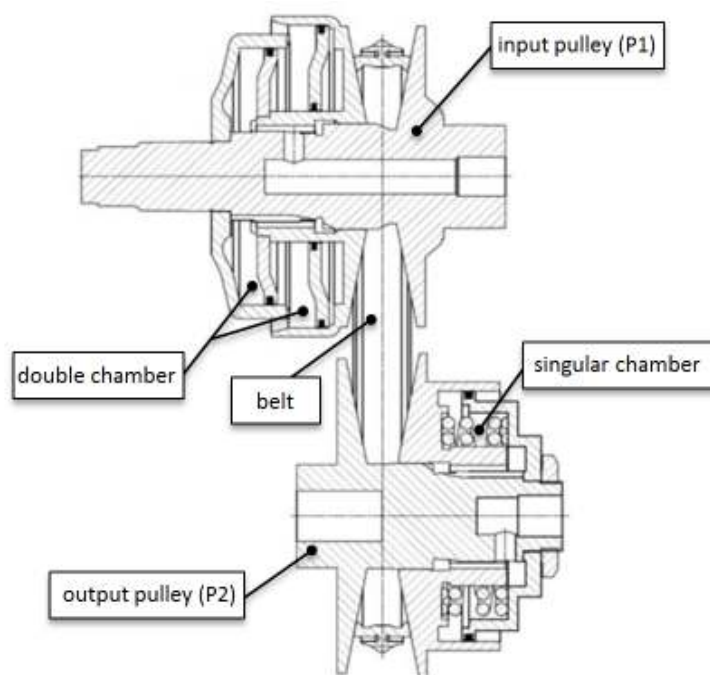
Fig. 3. Cross section of CVT
Source: Author's

First, test results for 0[rpm] are presented. These are the simplest among all scheduled tests because there is no heating disturbance phenomenon (caused by friction when turning the gearbox's shafts) and no oil flow perturbation caused by (small) axial oscillations of the pistons which occur when the transmission is turning - this phenomenon is described further.

Fig. 4 shows the test results for the P1 actuator and different values of oil temperature. The maximal value of leakage (0,65[l/min]) can be observed for the highest oil temperature (80[°C]) and pressure 3,5 [MPa]. The shape of the achieved curves is thought provoking. The higher the pressure, the lower the increase of leakage can be observed. This was particularly for the highest temperature range when leakages dropped a little at top pressure.

There could be two explanations of this phenomenon. First concerns the oil temperature - before the test the gearbox was warmed to the required temperature by turning the gearbox shafts. When the test started (for 0[rpm]) the oil inside CVT started to cool which caused a drop of leakage, regardless of the pressure increase. Nevertheless, the impact of this process should be slight because the whole test lasts only a few minutes. The second explanation relates to the sealings and their features. It is possible that due to higher pressure the sealing tightens which contributes to lower leakages. Most likely the answer is a combination of both mentioned theories.
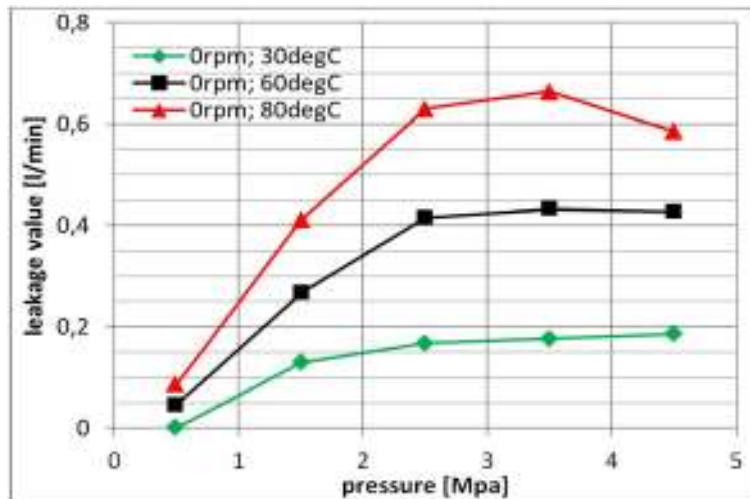
Fig. 4. Test results for P1 actuator, 0[rpm] and different values of oil temperature
Source: Author's

Fig. 5 shows test results for the P2 actuator, 0[rpm] and various values of oil temperature. The maximal value for 80[$°$C] is close to 1,2[l/min] which is noticeably more than for the P1 actuator. When compared to P1 results it can be observed different shape and there is no leakage fall when pressure is increased. Different properties can be explained by the distinct design of actuators presented in Fig. 3.
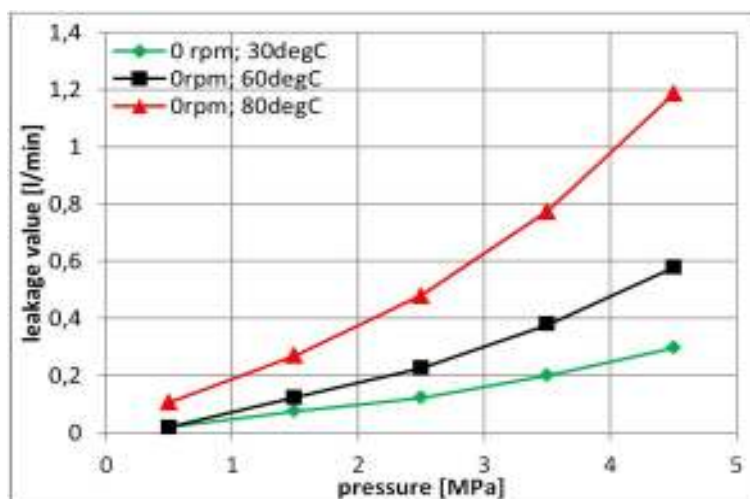
Fig. 5. Test results for P2 actuator, 0[rpm] and different values of oil temperature
Source: Author's

In Fig. 6 the leakage values are presented for the P1 actuator at 80[$°$C], at various rotational speeds. Based on the results from the mentioned graph, a general tendency can be observed for leakages for all values of rotational speed increase together with increased pressure. The next remark concerns the fact that the curves of higher values of rotational speed are steeper. A probable explanation is connected with temperature phenomena. Analogously, like the small drop of leakages from Fig. 4 was explained by the lowering of oil temperature at the contact area of belt and pulleys, this time higher rotational speed causes more severe warming of oil inside the gearbox (mainly because of friction). As shown in Fig. 6, leakages increase more rapidly during the test. The highest value of leakage slightly exceeds 0,8[l/min]. It was possible to control the T_1

temperature (the input one) but not the T_2 temperature (the output one) because it was not feasible to apply cooling inside rotating CVT (and its actuators). The fan (Fig. 2) was used to reduce this phenomenon.
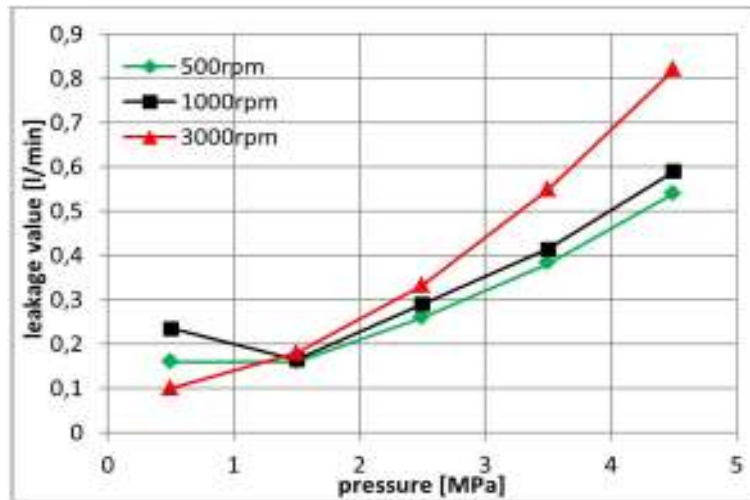
Fig. 6. Test results for P1 actuator, temperature of oil 80[°C] and different rotational speed values
Source: Author's

Fig. 7 depicts test results for P2 actuator at temperature 80[°C] and various values of rotational speed. Results are similar to those from Fig. 6. All previously mentioned relationships are also visible and true. The most significant difference concerns the value of leakages – such as for 0[rpm], leakages for P2 actuators are greater and for results from Fig. 7 achieve nearly 1,2[l/min] for 3000[rpm] and 4,5[MPa].
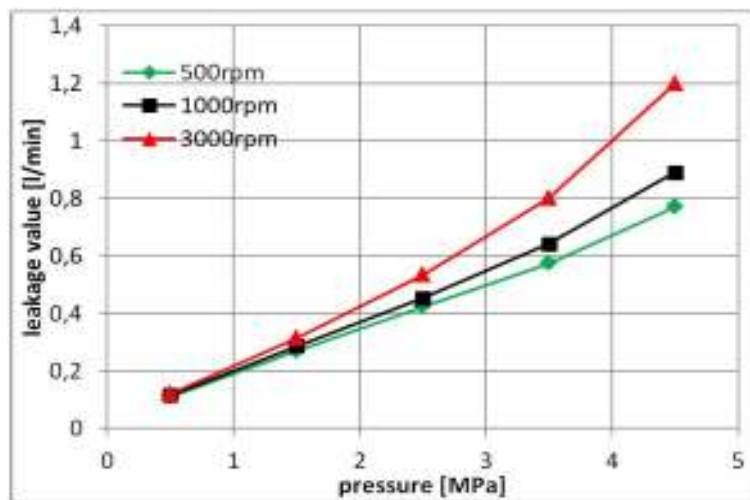
Fig. 7. Test results for P2 actuator, temperature of oil 80[°C] and different rotational speed values
Source: Author's

Noticed phenomena
Several phenomena were noticed while testing the CVT leakages:

- Initially there was an idea to use solenoid-valves to produce p_1/p_2 pressures. High oscillations of oil-flow value were noticed. Solenoid-valves were suspected to be the reason, so a new hydraulic circuit was made (presented earlier within the test bench scheme). Oscillations of oil-flow decreased significantly. What is more, it happened that solenoid valves became excited. This dangerous phenomenon is described in [23].
- Some oscillations still occur and are visible particularly when the pressure is low. The reason could be the axial movement of the pulley (it causes oscillations of oil inside the chamber), and as a result, in oil-flow. Those axial movements are more probable when axial force (pressure) is small.
- Initially, one flow-meter with a small range (1,6[l/min]) was scheduled to be applied. When strong disturbances of oil flow were noticed at the beginning of the test (with solenoid valves) a set of three

flow meters was employed in order to have an additional control of flows and make measurements more reliable. It was interesting how big was the difference between the sum of the value from flow-meter's "1" and "2" in comparison with the value indicated on flow-meter "3"- see Fig. 2. It was noticed that for most measurement points this difference is smaller than 0,05[l/min]. This proved the reliability of the flow-meter's precision.

▪ For some conditions a very high value of leakages was observed. This happens when the gearbox was not in use for a long time and the pressure inside the chambers decreased to zero. After such a long break, when a small amount of oil pressure was applied, the value of leakage could achieve even a few liter per minute. The reason may be in the type of sealing, which need significant pressure value to be tightened. The last remark is in accordance with the assumption that the shape of curves from Fig. 4 is explained by tightening the seals by increasing pressure.

▪ Curves presented in this paper are the averaged data from 2÷3 repeated series. Measurement repeatability is generally better for the secondary pulley which could be explained by a simpler structure when compared to the primary one (doubled piston, two sealing sets).

Summary and conclusions

Table below contains a few, the most representative values of elaborated leakages: for significant rotational speed, oil temperature 80[degC] and two values of pressure. Low pressure (0,15[MPa] is typical for low load of engine which occurs during driving with steady speed, high pressure (0,45[MPa]) represents full load of engine, during e.g. acceleration.

Table 1. Selected measurements of leakages

conditions / p [MPa]	80[degC], 3000[rpm]	
	P1 actuator [l/min]	P2 actuator [l/min]
0,15[MPa]	0,15	0,3
0,45[MPa]	0,82	1,2

Source: Author's

Presented research recognized the leakage phenomena in CVT. This outcome makes it possible to improve efficiency of CVT's hydraulic control system. The results are peculiarly relevant for mentioned TUL's solution which has a good chance to decline power losses of the transmission and vehicle's fuel consumption as well. Determined values enable to appropriate design of the proposed solution and optimization of its control algorithm.

According to the test results, there are two main factors which strongly influence leakages: pressure and temperature. It was expected that the higher the pressure, the higher the leakages. Generally, this rule is proved by test results. However, there are a few points of these principles which seem untrue - Fig. 4. This is most likely caused by the second main factor: temperature. Tests from Fig. 4 were performed at high temperature when the motion was stopped. After a few measurement points, the gearbox began to become cold, which probably disturbed the measurement. The opposite situation is visible at high rotational speed. The curve for 3000[rpm] has the highest slope because the transmission becomes hot very fast. This is also probably the reason the values of leakages are more or less the same at the beginning point of the test (0,5[MPa]) for all rotational speeds. The curve at 500[rpm] is sloped weakly, and stronger at 1000[rpm] and 3000[rpm] mostly. If the influence of centrifugal force would be significant, the layout of curves should look different: the difference between all curves (for different rpm) should be noticeable from the beginning and remain more or less the same, to the end of the curves (4,5[MPa]). That's why the influence of centrifugal force could be omitted here. Summarizing, the layout of temperatures inside the gearbox is hard to be determined precisely. It changes depending on current rotational speed. Changes of temperature inside the pulleys chamber result in changes of leakages.

Research was not directed to investigate the influence of wear on leakages but it is expected that wearing of sealings will result in higher values of leakages.

References

[1] BOSCH, Expansion by exceeding expectations, FISITA World Automotive Congress, Maastricht, 2014.

[2] F. Sluis, E. Noll, H. Leeuw, The success of the bushbelt CVT- status and development, JSAE Annual Conference, Yokohama, 2012.

[3] F. Sluis, S. Yildiz, A. Brandsma, P. Veltmans, M. Kunze, The CVT Pushbelt reinvented for Future Compact and Efficient Powertrains, JSAE Conference, Yokohama, 2017.

[4] J. Jantos, Zintegrowane sterowanie samochodowym, spalinowym układem napędowym o przełożeniu zmiennym w sposób ciągły, Opole University of Technology, Opole, 2003.

[5] C. Śliwiński, Kinetic energy recovery systems in motor vehicles, IOP Conf. Series: Materials Science and Engineering, 148 (2016) 012056.

[6] B. Radzymiński, Koncepcja hybrydowego układu napędowego samochodu osobowego wyposażonego w mechaniczny akumulator energii, Wpływ Młodych Naukowców na Osiągnięcia Polskiej Nauki, Poznań, 2015.

[7] Z. Dimitrova, F. Maréchal, Techno–economic design of hybrid electric vehicles and possibilities of the multi-objective optimization structure, Applied Energy 161 (2016) 746-759.

[8] Z. Dimitrova, F. Maréchal, Environomic design of vehicle energy systems for optimal mobility service, Energy 76 (2014) 1019-1028.

[9] Z. Dimitrova, P. Lourdais, F. Maréchal, Performance and economic optimization of an organic Rankine cycle for a gasoline hybrid pneumatic powertrain, Energy 86 (2015) 574-588.

[10] Z. Dimitrova, F. Maréchal, Gasoline hybrid pneumatic engine for efficient vehicle powertrain hybridization, Applied Energy, 151 (2015) 168-177.

[11] F. Sluis, T. Dongen, G.-J. Spijk, A. Velde, A. Heeswijk, Fuel Consumption Potential of the Pushbelt CVT, FISITA World Automotive Congress, Yokohama, 2006.

[12] T.W.G.L. Klaasen, The empact CVT: dynamics and control of an electromechanically actuated CVT, Technische Universiteit Eindhoven, Eindhoven, 2007.

[13] B. Bonsen, Efficiency optimization of the push-belt CVT by variator slip control, Technische Universiteit Eindhoven, Eindhoven, 2006.

[14] J. Goszczak, B. Radzymiński, Propozycja układu hydraulicznego zasilającego przekładnię CVT, Przegląd Mechaniczny, 7-8 (2017) 23-38.

[15] F. Sluis, A New Pump for CVT Applications, SAE Technical Paper 2003-01-3207 (2003)

[16] F. Sluis, G. Spijk, A. Velde, Efficiency Optimization of the Pushbelt CVT, SAE Technical Paper 2007-01-1457 (2007)

[17] P.F. van Oorschot, J. Pustjens, Polymer rectangular seal design for the inline CVT, Technische Universiteit Eindhoven, Eindhoven, 2009.

[18] D. Qu, W. Luo, Y. Liu, B. Fu, Y. Zhou, F. Zhang, Simulation and experimental study on the pump efficiency improvement of continuously variable transmission, Mechanism and Machine Theory 131 (2019) 137-151.

[19] Y. Xia, D. Sun, Characteristic analysis on a new hydro-mechanical continuously variable transmission system, Mechanism and Machine Theory 126 (2018) 457-467.

[20] T. Bradley, B. Huff, A. Frank, Energy Consumption Test Methods and Results for Servo-Pump Continuously Variable Transmission Control System, SAE Technical Paper 2005-01-3782 (2005).

[21] T. Bradley, A. Frank, Servo-Pump Hydraulic Control System Performance and Evaluation for CVT Pressure and Ratio Control, VDI CVT Congress, Munich, 2002.

[22] Y. Nagawa, Introducing Technologies of Jatco CVT7 Featurig an Auxilary Transmission, Jatco Technical Review 11 (2011) 23-29.

[23] J. Goszczak , B. Radzymiński, A. Werner, Z. Pawelski, PWM-controlled hydraulic solenoid valves for motor vehicles, The Archives of Automotive Engineering 75 (2017) 23-37.

Artur Stelęgowski

Lodz University of Technology, Faculty of Architecture, Civil and Environmental Engineering,
al. Politechniki 6, 90-924 Lodz, Poland, artur.stelegowski@edu.p.lodz.pl

CORRELATIONS BETWEEN AIR POLLUTANT CONCENTRATIONS IN SELECTED URBAN AND RURAL AREAS IN POLAND

Abstract

Correlations between concentrations of selected air pollutants were analyzed in different areas in central Poland from 2012-2016. Three neighboring voivodeships (Lower Silesian, Lodz, and Masovian), were selected for which specific measurement locations were designated in urban and rural areas. The characteristics of the location of monitoring stations allowed to distinguish the following types of measurement stations: "urban-transport", "urban-background", "suburban-background", "town-background", and "rural-background". Therefore, using the Pearson's linear correlation coefficient, it was possible to analyze the interrelations between the occurrence of air pollution in various types of areas. It was found that the coefficient changed along with the type of area. Moreover, it turned out that the coefficient decreased in each voivodeship along with a decrease in the population density of the analyzed areas. In addition, concentrations of various air pollutants in given areas were compared. Also, it was observed that the strongest correlations occur between the results of calculations from measurement stations located in the same province.

Key words
air pollution; statistical analysis; nitrogen dioxide; particulate matter

Introduction

Occurrence of air pollution depends on the characteristics of the tested area. Levels of contaminants differ in urbanized and industrialized areas, and in less urbanized, or agricultural areas [1−3]. In addition, air quality varies depending on the characteristics of the region [2−4]. Generally, the level of air pollution is lower at rural sites, and higher in large cities [1, 5−6]. This is because air quality is strongly affected by emission sources of air pollution [7−9]. Therefore, it is assumed that the presence of specific pollutants in the air may indicate the activity of selected types of emission sources [10−12]. For example, an increase in the concentration of nitrogen oxides and carbon monoxide in the air near a road can be associated with an increase in traffic intensity. While presence of PM_{10}, sulfur oxides and carbon monoxide in a residential area is often associated with the impact of individual home's fuel combustion. Also, meteorological conditions can affect the level of air quality. Nevertheless, the maximum and minimum daily concentrations at various areas could occur at a similar time (Fig. 1). For example, in Poland peak ground level ozone occurred usually at 15:00, nitrogen dioxide at 7:00-9:00 and 19:00-21:00, sulphur dioxide at 10:00-12:00, carbon monoxide at 6:00-8:00 and 20:00-22:00, PM_{10} at 7:00-9:00 and 20:00-22:00 [6].
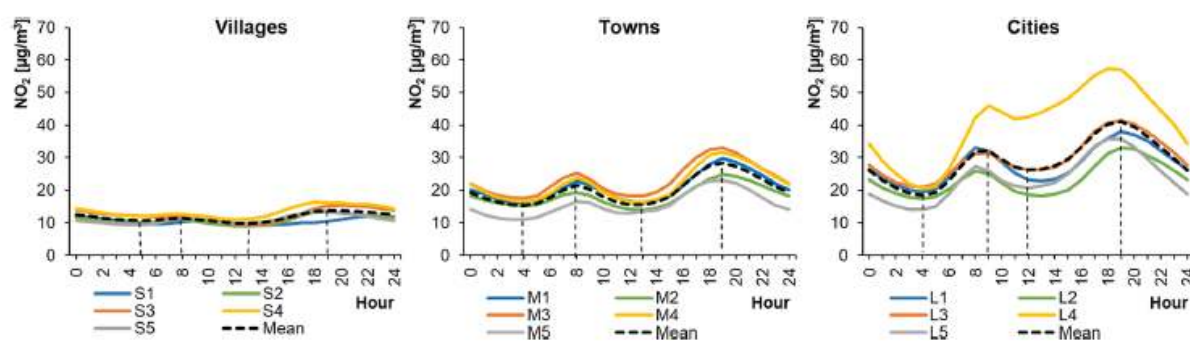

Fig. 1. Average hourly NO_2 concentrations in winter periods in selected villages, towns and cities in Poland in 2012-2016.
Source: [6]

Although the air quality, at a specific site, depend on many factors, some common characteristics of changes could be determined using statistical methods. Therefore, in literature, the correlation coefficient is often used as a statistical tool to analyze the nature of changes in air pollution [13−16]. Pearson's linear correlation coefficient is widely used, inter alia to analyze the dependencies between the presence of pollutants in the air, and various types of ailments and diseases occurring in the groups of people exposed to these pollutants [4,17]. By definition, this coefficient is used to determine the similarity of objects /variables and their linear interdependence [18−19]. When x and y are variables, the Pearson's linear correlation coefficient R can be calculated as follows (1):

$$R = \frac{\sum_{i=1}^{n}[(x_i - \bar{x}) \times (y_i - \bar{y})]}{\sqrt{(x_i - \bar{x})^2} \times \sqrt{(x_i - \bar{x})^2}} \quad (1)$$

Interpretation of the calculated coefficient depends on its value. The "stronger" are the interdependencies between variables, the higher is the coefficient. Therefore, specific ranges of the coefficient are determined, depending on the field of knowledge, to describe the "strength" of the interdependencies [19−20]. In this analysis, the interpretation of the R coefficient was adopted according to Table 1.

Table 1. Interpretation of R linear correlation coefficient.

R (-)	Interpretation
0.90–1.00	Very high correlation
0.70–0.89	High correlation
0.50–0.69	Moderate correlation
0.30–0.49	Low correlation
0.00–0.29	Little, if any, correlation

Source: [19]

The analysis was aimed at demonstrating the interdependence (or lack thereof) between the occurrence of air pollution in various types of areas, especially urban and rural areas within the same region. However, in the literature, usually only the correlations between various pollutants and their dependence on meteorological conditions are calculated [16, 21]. Unfortunately, there is a lack of comparative calculations, regarding relationships between different urban and rural areas. Therefore, in the analysis, Pearson's linear correlation coefficients were determined between the concentrations of the selected pollutant in the air in areas with different characteristics, i.e. in urban and rural areas in three voivodships in central Poland. The pollutants analyzed were: nitrogen dioxide (NO_2), sulfur dioxide (SO_2), ground-level ozone (O_3), and PM_{10}. Additionally, in selected locations, correlation coefficients between concentrations of different air pollutants were compared.

Method description
Interdependencies between hourly air pollutants concentrations in various areas were analyzed by determining the Pearson's linear correlation coefficient R. Occurrence of pollutants was compared in three voivodeships (Lower Silesian, Lodz, and Mazovian) in central Poland, at selected areas: "urban traffic" - UT, "city background" - CB, "suburb background" - SB, "town background" – TB, and "rural background" – RB (Table 2). The occurrence of NO_2, SO_2, O_3, CO, and PM_{10}, was analyzed. The parts of data used in the analysis were obtained from 15 selected automatic air quality monitoring stations in Poland, during 2012−2016. Therefore, around 43,000 measurements of a given air pollutant were obtained from a single monitoring station. However, as technical and maintenance breaks occurred in operation of measuring stations, only the parts of data with at least 75% completeness for a particular year and station, were used in the analysis.

Table 2. Location of measuring stations in selected voivodeships in Poland (where: UT – urban traffic, CB – city background, SB – suburb background, TB – town background, RB – rural background)

Province	Name of settlement	Type of settlement	Type of monitoring station
Lower Silesia	Wrocław	City	UT, CB, SB
	Kłodzko	Town	TB
	Osieczów	Village	RB
Lodz	Lodz	City	UT, CB, SB
	Piotrków Tryb.	Town	TB
	Gajew	Village	RB
Mazovia	Warsaw	City	UT, CB, SB
	Piastów	Town	TB
	Belsk Duży	Village	RB

Source: Author's

Results

Changes in concentrations of air pollutants in a given area often correlated with changes in concentrations in other areas. For example, such a relationship is presented in Fig. 2, where the increase in NO_2 concentration in the city's downtown (CB area) is associated with an increase in this pollutant concentration outside the city center (SB area).
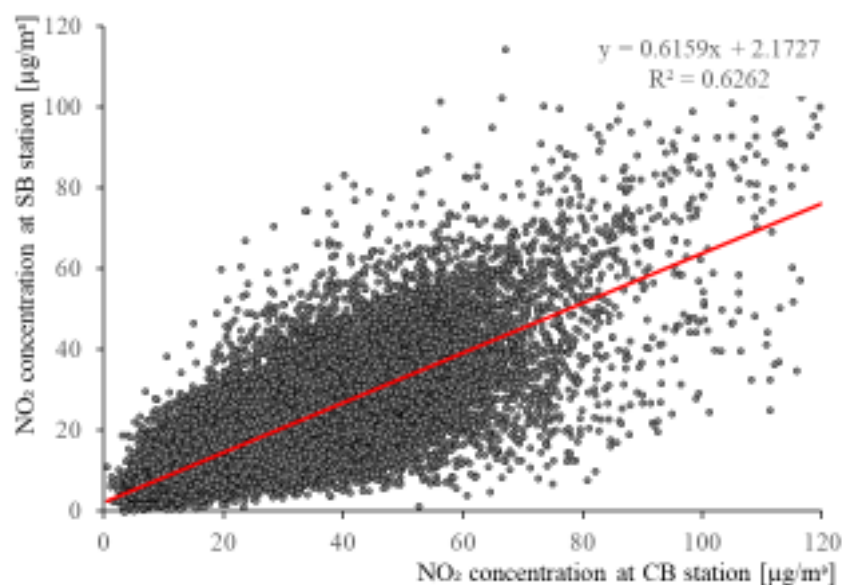
Fig. 2. Correlation between NO_2 concentrations at SB and CB stations in the city of Lodz.
Source: Author's

For NO_2, the correlation of results was medium–high between UT and CB (*R* ranged from 0.61 to 0.82), as well as between CB and SB (*R* from 0.61 to 0.82) (Table 3). The town background and rural background were most interdependent with the suburb background areas. However, the interdependencies between NO_2 concentrations were most visible in the areas within the same voivodeship. The highest correlation of coefficients were in the Lodz Voivodeship (*R* of 0.53-0.82) which varied less than in the other two voivodeships. This could indicate the similarity of conditions, such as traffic, urban planning, concentration of emission sources, affecting the change in pollution concentration. Generally, the correlation coefficient decreased as the area changed to less urbanized areas within the same voivodeship. This indicates an increase in the changes in the conditions of air quality along with "moving away" from city centers (UT, CB). The changes in hourly concentrations differed when approaching areas characterized by a smaller number and density of inhabitants

(SB, TB, RB). This corresponded to the observation that usually air pollution level is much lower in rural areas comparing to urban areas [1, 5−6]. Unfortunately, in the literature, there is a lack of comparative calculations, regarding relationships between different urban and rural areas.

Table 3. Correlation coefficient between NO_2 concentrations in different areas (correlation was significant at the 0.01 level, 2-tailed). Light grey shadowing was used to underline the correlation coefficints within the same region.

-		Lower Silesia					Lodz					Masovia				
		UT	CB	SB	TB	RB	UT	CB	SB	TB	RB	UT	CB	SB	TB	RB
Lower Silesia	UT	-														
	CB	0.63	-													
	SB	0.40	0.73	-												
	TB	0.39	0.49	0.49*	-											
	RB	0.12	0.43	0.43	0.39	-										
Lodz	UT	0.55	0.54	0.39	0.37	0.19	-									
	CB	0.50	0.61	0.46	0.47	0.33	0.82	-								
	SB	0.42	0.61	0.55	0.46	0.35	0.68	0.79	-							
	TB	0.23	0.48	0.45	0.39	0.45	0.53	0.61	0.59	-						
	RB	0.48	0.60	0.52	0.51	0.29	0.69	0.76	0.72	0.60	-					
Masovia	UT	0.56*	0.34	0.22	0.15	-0.02	0.47	0.38	0.39	0.15	0.39	-				
	CB	0.58	0.38	0.20	0.27	0.07	0.58	0.55	0.39	0.28	0.45	0.61	-			
	SB	0.42	0.52	0.47	0.43	0.24	0.59	0.67	0.65	0.54	0.69	0.53	0.55	-		
	TB	0.38	0.50	0.44	0.41	0.24	0.62	0.68	0.61	0.58	0.68	0.42	0.54	0.80	-	
	RB	0.22	0.38	0.33	0.36	0.43	0.37	0.49	0.44	0.55	0.48	0.08	0.27	0.44	0.49	-

*Correlation was insignificant at the 0.01 level

Source: Author's

The nature of SO_2, O_3, CO, and PM_{10} changes in Lodz voivodeship was similar to those of NO_2. Namely, the linear correlation coefficient within the same voivodeship decreased along with the change to a less urbanized type of area (Tables 4−7). Interdependencies in various areas were high (and very high) in the case of ozone, and of carbon monoxide, but medium (and high) for particulate matters, and for SO_2. This indicates a large similarity in the nature of changes in concentrations of these pollutants in the analyzed areas. Therefore, an increase of city background pollution occurred at a similar time as the increase in concentrations in other areas. The similarity was the greater, the more similar were the areas. Also, the analyzed correlations of the areas type (R = 0.52−0.95) were higher than correlations between air pollutants and weather conditions (R = ±0.01−0.89) in locations of other studies [21-22]. The calculated correlations were significant for the level 0.01, unless otherwise indicated in the tables. Unfortunately, some stations in the Lodz voivodship did not perform measurements of SO_2, O_3 and CO. Therefore, the corresponding cells were marked as "not applicable" (n/a).

Table 4. Correlation coefficient between SO_2 concentrations in Lodz Province.

SO_2	UT	CB	SB	TB	RB
UT	-				
CB	n/a	-			
SB	n/a	0.67	-		
TB	n/a	0.69	0.52	-	
RB	n/a	0.62	0.56	0.58	-

Table 5. Correlation coefficient between O_3 concentrations in Lodz Province.

O_3	UT	CB	SB	TB	RB
UT	-				
CB	n/a	-			
SB	n/a	0.95	-		
TB	n/a	0.90	0.87	-	
RB	n/a	0.86	0.84	0.88	-

Source: Author's

Table 6. Correlation coefficient between
CO concentrations in Lodz Province.

CO	UT	CB	SB	TB	RB
UT	-				
CB	0.90	-			
SB	0.80	0.83	-		
TB	0.78	0.78	0.70	-	
RB	n/a	n/a	n/a	n/a	-

Table 7. Correlation coefficient between
PM_{10} concentrations in Lodz Province.

PM_{10}	UT	CB	SB	TB	RB
UT	-				
CB	0.87	-			
SB	0.75	0.80	-		
TB	0.71	0.75	0.70	-	
RB	0.64	0.64	0.70	0.59	-

Source: Author's

The nature of air pollution changes in the Masovia voivodeship was similar to that of the Lodz voivodship. Linear correlation coefficients decreased along with the change to a less urbanized type of area, within the same voivodeship (Tables 8−11). Interdependencies between air pollutants concentrations were high (and very high) in the case of ozone, medium (and high) for PM_{10}, low (and medium) for SO_2, and for CO. This indicated large similarities in the character of changes in the level of ozone in the analyzed areas, but much lower similarities for other analyzed pollutants. The correlations were significant for the level 0.01, unless otherwise indicated in the tables. Unfortunately, some stations in the Masovia voivodship did not perform measurements of SO_2, O_3, CO and $PM_{10.}$ Therefore, the corresponding cells were marked as "not applicable" (n/a).

Table 8. Correlation coefficient between
SO_2 concentrations in Masovia Province.

SO_2	UT	CB	SB	TB	RB
UT	-				
CB	n/a	-			
SB	n/a	n/a	-		
TB	n/a	n/a	0.53	-	
RB	n/a	n/a	0.34	0.48	-

Table 9. Correlation coefficient between O_3
concentrations in Masovia Province.

O_3	UT	CB	SB	TB	RB
UT	-				
CB	n/a	-			
SB	n/a	n/a	-		
TB	n/a	n/a	0.94	-	
RB	n/a	n/a	0.82	0.84	-

Source: Author's

Table 10. Correlation coefficient between
CO concentrations in Masovia Province.

CO	UT	CB	SB	TB	RB
UT	-				
CB	0.53	-			
SB	n/a	n/a	-		
TB	n/a	n/a	n/a	-	
RB	0.35	0.54	n/a	n/a	-

Table 11. Correlation coefficient between
PM_{10} concentrations in Masovia Province.

PM_{10}	UT	CB	SB	TB	RB
UT	-				
CB	0.69	-			
SB	0.72	0.87	-		
TB	n/a	n/a	n/a	-	
RB	0.59	n/a	0.67[*]	n/a	-

*Correlation was significant at the 0.05 level

Source: Author's

Also, the nature of air pollution changes in the Lower Silesia voivodship was similar to that for the Lodz and Masovia voivodship. Linear correlation coefficients decreased along with the change of the type of area into less urbanized, within the same voivodeship (Tables 13−16). Interdependencies between air pollutants concentrations were high (and very high) in the case of ozone, but low (and medium) for SO_2. This indicated large similarities in the character of changes in the level of ozone in the analyzed areas, but much lower

similarities for other analyzed pollutants. The correlations were significant for the level 0.01, unless otherwise indicated in the tables. Unfortunately, some stations in the Lower Silesia voivodship did not perform measurements of SO_2, O_3, CO and PM_{10}. Therefore, the corresponding cells were marked as "not applicable" (n/a).

Table 12. Correlation coefficient between SO_2 concentrations in Lower Silesia.

SO_2	UT	CB	SB	TB	RB
UT	-				
CB	0.69	-			
SB	n/a	n/a	-		
TB	0.46	0.48	n/a	-	
RB	0.42	0.41	n/a	0.31	-

Table 13. Correlation coefficient between O_3 concentrations in Lower Silesia.

O_3	UT	CB	SB	TB	RB
UT	-				
CB	n/a	-			
SB	n/a	0.95	-		
TB	n/a	0.80	0.84[*]	-	
RB	n/a	0.82[*]	0.84	0.78	-

*Correlation was insignificant at the 0.01 level

Source: Author's

Table 14. Correlation coefficient between CO concentrations in Lower Silesia.

CO	UT	CB	SB	TB	RB
UT	-				
CB	0.77	-			
SB	n/a	n/a	-		
TB	n/a	n/a	n/a	-	
RB	n/a	n/a	n/a	n/a	-

Table 15. Correlation coefficient between PM_{10} concentrations in Lower Silesia.

PM_{10}	UT	CB	SB	TB	RB
UT	-				
CB	n/a	-			
SB	n/a	n/a	-		
TB	n/a	0.40	n/a	-	
RB	n/a	n/a	n/a	n/a	-

Source: Author's

In addition, the occurrence of various pollutants was compared within stations containing the largest number of data, i.e. stations located in urban (CB, SB, TB) areas, and rural (RB) areas in the Lodz region. Correlation was the strongest for NO_2, CO and PM_{10} (Tables 16-19). This could indicate the impact of emissions from road transport at similar times of the day [21]. Also, the analyzed correlations (R = -0.61–0.87) between air pollutants were comparable to other studies [21-22]. However, the O_3 concentrations had negative correlation with other pollutants. This was because in Poland the ground-level ozone reached the highest concentrations during early afternoon, resulting from occurrence of photo-chemical processes, while other pollutants had the highest concentrations in the morning, in the evening, or at night [6]. The calculated correlations were significant for the level 0.01, unless otherwise indicated in the tables. Unfortunately, RB station did not perform measurements of CO. Therefore, the corresponding cells were marked as "not applicable" (n/a).

Table 16. Correlation coefficient between air pollutants concentrations in CB area in Lodz Province.

City Background	NO_2	O_3	SO_2	CO	PM_{10}
NO_2	-				
O_3	-0.54	-			
SO_2	0.42	-0.32	-		
CO	0.70	-0.55	0.61	-	
PM_{10}	0.65	-0.44	0.61	0.84	-

Source: Author's

Table 17. Correlation coefficient between air pollutants concentrations in SB area in Lodz Province.

Suburb Background	NO$_2$	O$_3$	SO$_2$	CO	PM$_{10}$
NO$_2$	-				
O$_3$	-0.56	-			
SO$_2$	0.36	-0.21	-		
CO	0.69	-0.53	0.46	-	
PM$_{10}$	0.59	-0.34	0.45	0.74	-

Source: Author's

Table 18. Correlation coefficient between air pollutants concentrations in TB area in Lodz Province

Town Background	NO$_2$	O$_3$	SO$_2$	CO	PM$_{10}$
NO$_2$	-				
O$_3$	-0.55	-			
SO$_2$	0.51	-0.30	-		
CO	0.63	-0.45	0.71	-	
PM$_{10}$	0.60	-0.38	0.67	0.87	-

Source: Author's

Table 19. Correlation coefficient between air pollutants concentrations in RB area in Lodz Province

Rural Background	NO$_2$	O$_3$	SO$_2$	CO	PM$_{10}$
NO$_2$	-				
O$_3$	-0.61	-		`	
SO$_2$	0.35	-0.15	-		
CO	n/a	n/a	n/a	n/a	
PM$_{10}$	0.56	-0.27	0.43	n/a	-

Source: Author's

Conclusions

Calculated linear correlation coefficients for air pollutants had a similar tendency in the analyzed locations. Although the hourly concentrations of pollutants varied greatly depending on the area, some correlation between these results was observed. This was particularly visible within the same region, where the coefficients were the highest (*R* up to 0.82 for NO$_2$, 0.69 for SO$_2$, 0.95 for O$_3$, 0.90 for CO, 0.87 for PM$_{10}$). Correlation coefficient for air pollutants decreased along with the change of characteristics (UT, CB, SB, TB, RB) of the analyzed area to a less dense area. Results of measurements in the cities (UT and CB areas) were more strongly interrelated with each other, than results from a city (UT) and a village (RB). For example, PM$_{10}$ concentrations at urban traffic site in Lodz (Table 7) were highly correlated to city background (R = 0.87) suburb background (R = 0.75) and town background (R = 0.71), and moderate correlated to rural background (R = 0.64). However, interrelations between air pollutants in the same area were the strongest between NO$_2$, CO and PM$_{10}$ (Tables 16-19). Correlation coefficient between nitrogen dioxide and carbon monoxide was 0.70 in city background, 0.69 in suburb background, and 0.63 in rural background. For NO$_2$ and PM$_{10}$ the coefficient was from 0.56 at RB monitoring station to 0.65 at CB station. This could indicate the impact of emissions from road transport, which generates inter alia those three pollutants. However, ground-level ozone had a negative correlation to other analyzed pollutants, as its concentration is usually increasing in the afternoon, contrary to other air pollutants [6]. This could be a result of photochemical processes, affected by solar radiation and ambient temperature [21]. Those interrelations were similar to those of other studies [21–22]. However, it should be remembered, that the correlation coefficients do not prove the existence (or absence) of dependencies between the analyzed variables [24], but may indicate the occurrence of such

interdependencies. Also, the results from air quality measuring stations might not always adequately represent the air quality conditions in large, especially highly urbanized areas [25].

Generally, R values decreased along with the change in the type of area into less urbanized, within the same voivodeship. Therefore, it should be further investigated if the most significant impact to this phenomenon was related to similar weather conditions in the same region, or the urban spatial structure, or hourly profiles (patterns) of human activity. However, a strong influence from all factors was very likely related.

References

[1] J.P. Putaud, F. Raes, R. Van Dingenen, E. Brüggemann, M. Facchini, S. Decesari, S. Fuzzi, R. Gehrig, C. Huglin, P. Laj, G. Lorbeer, W. Maenhaut, N. Mihalopoulos, K. Müller, X. Querol, S. Rodriguez, J. Schneider, G. Spindler, A. Wiedensohler, A European aerosol phenomenology - 2: Chemical characteristics of particulate matter at kerbside, urban, rural and background sites in Europe, Atmos. Environ. 38 (2004) 2579−2595 https://doi.org/10.1016/j.atmosenv.2004.01.041

[2] R. Cichowicz, G. Wielgosiński, Analysis of variations in air pollution fields in selected cities in Poland and Germany, Ecol. Chem. Eng. S 25 (2018) 217−227 https://doi.org/10.1515/eces-2018-0014.

[3] R. Cichowicz, G. Wielgosiński, W. Fetter, Dispersion of atmospheric air pollution in summer and winter season, Environ. Monit. and Assess. 12 (2017) 189–605 https://doi.org/10.1007/s10661-017-6319-2

[4] C.F. Lee, J. Hsiao, S.J. Cheng, H.H. Hsieh, Identification of regional air pollution characteristic and the correlation with public health in Taiwan, Int. J. Environ. Res. Public Health 4 (2007) 106−110

[5] A. Hagenbjörk, E. Malmqvist, K. Mattisson, N.J. Sommar, L. Modig, The spatial variation of O_3, NO, NO_2 and NO_x and the relation between them in two Swedish cities. Environ. Monit. Assess. 189 (2017) 189-161 https://doi:10.1007/s10661-017-5872-z

[6] R. Cichowicz, A. Stelęgowski, Average Hourly Concentrations of Air Contaminants in Selected Urban, Town, and Rural Sites, Arch. Environ. Contam. Toxicol. (2019) https://doi.org/10.1007/s00244-019-00627-8

[7] G. Wielgosiński, J. Czerwińska, O. Namiecińska, R. Cichowicz, Smog episodes in the Lodz agglomeration in the years 2014-17, E3S Web Conf 28 (2018) 01039 https://doi.org/10.1051/e3sconf/20182801039

[8] R. Cichowicz, A. Stelęgowski, Effect of thermal sludge processing on selected components of air quality in the vicinity of a wastewater treatment plant, Chemical Papers (2018) https://doi.org/ 10.1007/s11696-018-0636-y

[9] R. Cichowicz, G. Wielgosiński, A. Targaszewska, Analysis of CO_2 concentration distribution inside and outside small boiler plants, Ecol. Chem. Eng. S 23 (2016) 49−60 https://doi.org/10.1515/eces-2016-0003

[10] L. Pan, B. Sun, W. Wang, City air quality forecasting and impact factors analysis based on grey model, Proceedia Engineering 12 (2011) 74−79 https://doi.org/ 10.1016/j.proeng.2011.05.013

[11] R. Cichowicz, Spatial distribution of pollutants in the area of the former CHP plant, E3S Web Conf 28 (2018) 01007 https://doi.org/10.1051/e3sconf/20182801007

[12] R. Cichowicz, A. Stelęgowski, Selected Air Pollutants In Urban And Rural Areas, Under The Influence Of Power Plants, Acta Innovations 29 (2018) 41−52 https://doi.org/10.32933/ActaInnovations.29.5

[13] L.R. Sonkin, V.D. Nikolaev, Synoptic analysis and atmospheric pollution forecast, Russian Meteorology & Hydrology 5 (1993) 10−14

[14] P.I. Coyne, G.E. Bingham, Carbon Dioxide Correlation with Oxidant Air Pollution in the San Bernardino Mountains of California, J. Air Pollut. Control Assoc. 27 (1977) 782−784 https://doi.org/ 10.1080/00022470.1977.10470493

[15] F. Karaca, Determination of air quality zones in Turkey, J AIR WASTE MANAGE 62 (2012) 408−419 https://doi.org/10.1080/10473289.2012.655883

[16] R. Keresztes, E. Rapo, Statistical analysis of air pollution with specific regard to factor analysis in the Ciuc basin, Romania, Studia Ubb Chemia 3 (2017) 283−292 https://doi.org/10.24193/subbchem.2017.3.24

[17] X. Liu, Y. Liang, D. Yuan, Relationship between Air Polllution Index (API) and Crowd Health in Nanchang City, J. Geosci Environ. Protect. 4 (2016) 26−31 https://doi.org/ 10.4236/gep.2016.44005

[18] B. Thompson, Canonical correlation analysis – Uses and Interpretation, Sage Publications, London, 1984.

[19] A.G. Asuero, A. Sayago, A.G. Gonzalez, The correlation coefficient: an overview, Crit. Rev. Anal. Chem. 36 (2006) 41−59 https://doi.org/ 10.1080/10408340500526766

[20] H. Akoglu, User's guide to correlation coefficients, Turkish Journal of Emergency Medicine 18 (2018) 91–93 https://doi.org/10.1016/j.tjem.2018.08.001

[21] D.M. Agudelo-Castaneda, E.C. Teixeira, F.N. Pereira, Time-series analysis of surface ozone and nitrogen oxides concentrations in an urban area at Brazil, Atmos. Pollut. Res. 5 (2014) 411−420 https://doi.org/ 10.5094/APR.2014.048

[22] D. Pudasainee, B. Sapkota, M.L. Shrestha, A. Kaga, A. Kondo ,Y. Inoue, Ground level ozone concentrations and its association with NOx and meteorological parameters in Katmandu valley, Nepal, Atmos. Environ. 40 (2006) 8081–8087 https://doi.org/ 10.1016/j.atmosenv.2006.07.011

[23] E.C. Teixeira, E.R. de Santana, F. Wiegand, J. Fachel, Measurement of surface ozone and its precursors in an urban area in South Brazil, Atmos. Environ. 43 (2009) 2213–2220 https://doi.org/ 10.1016/j.atmosenv.2008.12.051

[24] A.K. Sharma, Text book of correlation and regression, Discovery Publishing House, New Delhi, 2005.

[25] I.F. Goldstein, L. Landovitz, G. Block, Air pollution patterns in New York City, J. Air Pollut. Control Assoc. 24 (1974) 148−152 https://doi.org/10.1080/00022470.1974.10469906

Aleksandra Kowalska, Robert Banasiak, Andrzej Romanowski, Dominik Sankowski
Lodz University of Technology, Institute of Applied Computer Science
Stefanowskiego 18/22, 90-924 Lodz, akowalska@iis.p.lodz.pl

A STUDY OF THE POSSIBILITY OF USING 3D MODELLING AND 3D PRINTING FOR ELECTRICAL CAPACITANCE TOMOGRAPHY SENSOR

Abstract
Nowadays, the optimization of energy consumption and resources is one of the most urgent topics in worldwide industry. The energy consumption monitoring and control in various multiphase flow industrial applications, where a proper flow characteristic and an optimal phase mixture control is crucial, is hard to perform due to the physical and chemical complexity of the processes. The Electrical Capacitance Tomography (ECT) is one of the relatively cheap non-invasive measurement methods that can help in the monitoring and control of optimal energy and resources dozing in industrial processes. ECT diagnostics systems use unique sensors that can non-intrusively detect spatial capacitance changes caused by spatial changes in the electrical permittivity of industrial process components. One of the latest ECT extensions is a three-dimensional measurement strategy that uses a multilayer structure of the capacitance sensor. In this paper, the authors propose a novel approach to the 3D ECT sensors fabrication process that uses 3D computer modelling and 3D printing to easily get any sensor shape, electrode layout, scale and shielding strategy. This study compares the measurement abilities of a 3D ECT sensor fabricated using a traditional hand-made technique with the 3D printed device. The results have proven the potential of the new 3D print-based sensor regarding its significant fabrication time reduction as well as the improvement of the overall 3D ECT sensor measurement accuracy and stability.

Key words
Electrical Capacitance Tomography, 3D printing, industrial processes, optimization, energy, resources

Introduction
Advanced automation and control of production processes play a crucial role in keeping the world economy competitive in their environmental aspect. While costly process equipment and production lines can be seen as the heart of industrial production, modern monitoring and control systems driven by information technology are its brain. They provide the flexibility to adjust production processes quickly in order to achieve efficiency at the lowest possible amount of resources and energy consumption costs. Hence, the development and application of advanced diagnostic systems is one of the most effective levers for immediate and long-term gross energy savings. One of the modern monitoring techniques that can meet these requirements is an electrical process tomography. It is a relatively young imaging method for industrial diagnostics, undergoing dynamic development [1] [2]. Electrical process tomography is now considered an up-to-date method of visualization and it effectively competes with other well-known imaging techniques such as observations of physical-chemical phenomena by using optical cameras or their recording on photographic film. Tomographic imaging allows observation of the structure of the interior of an object without any necessity of interfering or taking an invasive look into its interior. The process of constructing a tomographic image is based on acquiring and processing measuring signals from a sensor or a set of sensors used to study a given object or process. Process tomography offers unique possibilities of visualising industrial processes: structures of solid objects, fluids, gases and multiphase mixtures, as well as the parameters of their flows [3], and, what is more, in real time. The information about the process gained in this manner can be useful for further development of research or as a rich source of knowledge in the field of diagnostics, monitoring and control towards an energy and resource saving. Process tomography systems are those into which theoretical bases, devices [4], algorithms [5] and approaches used in medical tomography are integrated. This can be observed especially in the case of two- and three-dimensional Electrical Impedance Tomography (EIT) and Electrical Resistance Tomography (ERT). These techniques are now acknowledged worldwide as non-invasive visualization methods of rapidly changing physiological processes used for heart or lung diagnostics [6] and solving environmental issues as well [7]. In the case of Electrical Capacitance Tomography (ECT), as opposed to resistance and impedance methods, the measurement itself is fully non-invasive, and we deal with the environment of non-

conductive and typically dielectric properties. Such environments are common in numerous industrial processes. For many years electrical capacitance tomography systems have been regarded as an effective tool for non-invasive diagnosis and monitoring of two-phase, gas-liquid flows, pneumatic conveying of bulk materials in vertical and horizontal pipelines as well as in gravitational transport processes [3][8][9]. Initially capacitance tomography imaging method was used for two-dimensional visualization of an industrial process interior. The acquired measurement data enabled reconstruction of cross-sectional images of the process under test. Such an image allowed one to make only an approximate evaluation of an industrial process state, since the information obtained from measurement data was simplified and applied only to a specific industrial process section. In reality, however, industrial processes are of a spatial nature and require the use of fully three-dimensional imaging technique [10-17] in real-time as well [18]. Main functional components of 3D ECT system have been shown in Fig. 1.
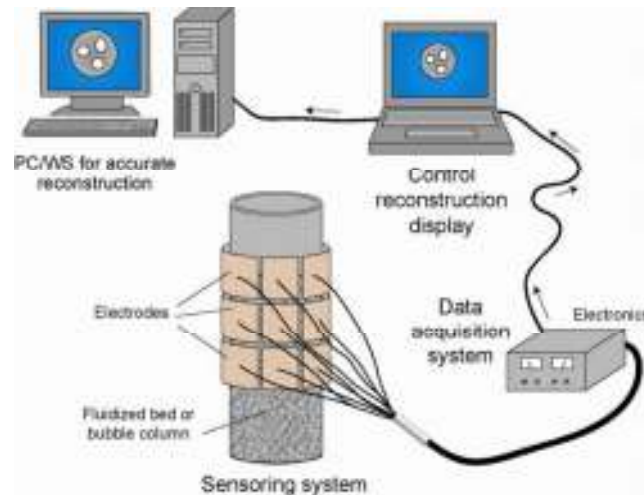

Fig. 1. Example 3D ECT system diagram and its components.
Source: [2]

In the case of a 3D ECT the basic structure of the sensors and the measurement concept are the same as in a 2D tomography (see Fig 2) [14]. The sensor is composed of a set of electrodes, each with a relatively high area of active surface [16]. The difference lies in their layout. In 2D ECT, with its cross-sectional arrangement of electrodes, some inhomogeneities (i.e. objects) can be difficult to distinguish and properly locate in 3D space as presented in Fig 3-A. 3D capacitances tomography uses a unique extended multilayer sensor structure where capacitance measurements are obtained by exciting electrodes from different layers as well and therefore any inhomogenity under test can affect all the measurements and can be distinguished in the final reconstructed image – Fig 3-B [19][20].
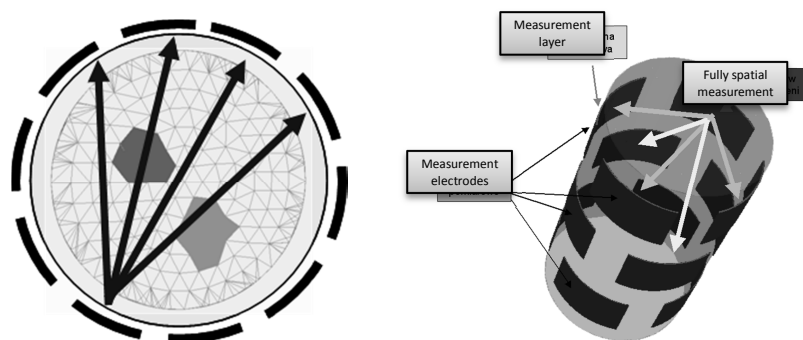

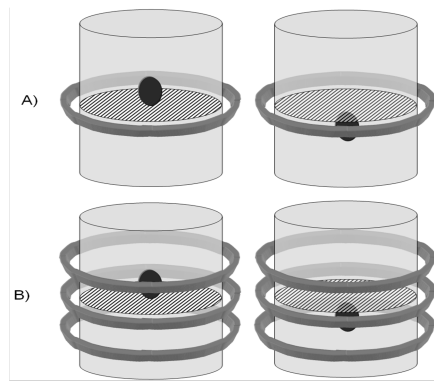Fig 2. 2D and 3D Tomography**.**
Source: [19]

Fig 3. Problem with object location in classic 2D tomography.
Source: [19]

The most common and widely used method of building a 3D ECT sensor is to use a PVC or PMMA pipe and equip it with conductive plates on the outer surface connected with wires. There are two major drawbacks of such an approach. Firstly, a PVC or PMMA pipe has a thickness that can unfavorably reduce an electric field penetration strength. Secondly, manual mounting of these components at specific positions is a sort of "more or less" work and it can bring various disturbances of a proper geometry of sensor structure. An improvement of these issues may be important to a better electric field detection efficiency and may provide more reliable industrial process monitoring and control decision-making – as it is important for energy and resource savings. In this paper, the authors propose a novel approach to the 3D ECT sensor fabrication process that uses 3D computer modelling and 3D printing to easily get any sensor shape, electrode layout, scale and shielding strategy. The proposed solution is a significant step into optimization of a 3D ECT sensor structure and consequently a step into better monitoring efficiency of the industrial process. This study compares the electric field sensing efficiency and measurement abilities of a 3D ECT sensor fabricated using a traditional hand-made technique with the 3D printed device.

3D printing of capacitance sensors
3D printing typically refers to fabrication processes in which various materials are joined or solidified under computer control to create a three-dimensional object. 3D printing is used in both rapid prototyping and additive manufacturing. Objects can be of any shape or any geometry and typically are produced using digital model data from a 3D model or another electronic data source. In an additive process an object is created by putting down successive layers of heated and melted material until the object is completed. Each of these layers can be seen as a thinly sliced horizontal cross-section of the eventual object. In this study, Fused Filament Fabrication technology was used in this research to build a new structure of capacitance sensor. To develop a new mechanical structure of a precise 3D ECT sensor, its computational design has to be prepared as a first. To achieve this goal, a Blender 3D modeller was used for designing a structure of the sensor model and its components. The 3D ECT sensor model has to be designed according to various 3D printing constraints and must be examined for mesh structure errors so that a significant effort has to be put on avoiding very thin walls, redundant mesh points, faces, overhangs, intersections, etc. The mesh model has to be kept as manifold as possible to be 3D printed properly. Blender software is able to generate a 3D sensor output mesh in Stereolithography (STL) format which is widely used 3D printing format. There was a need for splitting a sensor model into two separate symmetric parts due to being limited to a 200mm height of printing. Both parts were redesigned to have special holes and inserts to arrange and connect both parts precisely. The Z-axe outermost electrode layout separation walls and joints have been printed with a half of their thickness to keep it uniform for all 3D ECT sensor model structure. The next step was to prepare 3D printing configuration. In this study the Ultimaker 3 printer with PLA (polylactic acid) printing material and the CURA printing software were used for the building and control of the printing process. The 3D printing solution we used in this research is able to build very precise 3D structures of the ECT sensor with unlimited shapes and wide range of scale. The current maximum resolution of the used printer is 0.4mm for XY axes and 0.06mm for Z axe (print layer thickness) and can be extended by using higher resolution printing modules in the future. The high 3D printing XY resolution was used here to generate very thin sensor wall for keeping distance between electrodes and scanning volume as low as possible. In the past it was very hard or even impossible to achieve in previous classic PMMA (or PVC) pipes-based 3D ECT sensors. Due to the fact that the 3D ECT sensor print model has hanging inter-plane

separation walls the dual printing heads approach has been applied using PVA water-dissolvable material for generating special supports. Finally the printed model was equipped with common electrical elements: electrode plates, wiring and screening system. The main stages of the developed 3D ECT sensors printing workflow have been illustrated in Fig 3.

Fig. 3. The main steps of modelling, design and finishing 3D printed ECT sensor.
Source: Author's

Forward and inverse 3D modelling

The 3D ECT technique is based on measuring the changes in the electric capacitance between the capacitor planes as a result of changes in the dielectric properties of an object under test, located between these planes. The general capacitance tomography measurement concept is as follows: the positive potential on one of the electrodes (excited electrode) is set, while others are grounded. The measured capacitances are collected and then the other electrodes are excited. A limited set of measurements can then be used in image building. The forward problem for 3D electrical capacitance tomography is the simulation of M measurement data for given value of excitation for N electrodes and material permittivity distribution (ε ̂). The main goal of an inverse solution is to approximate of material permittivity distribution (ε ̂) inside of sensor volume using capacitance data C_M and electric field sensitivity matrix S_{MxN}. This general idea is illustrated in Fig. 4.
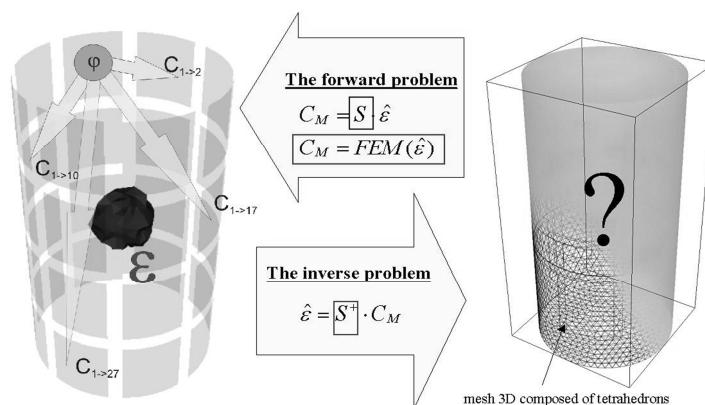

Fig. 4. 3D ECT forward and inverse problem scheme.
Source: Author's

Let's take and assume no internal charges. Then the following equation holds:
$$\nabla \cdot \varepsilon \nabla u = 0 \ \text{in} \ \Omega, \quad (1)$$
where: u is the electric potential, ε is dielectric permittivity and Ω represents the region containing the electric field. The potential on each electrode is known as:
$$u = \nu_k \ at \ e_k, \quad (2)$$
where: e_k is the k-th electrode held at the potential ν_k. Using the Finite Elements Method we obtain:
$$\mathbf{K}(\varepsilon)\boldsymbol{\varphi} = \mathbf{B}, \quad (3)$$
where: the matrix **K** is the discrete representation of the operator $\nabla \cdot \varepsilon \nabla$, the vector **B** is the boundary condition term and $\boldsymbol{\varphi}$ is the vector of electric potential solution. The electric current on the k-th electrode e_k is given by:
$$I_k = \int_{e_k} \varepsilon \frac{\delta u}{\delta n} dx^2, (4)$$
where: n is the inward normal on the k-th electrode e_k.

To calculate simulated capacitance data, the forward model of the 3D capacitance sensor has to be developed. There are a few ideas of 3D ECT sensor forward modelling [21]. The inverse problem is the imaging result for a given set of measurement data. To solve the inverse problem, we need to find the remedy for the forward problem as a first and to calculate sensitivity maps for the 3D ECT sensor. To obtain a distribution of sensitivity inside the sensor volume, the Fréchet derivative of the measured capacity is calculated in relation to the disturbances that occur in the permeability distribution ε ignoring there by the higher order terms [12] [14].This can simply be extended to a formal proof using operator series and a derivation of sensitivity formula has been given in [6] [12] [14]. In order to obtain a change in the load Q on electrode e_i when e_j is excited, the potential φ_i is applied when electrode e_i is driven and φ_j when e_j is driven [14]. The sensitivity formula can be written as follows:

$$\delta Q_{ij} = \int_{\Omega_p} \delta\varepsilon \nabla\varphi_i \cdot \nabla\varphi_j dx^3, \qquad (5)$$

where: Ω_p represents the capacitance sensor volume perturbed by electrical permittivity distributionε. Here φ_i and φ_j can be calculated by the solution of the forward problem while electrodes e_i and e_j are excited.

Experimental setup

The experimental part of this study was performed entirely in the Process Tomography Research Laboratory at the Institute of Applied Computer Science at the Lodz University of Technology. To compare 3D printed ECT sensor with traditionally made device, the experimental setup consists of two 3D ECT sensors, the Agilent E4980A impedance precision meter and 64-channel computer-controlled multiplexer has been applied. Both sensors were built in accordance with the 3D ECT measurement concept and equipped in 32 electrodes (4 layers with 8 electrodes at each layer). The electrode excitation strategy uses m=496 independent measurement data for n_el without mutual repetitions according to the formula:

$$m = \frac{n_{el}(n_{el}-1)}{2}, \quad (6)$$

Both sensors have two external planes (1st and 4th) and two internal planes (2nd and 3rd). The conventionally-made sensor (we named it: Sensor1) is the sensor we have used in our previous research [9][14]. It was devised and built using the traditional "hand-made" method. The sensor mounting pipe is made of PMMA (polymethyl methacrylate), the sensor total height is 304 mm and its external diameter is 158mm [14]. The mounting pipe thickness is 4mm. Outer electrode layers height is 70mm and inner electrode layers height is 30mm. The electrodes are located on the external surface of the sensor mounting cylinder. The novel sensor (we named it: Sensor2) is based on the 3D modeller design and it was printed using 3D printer [14]. The transparent PLA printing material was used to generate the sensor mechanical structure. Differently from Sensor 1, the outer layers have a height of 40mm of and inner layers have 25mm. The pipe thickness is 0.4mm which is a significant improvement compared to the Sensor 1 structure. It simultaneously assures the insulation of electrodes from industrial process components and keeps the measurement penetration distance and as low as possible. It may have significant positive influence on sensitivity in central area of a sensor. For both sensors, an electrode area and height asymmetry have been applied for outer and inner layers to keep a distant, inter-plane measurement signal detectable by a measurement unit [14].

Fig. 5. The main components of the experimental setup used in this study – a measurement system and two 3D printed test phantoms filled in PE granulate.
Source: Author's

Both sensors structures include a full shielding arrangement including copper-made outer screens and boundary screens. During the measurement, the following strategy was applied: firstly, the sender electrode has a positive potential (5V excitation voltage value has been applied) while the rest of the electrodes are grounded. Each electrode is switched made the sender in turn. [14][24].

Table 1. Experimental Sensor1 and Sensor2 key dimensions and parameters.

	Sensor height [mm]	Electrode Height [mm]	Electrode Width [mm]	Total active area [cm^2]
Sensor1	200	70/30	57	456
Sensor2	130	40/25	55	286

Source: Author's

For the experimental stage, two different experimental permittivity distributions (test1, test2) have been used. The testing phantoms were objects built using 3D printing technique (PLA) and filled in two ways with 3mm PE (polyethylene) granulates. The arrangement of tested phantom has been visualised in Fig 6. The experimental datasets have been normalized using capacitance data for high C_{full} and low C_{empty} uniform permittivity distributions (PE granulate − 3, an air − 1 as a background). In this study the normalization of experimental capacitance data C_n has been calculated according to formula:

$$C_n = \frac{C - C_{empty}}{C_{full} - C_{empty}}, \qquad (7)$$

To compare both sensors a full cycle and the first electrode with the full 31 measurement cycles were taken into consideration.
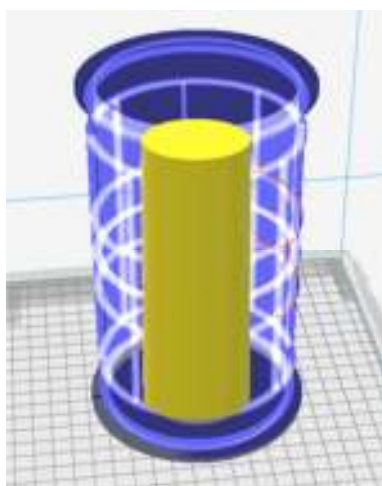

Fig. 6. The arrangement of a tested phantom inside a 3D ECT sensor volume for two options: test1 - a cylinder with 75mm of diameter filled with PE inside; test2 - a cylinder with 75mm of diameter filled with PE outside.
Source: Author's

Results and discussion

In this study we have mainly focused on the of the comparison of detection abilities of Sensor1 and Sensor2 and their responsivity on tested electrical permittivity phantoms test1 and test2. The Sensor1 has already been successfully verified for many industrial applications (two-phase flows, hopper flows) in our laboratory in the past [10]. In this study we treated it as a reference device. The full measurement cycle for test1 object (a PLA printed cylinder filled by PE granulate) and both sensors has been shown in Fig. 7.
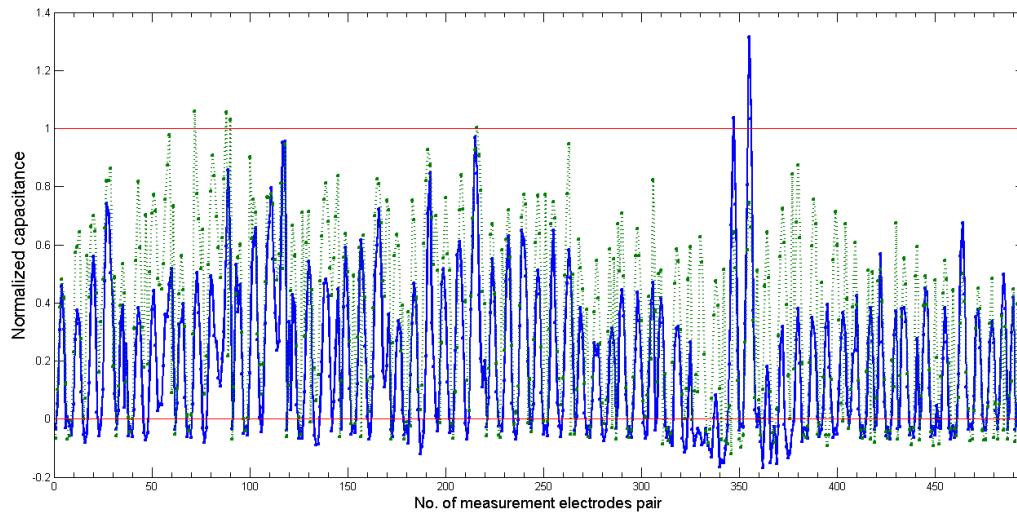
Fig. 7. The full measurement cycle for test1 and Sensor1 – green dotted line, Sensor2 – blue solid line. Red lines determine calibration limits (0;1).
Source: Author's

Both sensors were able to provide reliable calibration data to get stable in time the normalized capacitance vectors. The obtained experimental capacitance data full measurement cycle characteristics for test1 proved the similar abilities of these two devices to detect small objects in the centre of the scanning area. The mean value of the normalized capacitance dataset for Sensor1 is 0.3387 and the standard deviation is 0.3019. The mean value 0.1809 of Sensor2 normalized signal response is lower. This indicates that acquired signal response is weaker.

It points out the slight advantage of Sensor1 over Sensor2. However, the standard deviation is 0.2472, which indicates a better signal stability for Sensor2. We have to keep in mind that Sensor1 has around a 60% larger total area of electrode array in comparison to the 3D printed Sensor2 that surely can provide higher values of electric field intensity inside an investigation area. Fig 8 presents 1st electrode measurement cycle taken from full capacitance data set. This confirms the tendency and comparison results visible for full cycle.

Fig. 8. The 1st electrode measurement cycle (with 2..32) for test1 and Sensor1 – green dotted line, Sensor2 – blue solid line. Red lines determine calibration limits (0;1).
Source: Author's

Test2 investigates the ability of both sensors to detect permittivity distribution close to electrodes array. The full measurement cycle for test2 object (a PLA printed cylinder with an air inside surrounded by PE granulate) and both sensors have been shown in Fig 9. The mean value of normalized capacitance dataset for Sensor1 is

0.5801 and standard deviation is -0.1043. Regarding to test2 we also calculated a standard deviation value for both sensors: Sensor1 - 0.8103 and Sensor2 – 0.4730. This test showed a better performance of Sensor2 comparing to Sensor1 for an object located in the neighbourhood of the electrode array. The signal from Sensor2 better fits calibration limits and is more stable as well. The mean value of Sensor1 is negative (there are few negative normalized capacitance values below -1.5 for the most distant electrode pairs). It can indicate that capacitance measurement for the most distant electrodes is too low to generate positive normalized capacitance data. This confirms some benefits of using 3D printing technology over traditional method.

Fig. 9. The full measurement cycle for test2 and Sensor1 – green dotted line, Sensor2 – blue solid line. Red lines determine calibration limits (0;1).
Source: Author's

Fig. 10 presents first electrode measurement cycle graph subtracted from full capacitance data set. The blue line represents 3D printed 3D ECT Sensor2 capacitance data subset for first electrode and the green dotted line represents Sensor1. Capacitance measurement for electrode pair 1-28 is typically the most distant from all of the electrodes array and the hardest to measure due to the limitations of tomography hardware. The new sensor raises this capacitance minimum value to the level that might be acceptable for existing tomography systems [22]. This figure shows the measurement values normalized by means of calibration. It is known that the values should be in the range from 1 to 0 with the accuracy of the amplitude of the noise in the signal. Although neither sensor1 nor sensor2 fall into these values - it can be seen that sensor2 better adapts to the above range.
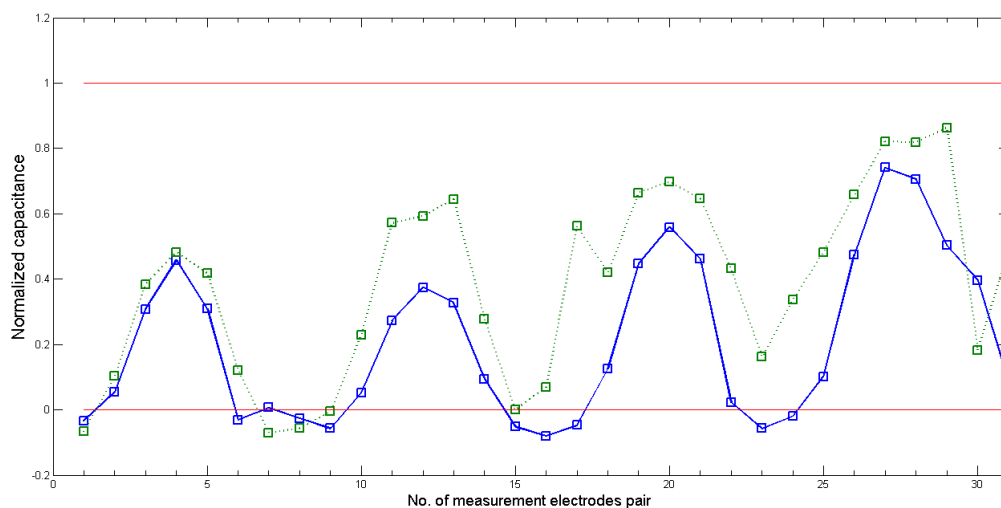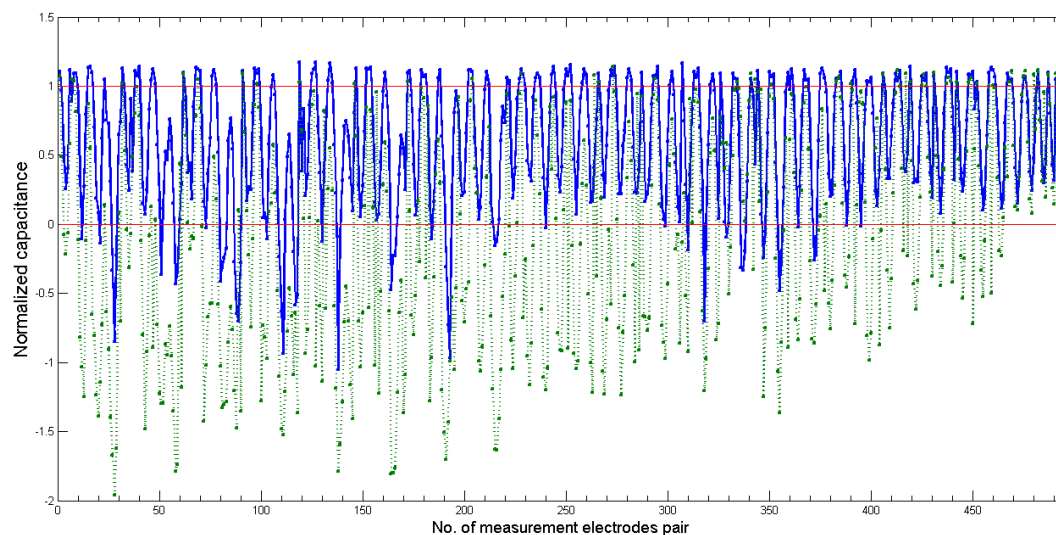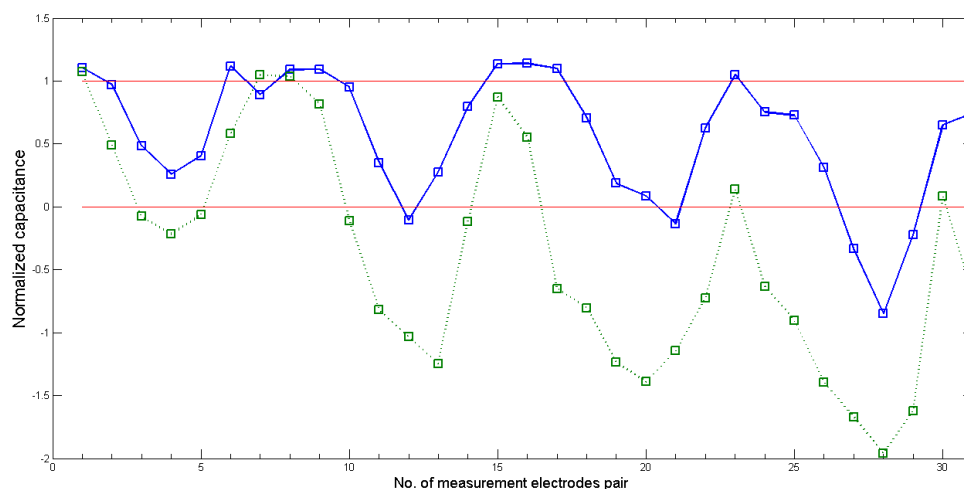

Fig. 10. The first electrode measurement cycle (with 2..32) for test2 and Sensor1 – green dotted line, Sensor2 – blue solid line. Red lines determine calibration limits (0;1).
Source: Author's

Conclusions and future work

In this research work a novel method for high precision design, modelling and build of 3D electrical tomography capacitance sensor was proposed and discussed. A developed solution combines modern 3D printing technique with a knowledge of 3D capacitance imaging and can extend 3D ECT tomography monitoring abilities to an efficiency level inaccessible for process tomography society in the past. The 3D printed ECT sensor advantages over traditionally hand-made made known 3D ECT sensors. It offers very thin wall between electrode array and can be built as a one-piece complex structure that may be easily fitted to industrial process under test. The accuracy of the 3D printed sensor structure is very high due to the reliability, repeatability and high resolution of 3D printing. In this research work, a 3D printed sensor model was compared to a well-known and reliable device used in the previous research. For most tests, we achieved better results of sensor detectability for tested phantoms. The conducted experiments have shown the great potential of using 3D printing technology for making ECT sensors. It seems to be a giant step forward towards high resolution and high precision electrical capacitance tomography systems. The proposed method brings a new era to the ECT sensor making process and now, even the most complex electrode arrays and sensor structures can be easily designed and 3D-printed in a short time. It also drives ECT non-invasive diagnostic technique towards a better and more robust industrial process monitoring and control that can lead to optimize strategy of energy and resources usage. As a future project, some new 3D ECT optimized and complex sensor designs will be tested and developed including: an increasing number of electrodes, changing electrode array shape and screening structures. Another direction could be the design and printing of the 3D ECT sensor optimized and fitted it to a given industrial process that runs in non-circular curved pipes and custom shape tanks or silos. Finally it will be interesting to research on the possible influence of the proposed 3D printing sensor methodology on the efficiency, performance and accuracy of hybrid systems employing contextual data processing or human crowd-computer data processing algorithms [12][21][23].

Acknowledgements

References

[1] C.G. Xie, S.M. Huang, C.P. Lenn, A.L. Stoll, M. S. Beck, Experimental evaluation of capacitance tomographic flow imaging systems using physical models, IEE Proc. – Circuits Devices Syst. 141 (1994) 357-368.

[2] A. Pląskowski, M.S. Beck, R. Thorn, T. Dyakowski, Imaging Industrial Flows – Applications of electrical process tomography, IOP Publishing Ltd - Taylor & Francis, 1995.

[3] K. Grudzien, A. Romanowski, D. Sankowski, R.A. Williams, Gravitational Granular Flow Dynamics Study Based on Tomographic Data Processing, Particulate Science and Technology, 26 (2007) 67-82, DOI: 10.1080/02726350701759373

[4] J. Kryszyn, W. T. Smolik, B. Radzik, T. Olszewski, R. Szabatin, Switchless charge-discharge circuit for electrical capacitance tomography, Meas. Sci. Technol., 25 (2014) 115009.

[5] W. Q. Yang, L. Peng, Image reconstruction algorithms for electrical capacitance tomography, Meas. Sci. Technol. 14 (2003) R1–R13.

[6] Ł. Mazurkiewicz, R. Banasiak, R. Wajman, T. Dyakowski, D. Sankowski, Towards 3D Capacitance Tomography, proc. 4th World Congress Industrial Process Tomography, Aizu, 2005, pp. 546-551.

[7] T. Rymarczyk, Using electrical impedance tomography to monitoring flood banks, Int. J. Appl. Electromagn. Mech. 4 (2014) 1–4.

[8] G. Rybak, Z. Chaniecki, K. Grudzień, A. Romanowski, D. Sankowski, Non–invasive methods of industrial processes control, IAPGOS - Informatics, Control. Meas. Econ. Environ. Prot. 4 (2014) 41–45.

[9] I. Jelliti, A. Romanowski, K. Grudzien, Design of crowdsourcing system for analysis of gravitational flow using x-ray visualization, in proc. FedCSIS'16, ACSIS, vol. 8. IEEE, 2016, pp. 1613–1619.

[10] R. Wajman, R. Banasiak, Tunnel-based method of sensitivity matrix calculation for 3D-ECT imaging, Sens. Rev. 34 (2014) 273–283.

[11] Q. Marashdeh, F. Wang, L.S. Fan, W. Warsito, Velocity measurement of multi-phase flows based on electrical capacitance volume tomography, in Proceedings of IEEE Sensors, 2007, pp. 1017–1019.

[12] R. Banasiak, R. Wajman, M. Soleimani, An efficient nodal Jacobian method for 3D electrical capacitance tomography image reconstruction, Insight Non-Destructive Test. Cond. Monit. 51 (2009).

[13] R. Wajman, P. Fiderek, H. Fidos, T. Jaworski, J. Nowakowski, D. Sankowski, R. Banasiak, Metrological evaluation of a 3D electrical capacitance tomography measurement system for two-phase flow fraction determination, Meas. Sci. Technol. 24 (2013) 11, DOI: 10.1088/0957-0233/24/6/065302.

[14] R. Banasiak, R. Wajman, D. Sankowski, M. Soleimani, Three-dimensional nonlinear inversion of electrical capacitance tomography data using a complete sensor model, Progress In Electromagnetics Research PIER, 100 (2010) 219-234.

[15] K. Grudzień, Visualization System for Large-Scale Silo Flow Monitoring Based on ECT Technique, IEEE Sensors Journal. 24 (2017) 8242-8250.

[16] R. Wajman, R. Banasiak, Ł. Mazurkiewicz, T. Dyakowski, D. Sankowski, Spatial imaging with 3D capacitance measurements, Measurement Science and Technology 17 (2006) 2113-2118.

[17] F. Wang, Q. Marashdeh, L.-S. Fan, W. Warsito, A Review: Electrical Capacitance Tomography: Design and Applications, Sensors 10 (2010) 1890-1917.

[18] M. Soleimani, C. N. Mitchell, R. Banasiak, R. Wajman, A. Adler, Four-Dimensional Electrical Capacitance Tomography Imaging Using Experimental Data, Prog. Electromagn. Res. 90 (2009) 171–186.

[19] R. Banasiak, Ł. Mazurkiewicz, R. Wajman, 3D Graphics Hardware and Software Acceleration Features for 3D Tomography, proc.3rd International Symposium on Process Tomography in Poland, Łódź, 2004, pp. 19-23.

[20] R. Banasiak, R. Wajman, Ł. Mazurkiewicz, Study of electrodes layout for three-dimensional electrical capacitance tomography sensors, proc. PROCTOM 2006 - 4th International Symposium on Process Tomography in Poland, Warszawa, 2006, pp. 147-150.

[21] C. Chen, P. Wozniak, A. Romanowski, M. Obaid, T. Jaworski, J. Kucharski, K. Grudzien, S. Zhao, M. Fjeld, Using Crowdsourcing for Scientific Analysis of Industrial Tomographic Images, ACM Trans on Intelligent Systems and Technology 52 (2016) 25.

[22] P. Brzeski, J. Mirkowski, T. Olszewski, A. Pląsowski, W. Smolik, R. Szabatin, Multichannel capacitance tomograph for dynamic process imaging, Opto-Electronics Rev. 11 (2003) 175–180

[23] A. Romanowski, K. Grudzień, P. Woźniak, Contextual processing of ECT measurement information towards detection of process emergency states, In proc. Thirteenth International Conference on Hybrid Intelligent Systems (HIS 2013), Tunis, 2013, pp. 292-298.

[24] R. Banasiak, M. Soleimani, Shape based reconstruction of experimental data in 3D electrical capacitance tomography, NDT & E International, 43 (2010) 241-249.

Małgorzata Zakłos-Szyda, Nina Pawlik
Lodz University of Technology, Faculty of Biotechnology and Food Sciences, Institute of Technical Biochemistry
Stefanowskiego 4/10, 90-924 Lodz, Poland, nina.pawlik@edu.p.lodz.pl

THE INFLUENCE OF *VIBURNUM OPULUS* POLYPHENOLIC COMPOUNDS ON METABOLIC ACTIVITY AND MIGRATION OF HELA AND MCF CELLS

Abstract
In recent years, research of antitumor activity of natural compounds isolated from plant material has increased. Polyphenols have gained significant attention due to their proapoptotic abilities and their involvement in migration and inhibition of metastasis processes. The anticancer effects of polyphenolic extracts of *Viburnum opulus* fruit against human breast (MCF-7) and cervical (HeLa) cancer cell lines have been confirmed in this study. It was demonstrated that the tested preparations (methanol – M and acetone – A from pomace, juice – J and juice after extraction to the solid phase SPE – PF) show cytotoxic activity and regulate the migration process of cancer cells. The degree of inhibition of cell migration was measured at two times - 24 h and 48 h after addition of the tested preparations. The highest toxicity towards both cell lines was demonstrated by the polyphenol fraction obtained after juice purification SPE (IC_{50} values at concentration of 63,541 and 19,380 µg/mL for HeLa and MCF cell lines, respectively). At the same time, the same preparation inhibited cell migration the most (nearly 70% compared to controls at both times at the concertation of 15 and 30 µg/mL). All preparations showed the antioxidant ability, but the *Viburnum opulus* juice (200 and 350 µg/mL) and the preparation after its purification (15 and 30 µg/mL) have larger ability to inhibit the intracellular oxidative stress (30-40%) than preparation obtained from pomace (nearly by 20% at concentration of 20 and 50 µg/mL of M and A). Despite the antioxidative capacity of the preparations, they simultaneously decreased cellular mitochondrial potential. The results obtained indicate the high potential of components of *Viburnum opulus* polyphenolic compounds can be used in the production of innovative dietary supplements or pharmacological preparations for people with an increased risk or inclination towards developing breast or cervical cancer.

Key words
Viburnum opulus, polyphenols, cancer cells migration, mitochondrial potential, anti-oxidant effect.

Introduction
Despite significant advances in medical technology cancer remains one of the most aggressive and debilitating diseases worldwide. Surgery, chemotherapy and radiotherapy are commonly used for cancer treatment, however due to the harmful and painful side effects of these treatments, patients usually do not cope well with them [1]. Recently, much attention has been paid to the identification of natural chemopreventive substances capable of inhibiting, delaying or reversing the process of multistage carcinogenesis. Most of these naturally occurring phytocompounds retain antioxidant and anti-inflammatory properties that seem to contribute to their chemoprevention. Antioxidants, such as vitamins and polyphenols, include many compounds that can capture reactive oxygen species. Therefore, it has been proposed that antioxidants have potential benefits for the prevention and treatment of diseases associated with increased generation of reactive oxygen species and can be effective in reduction of carcinogenesis [2].

Viburnum opulus belongs to the Adoxaceae plant family, which can be found in eastern, north-eastern, western and central Europe and Turkey. The fruits are quite small, have a red color and are very acidic. They contain a large amount of polyphenols, as well as ascorbic acid and L-malic acid. According to several authors, *Viburnum opulus* juice is a source of flavonoids that contain (+) – catechin, (-) – epicatechin and quercetin glycosides. The juice also contains a large amount of chlorogenic acid (54% of the total phenolic compound) and carotenoids, coleoic acid, epigallocatechin gallate, and quercetin [3, 4]. Due to the presence of these ingredients, it has a strong antioxidant effect and can be used in treatment of certain diseases, such as menstrual cramps, disorders of the nervous system as well as liver and biliary disorders. Recent studies have

shown that it has a high antimicrobial potential and antioxidant activity, which are considered effective in reduction of risk of cancer[2].

Global data indicates that Western European countries have the highest rate of incidence of breast and cervical cancer. For many years researchers have been trying to identify the risk factors and to develop effective methods for their prevention and treatment [5]. Due to these reports we decided to investigate the effects of polyphenolic extracts obtained from *Viburnum opulus* fruits as anti-tumor agents able to counteract metastases. As cellular models, HeLa and MCF-7 cell lines were chosen. Furthermore, we focused on determining the antioxidative capacity of preparations of such polyphenolic extracts and their impact on potential cellular mitochondrial regulation. The research aimed to determine the usefulness of *Viburnum opulus* fruits in the development of preparations and dietary supplements dedicated for people with an increased risk of breast and cervical cancer with a tendency to metastasis.

Materials and methods
In order to obtain polyphenol extracts, the fruits of *Viburnum opulus* were homogenized and then centrifuged at 5000 rpm for 10 min at 16°C. The obtained juice was divided into a fraction enriched with polyphenols by solid phase extraction (SPE) on a Waters Sep-Pak® C_{18} 35 cc Vac (10 g sorbent per cartridge) under pressure. The enriched polyphenol fraction was eluted with methanol at a volume equal to twice the bed volume. The pulp was further extracted with methanol: acetone: water (2:2:1 v/v/v) in a ratio of 1:10 w/v on the stirrer at 800 rpm for 30 min and then centrifuged at 5000 rpm for 10 min at 16°C. The residue was back-extracted with a 70% acetone solution in a ratio of 1:10 w/v and again centrifuged. The extracts obtained - polyphenols enriched, methanol and acetone - were concentrated at 40°C in a vacuum rotary evaporator (Büchi, Switzerland) and lyophilized.

The content of the total polyphenols was determined by using the Folin-Ciocalteu method. In a 96-well plate 10 µL of extract or water (control) was mixed with 40 µL of 10-times diluted Folin-Ciocalteu reagent. The reaction was initiated by adding 20 µL of 20% (w/w) Na2CO3. The volume of reaction mixture was adjusted to 200 µL with distilled water. After incubation at room temperature for 20 min the absorbance was measured at 760 nm (Synergy™ 2, BioTek Instruments Inc.). Total polyphenols content was expressed as mg of gallic acid equivalent (GAE) per g of lyophilized material.

For biological activity assays, centrifuged juice (J) and preparations of polyphenol fraction (PF), methanol (M) and acetone (A) extracts dissolved in a 50% DMSO solution were used. Samples were stored at -20°C before usage.

All cell culture reagents were obtained from Life Technologies (Carlsbad, USA). Human cervix adenocarcinoma HeLa cell line and human breast adenocarcinoma MCF-7 cell line were purchased from the American Type Cell Collection (ATCC). Cells were maintained at 37°C in a humidified incubator containing 5% CO_2 and 95% air. They were grown in DMEM medium with 10% fetal bovine serum (FBS), 100 µg/mL ampicillin, 100 µg/mL streptomycin and 100 IU/mL penicillin.

To determine the maximum non-toxic concentration and the IC_{50} dose, cells were seeded into 96-well plates at 10^4 cells per well in complete medium and grown for 20 h, then incubated in the presence of the extract diluted in DMSO and culture medium for 24 h. Following incubation, 10 µl of PrestoBlue cell viability reagent (Life Technologies, Van Allen Way, CA, USA), a resazurin-based solution, was added into each well and incubated further for 30 min at 37°C with 5% CO_2 and 95% air. Cell viability was determined by measuring the fluorescent signal at F530/620 nm (Excitation/Emission) on a Synergy 2 Microplate Reader (Bio-Rad, CA, USA). The obtained fluorescence magnitudes were used to calculate cell viability expressed as a percent of the viability of the untreated control cells.

To investigate the effect of the preparations on cell migration, cells were seeded into 96-well plates containing cell seeding stoppers (ORIS™ method) at a ratio of $4 \cdot 10^4$ per well for HeLa cells and $5 \cdot 10^4$ per well for MCF-7 cells in complete medium. After 24 h of incubation the stoppers were removed and cells were incubated in serum free medium in the presence of the extract diluted in DMSO and cultured medium for 24 h. Closure of the cell-free space was measured and recorded with a Leica M205C microscope (MDG4 model) using the Leica program, both immediately and at 24 h and 48 h after removing the stoppers, and then compared to the initial

cell-free space size at 0 h. The extent of migration was defined as the ratio of the difference between the original and the remaining wound areas compared with the original wound area. As a positive control, 10% FBS was used.

The mitochondrial membrane potential was assayed with a JC-1 probe. After treatments with the studied compounds, the medium was changed and JC-1 (1 µg/mL) was added for 20 min. Then, the cells were washed with serum-free medium and the fluorescent signal was measured at F530/620 nm, F485/528 nm, 485/620 nm. As a positive control, the known mitochondrial uncoupler CCCP (carbonyl cyanide 3-chlorophenylhydrazone) was used at a concentration of 50 µM. To determine the effect of the *Viburnum opulus* extracts on the intracellular generation of ROS, the DCFH-DA assay was performed. After incubating the cells for 20 h with extracts, they were washed with PBS and loaded with the DCFH-DA dye at a final concentration of 1 µM in serum-free medium for 40 min. The cells were then washed twice with PBS and the fluorescent signal at F485/528 nm was measured.

Results and discussion

There are few reports on *Viburnum opulus* composition and even fewer on its biological activity. However, it is known that guelder rose fruits contain large amounts of polyphenolic compounds corresponding to 65 mg of polyphenols per 1 g of fruit [6, 7]. Gallic acid was identified as the main polyphenolic compound in an amount of 8.29 g/kg fresh weight. Further compounds identified were chlorogenic acid, catechin, epicatechin, rutin, quercetin flavonoids, procyanidin B2, procyanidin trimer and proanthocyanidin dimer monoglycoside [8]. While discussing the results of the research we suggest the presence of the mentioned phytochemicals in the obtained preparations. Ulger et al. reported that the total number of tumor lesions were reduced in mice with colon cancer when treated with 1,2-dimethylhydrazine drinking water enriched with guelder juice at the initiation stage of tumorgenesis [9]. In this report we demonstrated that polyphenolic extracts of *Viburnum opulus* fruit exhibit anticancer activity with simultaneous decrease of cell metabolic activity and antioxidant properties.

PrestoBlue assay was used to assess the cytotoxicity of the preparations. Firstly, we determined the concentrations able to inhibit the viability of HeLa and MCF-7 cells at 50% compared to controls as well as the highest non-toxic concentrations. The obtained IC_{50} and IC_0 parameters are listed in Tab. 1. Fig. 1 demonstrates the influence of preparations on cellular viability. The highest cytotoxic activities against both cell lines were observed for the preparation obtained by extraction of solid phase (PF) from centrifuged juice. The IC_{50} parameters values are 63.541 µg/mL and 96.909 µg/mL for the HeLa and MCF-7 cells, respectively. In turn, the results indicate the lowest cytotoxicity of juice in both studied biological models. The lowest influence of a 50% decrease of cell viability was observed for centrifuged juice. The dependencies for both formulations seem to be justified. During the extraction to the solid phase we isolated certain flavonoid fractions, as well as flavonoid aglycons. We obtained a preparation free from proteins, polysaccharides and nucleic acids, which was chemically cleaner than the centrifuged juice [10]. For the other preparations (M and A), higher IC_{50} parameter values were observed, in comparison to the PF preparation, however they were lower than for the juice. This means that the most bioactive compounds affecting the viability of cells are found in the solid phase extracted preparation. The methanolic and acetone extracts were extruded from the pomace and contained higher amount of polyphenolic compounds than the centrifuged juice. Using an MTT assay, Waheed et al. showed that almost twice the dose (200 µg/mL) of methanolic extract of *Viburnum foetens* inhibited the metabolic activity of Caco-2 cells by 50%. Significantly lower inhibition (about 20%) with the same dose was obtained by Waheed against the MDA MB-468 cell line. In the presented studies all preparations showed higher toxicity to the cervical cancer cell line (HeLa) [11].
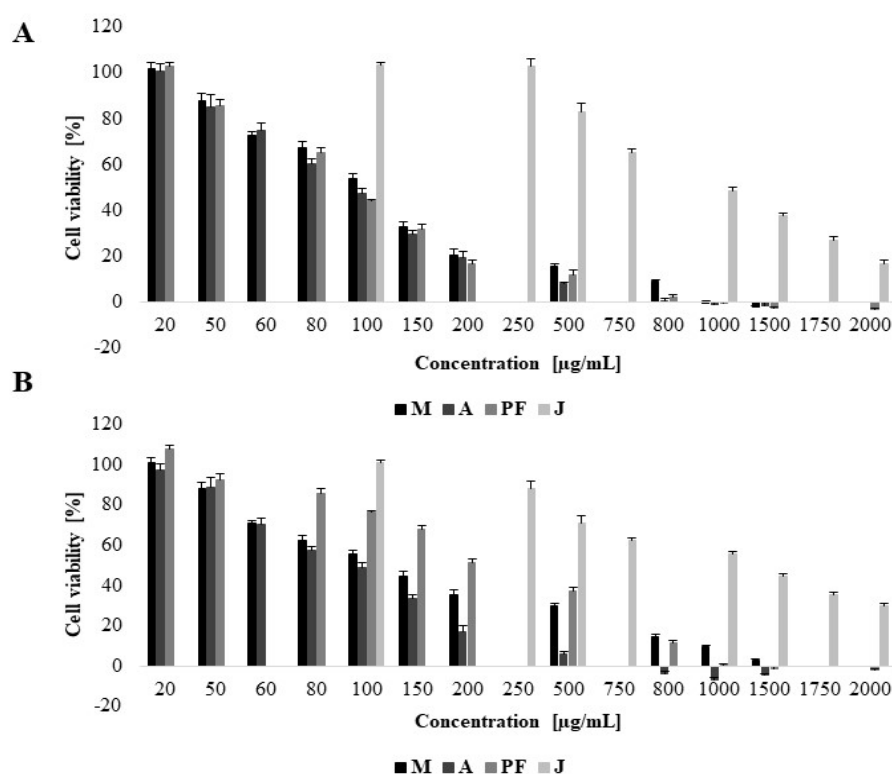
Fig. 1. Effect of *Viburnum opulus* fruit preparations on the viability of HeLa cells (A) and MCF cells (B) after 24 h incubation; values are mean ± standard deviation from at least eight independent experiments; the abbreviations used indicate the type of preparation M – methanol; A – acetone; PF – polyphenolic fraction; J – juice.
Source: Author's

Table 1. IC_{50} and IC_0 parameters of extracts obtained for HeLa and MCF-7 cells; values are means ± standard deviations from at least three independent experiments

Preparations	HeLa		MCF-7	
	IC_{50} (µg/mL)	IC_0 (µg/mL)	IC_{50} (µg/mL)	IC_0 (µg/mL)
Methanol: acetone: water	100,867 ± 0,101	20,173 ± 0,078	121,466 ± 0,121	24,293 ± 0,487
70% acetone	100,046 ±0,1	20,009 ± 0,128	243,641 ± 0,247	48,728 ± 0,307
Polyphenol fraction	63,541 ±0,162	12,781 ± 0,43	96,909 ± 0,097	19,380 ± 0,154
Juice	1031,512 ± 0,024	206,302 ± 0,362	1134,535 ± 1,135	226,907 ± 0,783

Source: Author's

The yield of inhibition of migration of the cells pre-treated with *Viburnum opulus* changed over time, which means that polyphenolic compounds contained in the preparations had a short-term effect. On the second day the number of actively migrating cells increased unambiguously, however the observed effect was stronger in HeLa cells (Fig. 2-3).
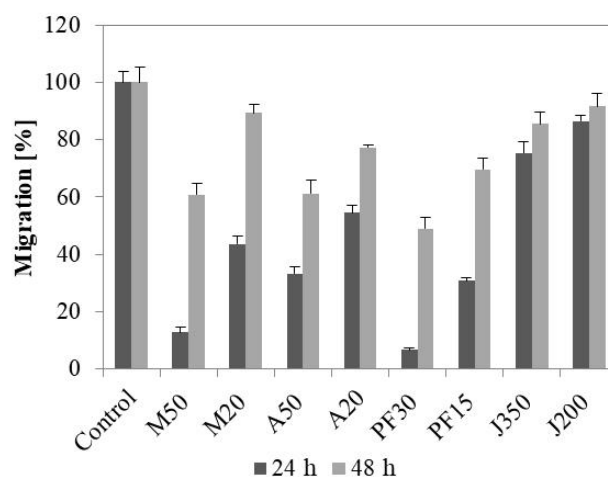
Fig. 2. Effect of *Viburnum opulus* fruit preparations on the rate of migration of the cervical cancer cell line (HeLa) for two incubation times (24 h and 48 h); values are means ± standard deviations from at least seven independent experiments; the abbreviations used indicate the type of preparation and the concentration used (for example M50 - methanol extract at concentration of 50 μg/mL)
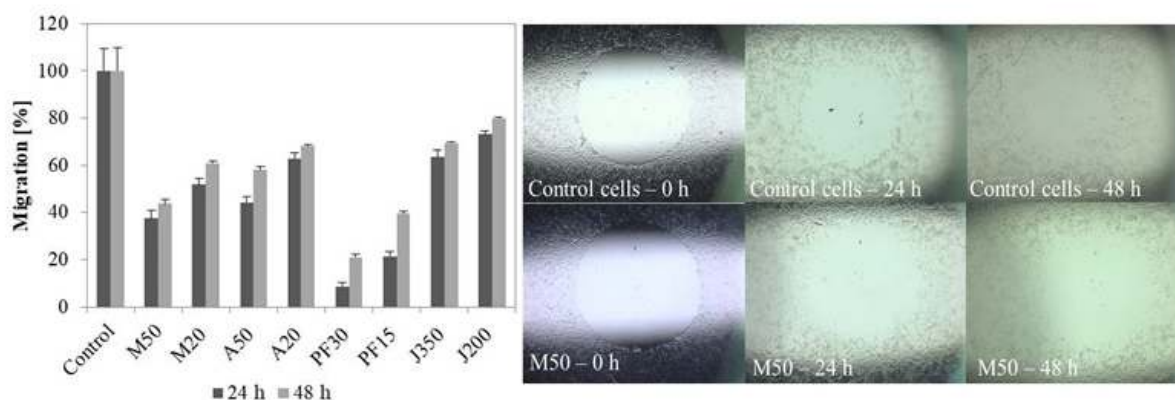*Source: Author's*

Fig. 3. Effect of *Viburnum opulus* fruit preparations on the rate of migration of the breast cancer cell line (MCF-7) for two incubation times (24 h and 48 h) and observed wound area of representative experiment; values are means ± standard deviations from at least seven independent experiments; the abbreviations used indicate the type of preparation and the concentration used (for example, M50 - methanol extract at concentration of 50 μg/mL)
Source: Author's

The anti-cancer properties of *Viburnum opulus* preparations are supported by a high content of polyphenolic compounds, like quercetin, epigallocatechin gallate (EGCG) and orgallic acid [13]. To the best of our knowledge there are no reports on the influence of extracts rich in polyphenolic compounds on the migration of tumor cells, but only reports of individual phytochemicals. Yu et al. analyzed the effect of quercetin (20 μM, 40 μM, 80 μM) on the migration of pancreatic cancer cells using the scratch test and the Transwell chamber. In all cases, after 24 h incubation the obtained results showed a correlation between the increase in the concentration of quercetin and a decrease in the number of cells that actively migrated. The inhibition of the rate of overgrowth observed was associated with the inhibition of migration, but also with a cytotoxic effect caused by quercetin [14]. In 2017, Farabegoli reported an inhibiting effect of EGCG at 25 μg/mL on MFC-7 cells migration based on the scratch assay. The concentration used did not demonstrate cytotoxicity to MCF-7 cells, but migration was inhibited by about 35% in comparison to cells cultured without polyphenols. After 48 hours the migration level was 37% lower. The effect of reduction of level of migration persisted for 72 hours and reached 45%. The study suggests that MFC-7 cells are susceptible to EGCG in the context of suppression of the migration process. This is also the basis for confirming the correctness of the results obtained in this work [15]. Another research study proved that polyphenol extract from *Phyllanthus emblica* (PEEP) tan grass leaves obtained by extraction with 70% acetone, inhibited proliferation of HeLa cells by 39% at a dose of PEEP 150 mg/mL [16]. The results of our work indicate that the preparation made with the same extraction method inhibits the migration of HeLa cells by about 85% the first day and by 40% on the second day at a non-toxic 50 μg/mL concentration.

The reduction of tumor invasiveness by lowering the rate of cell migration may have a different molecular basis. In counteracting tumor growth, modern medicine is based on reduction of the activity of small GTPases from the Rho protein family, metalloproteinases (MMP), vascular endothelial growth factor (VEGF), as well as the reduced expression of focal adhesion kinase (FAK) and c-Jun N-terminal kinases (JNK) [17, 18]. The debilitating factor of tumor cell invasiveness is mitochondrial dysfunction, which is accompanied by decrease of the mitochondrial potential, and in consequence, apoptotic cell death. Depolarization of mitochondrial membrane is caused by excessive production of reactive oxygen species (ROS), fragmentation of mitochondrial DNA (mtDNA), protein cross-linking and peroxidation of membrane phospholipids [19].

Mitochondrial dysfunction can promote progression of a cancer to an apoptosis-resistant/chemo-resistant and/or invasive phenotype by various mechanisms. During oncogenesis and tumor progression these mitochondrial alterations can activate cytosolic signaling pathways from mitochondria to the nucleus and ultimately alter nuclear gene expression for neoplastic transformation [20]. Chen et al. reported that caffeic acid phenethyl ester (CAPE), an active component isolated from honeybee propolis, induced apoptosis in human pancreatic cancer cells at 10 μg/mL, significantly decreased transmembrane potential of the mitochondrion in BxPC-3 cells and induced morphological changes of typical apoptosis (a 2-fold increase in caspase-3/caspase-7 activity in comparison to control cells) [21].

These reports have led us to attempt to determine the effect of *Viburnum opulus* on the mitochondrial potential and to link this phenomenon with a reduction in the rate of migration of tumor cell lines HeLa and MCF-7. For this purpose, we performed a test using a cationic dye (5,5',6,6'-tetrachloro-1,1',3,3'-tetraethylbenzimidazolylcarocyanine iodide), which signals the mitochondrial membrane potential decrease. In healthy cells, the negative charge of the membrane allows the cationic dye to pass into the mitochondrial matrix where it accumulates into red aggregates with fluorescence when measured at 530/620 nm (it is excited by green light). In apoptotic cells, the mitochondrial potential decreases and the charge of the vines change, so that the cationic dye cannot accumulate in the mitochondria and accumulates in the cytoplasm in a monomeric form emitting green fluorescence, which is measured at 485/528 nm when excited by blue light. The ratio of red to green fluorescence is defined as the health of cells. The wavelength of 485/620 nm is used to measure fluorescence, which presents the degree of polarity of the mitochondrial membrane [22].

The results of the JC-1 test are shown for the HeLa cervical cancer cell line (Fig. 4) and for the human breast cancer cell line (Fig. 5). For both lines, at each concentration of preparations, a decrease of mitochondrial potential, as well as a decrease in metabolic activity, were noticed. These results were closely correlated with the applied concentration of formulations as well as the degree of migration of HeLa and MCF-7 cells. Again, the most active was a highly purified PF preparation. The preparations reduced the polarity of the mitochondrial membrane by nearly 50% at a non-toxic IC_0 concentration, and at a concentration of 30 μg/mL by nearly 60%, which was comparable to the CCCP used as positive control. It is worth noting that all tested preparations showed a higher ability to induce a decrease in potential and metabolic activity in the MCF-7 breast cancer line, which could also be noted in the long-term inhibition of the proliferation rate of these cells. An equally high depletion of mitochondrial potential was observed for centrifuged juice, however it worked more strongly against the MCF-7 than HeLaline. Significant differences in the effects on the two cell lines were observed for the M and A formulations. This time, the methanol: acetone: water (v/v/v) preparation was more active against the HeLa line than the MCF-7. However, the preparation extracted with 70% acetone reduced the mitochondrial potential and metabolic activity to the same extent for both cell lines.
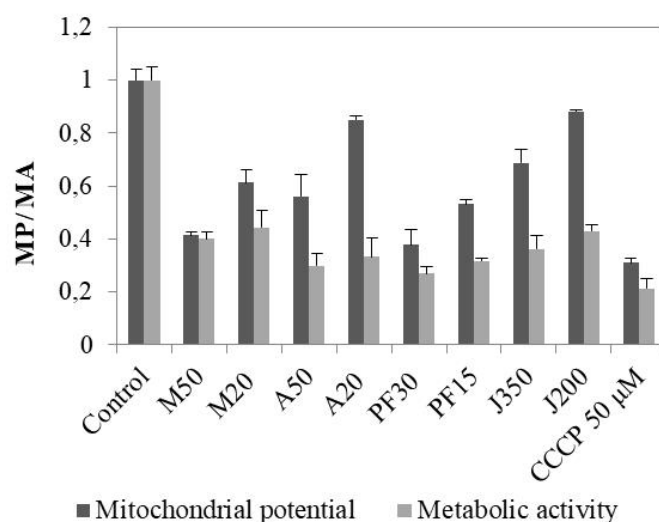
Fig. 4. Effect of *Viburnum opulus* fruit preparations on mitochondrial potential (MP) and metabolic activity (MA) of cervical carcinoma cell lines (HeLa); values are means ± standard deviations from at least three independent experiments; the abbreviations used indicate the type of preparation and the adjusted concentration (for example M50 - methanol extract in a concentration of 50 µg/mL)
Source: Author's
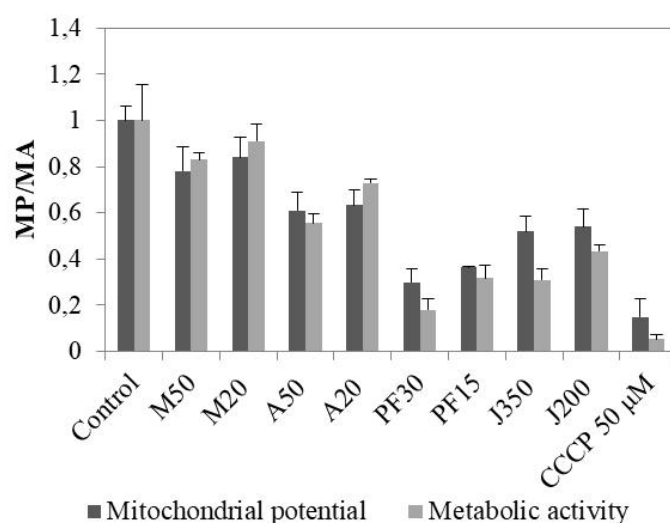
Fig. 5. Effect of *Viburnum opulus* fruit preparations on mitochondrial potential (MP) and metabolic activity (MA) of breast cancer cell lines (MCF-7); values are means ± standard deviations from at least three independent experiments; the abbreviations used indicate the type of preparation and the concentration used (for example, M50 - methanol extract at a concentration of 50 µg/mL)
Source: Author's

Drastic reduction of mitochondrial potential with simultaneous loss of cell biological activity usually lead to cellular apoptosis. Resistance to apoptosis is the main cause of cancer's insensitivity to conventional therapies. Therefore, one of the strategies employed is to look for factors that lead to cellular apoptosis induction. The latest reports showed that caffeic acid phenethyl ester (CAPE), a functional ingredient isolated from propolis, effectively reduced the number of proinflammatory cytokines and inflammatory mediators by inhibiting the transcription of the nuclear factor κ-light chain inhibitor of activated B cells (NF-κB). Several papers focused on the protective role of CAPE against general tumor models, both in vivo and in vitro for melanomas, lung and prostate cancers [23]. CAPE is a natural phenolic compound and an ester of phenethyl alcohol in the form of caffeic acid. Its presence was also found in the fruit of *Viburnum opulus* [8]. These reports lead us to conclude that the *Viburnum opulus* preparations we examined are capable of inducing mitochondrial dysfunction. This was proven by the reduction of the mitochondrial potential and the decrease in the metabolic activity of cancer cells. This resulted in the activation of caspase-3 and caspase-7, inhibition of the NF-κB factor, activation of the

Fas signal and ultimately in apoptosis induction. Analogous results for MCF-7 breast cancer were obtained by Liao et al., which were simultaneously proven in many independent studies with other cell lines [24].

The reduction of mitochondrial potential and dysfunction is accompanied by damage to the respiratory chain and overproduction of reactive oxygen species (ROS). This is observed due to the increased number of reduced forms of electron and proton transporters, such as the reduced form of nicotinamide adenine dinucleotide (NADH + H+) and flavin adenine dinucleotide (FADH2). The consequence of this process is the hyperpolarization of the internal mitochondrial membrane by increased electron flow through the respiratory chain. Finally, it stops the transformation of the respiratory chain at the complex III and the increased production of superoxide anion horn and mitochondrial dysfunction [25]. Taking this into consideration, we performed a study of the preparations influence on the intracellular oxidative stress using the DCFH-DA probe. This method consists of oxidizing the substrate (2',7'-dichlorodihydrofluorescein) introduced into the system in the form of an ester (diacetate, H2DCF-DA). The ester undergoes spontaneous hydrolysis reaction or a hydrolysis reaction which is catalyzed by hydrolases with the release of the product in the form of an oxidized DCF-DA, which can be recorded.

The results indicated the antioxidant capacity of the studied preparations of *Viburnum opulus* (Fig. 6). The highest decrease in ROS was observed for the PF preparation, as well as for the juice. At the IC_{20} concentration of PF, intracellular oxidative stress was reduced by 40% for HeLa and by 20% for MCF-7 cells. M and A formulations at IC_0 and IC_{20} resulted in the reduction of ROS concentrations by approximately 20%. It is clear that polyphenols contained in plant extracts have the ability to inhibit the production of free radicals, however, during mitochondrial dysfunction the apoptosis-induced ROS concentration in cells increase [18]. In 2016, Li et al. demonstrated that green tea preparation influenced internal oxidative stress of MCF-7 cells with an approximately 11-fold increase in ROS accumulation at 50 mg/mL dosage of preparation. Payen et al. showed that in SiHa-F3 cells EGCG at concentrations of 100 nM, 1 μM, 10 μM and 100 μM revealed a growing antioxidant effect which was correlated with the EGCG concentration [26].
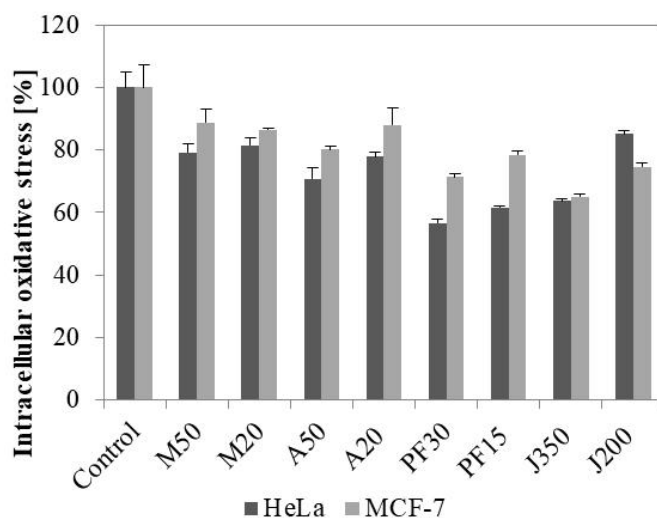
Fig. 6. Effect of *Viburnum opulus* fruit preparations on intracellular oxidative stress of cervical carcinoma cell line (HeLa) and breast cancer cell line (MCF-7); values are means ± standard deviations from at least three independent experiments the abbreviations used indicate the type of preparation and the concentration used (for example, M50 - methanol extract at a concentration of 50 μg/mL)
*Source: Author's*

Summary and conclusions
In summary, there is great interest in polyphenolic compounds in the context of antitumor activity, as well as in their inhibition of tumor cell migration and metastasis. In recent years a number of studies have been carried out showing a relationship between the increase of the concentration of various polyphenolic compounds (such as caffeic acid, gallic acid, quercetin, epigallocatechin gallate) and a decrease of migration process. The conducted studies showed that polyphenolic preparations obtained from *Viburnum opulus* fruits inhibit the migration of tumor cells. In some cases there is a drastic reduction in the number of migrating cells (up to 90%

- PF in the concentration of 30 µg/mL) for both of cell lines. At the same time, they show the ability to reduce the mitochondrial potential and metabolic activity of cells (up to 80% for PF for MCF cells), which was probably correlated with the degree of reduction of actively migrating cells. Despite the ability to drastically decrease the polarization of the mitochondrial membrane, the tested extracts showed antioxidant properties, which seem to also have a beneficial effect. The results obtained indicate the high potential of *Viburnum opulus* polyphenolic compounds as components that can be used in the production of innovative dietary supplements or pharmacological preparations dedicated to people with increased risk or inclination of breast or cervical cancer.

References
[1] A. Jemal, R. Siegal, E. Ward, Y. Hao, J. Xu, T. Murray, M.J. Thun, Cancer statistics, A Cancer Journal for Clinicians. 58 (2008) 71-96.

[2] D. Ceylan, A. Aksoy, T. Ertekin, A.H. Yay, M. Nisari, S.G. Karatoprak, H. Űlger, The effects of gilaburu (*Viburnum opulus*) juice on experimentally induced Ehrlich ascites tumor in mice, Journal of Cancer Research and Therapeutics. 14 (2018) 314-320.

[3] M. Çam, Y. Hişil, Comparison of chemical characteristics of fresh and pasteurised juice of gilaburu (*Viburnum opulus L.*), Acta Aliment. 36 (2007) 381-385.

[4] M.V. Gavrilin, M. Markova, T. Likhota, A. Izmailova, Optimization of the procedure of vitamin determination in Viburnum oil, Pharmaceutical Chemistry Journal. 41 (2007) 101-104.

[5] K.D. Miller, R.L. Siegel, C.C. Lin, A.B. Mariotto, J.L. Kramer, J.H. Rowland, K.D. Stein, R. Alteri, A. Jemal, Cancer treatment and surivorship statistics, A Cancer Journal for Clinicians. 66 (2016) 271-289.

[6] M. Zakłos-Szyda, I. Majewska, M. Redzynia, M. Koziołkiewicz, Antidiabetic Effect of Polyphenolic Extracts from Selected Edible Plants as α-Amylase, α -Glucosidase and PTP1B Inhibitors, and β Pancreatic Cells Cytoprotective Agents - A Comparative Study, Current Topics in Medicinal Chemistry. 15 (2015) 2431-2444.

[7] O. Rop, V. Recnicek, M. Valsikova, T. Jurikova, J. Milcek, D. Kramarova, Antioxidant Properties of European Cranberrybush Fruit (*Viburnum opulus* var. edule), Molecules. 15 (2010) 4467-4477.

[8] H. Singh, M.K. Lily, K. Dangwal, *Viburnum mullaha* D. DON fruit (Indian cranberry): A potential source of polyphenol with rich antioxidant, anti-elastase, anti-collagenase, and anti-tyrosinase activities, International Journal of Food Properties. 20 (2017) 1729-1739.

[9] H. Ulger, T. Ertekin, O. Karaca, O. Canoz, M. Nisari, E. Unur, F. Elmal, Influence of gilaburu (*Viburnum opulus*) juice on 1,2-dimethylhydrazine (DMH)-induced colon cancer, Toxicology and Industrial Health. 29 (2013) 824-829.

[10] M. Machowski, D. Kaliszewska, A. Kiss, Chromatograficzne metody izolacji i identyfikacji flawonoidów i saponin (Chromatographic methods of isolation and identification of flavonoids and saponin), Biuletyn Wydziału Farmaceutycznego Warszawskiego Uniwersytetu Medycznego. 4 (2010) 27-37.

[11] A. Waheed, Y. Bibi, S. Nisa, F.M. Chaudhary, S. Sahreen, M. Zia, Inhibition of human breast and colorectal cancer cells by Viburnum foetensL. extracts in vitro, Asian Pacific Journal of Tropical Disease. 3 (2013) 32-36.

[12] Ch. Decaestecker, O. Debeir, P Van Ham, R. Kiss, Can Anti-Migratory Drugs Be Screened In Vitro? A Review of 2D and 3D Assays for the Quantitative Analysis of Cell Migration, Medicinal Research Reviews. 27 (2007) 149-176.

[13] A. Konarska, M. Domaciuk, Differences in the fruit structure and the location and content of bioactive substances in *Viburnum opulus* and *Viburnum lantana* fruits, Springer Open Choice. 255 (2018) 23-41.

[14] D. Yu, T. Ye, Y. Xiang, Z. Shi, J. Zhang, B. Lou, F. Zhang, B. Chen, M. Zhou, Quercetin inhibits epithelial–mesenchymal transition, decreases invasiveness and metastasis, and reverses IL-6 induced epithelial–mesenchymal transition, expression of MMP by inhibiting STAT3 signaling in pancreatic cancer cells, OncoTargets and Therapy. 10 (2017) 4719-4729.

[15] F. Farabegoli, M. Govoni, A. Papi, EGFR inhibition by (-)-epigallocatechin-3-gallate and IIF treatments reduces breast cancer cell invasion, Bioscience Reports. 37 (2017) 170-178.

[16] X. Zhu, J. Wang, Y. Ou, W. Han, H. Li, Polyphenol extract of *Phyllanthusemblica* (PEEP) induces inhibition of cell proliferation and triggers apoptosis in cervical cancer cells, European Journal of Medical Research. 18 (2013) 46.

[17] C. Bonnas, J. Chou, Z. Werb, Remodelling the extracellular matrix in development and disease, Nature Reviews Molecular Cell Biology. 15 (2014) 786-801.

[18] T.Y. Forbes-Hernández, F. Giampieri, M. Gasparrini, L. Mazzoni, J.L. Quiles, J.M. Alvarez-Suarez, M. Battino, The effects of bioactive compounds from plant foods on mitochondrial function: A focus on apoptotic mechanisms, Food and Chemical Toxicology. 68 (2014) 154-182.

[19] G.L. Nicolson, Mitochondrial Dysfunction and Chronic Disease: Treatment With Natural Supplements, Integrative Medicine. 13 (2014) 35-43.

[20] C.C Hsu, L.M. Tseng, H.C. Lee, Role of mitochondrial dysfunction in cancer progression, Experimental Biology and Medicine. 241 (2016) 1281-1295.

[21] M.J., Chen, W.H. Chang, C.Y. Liu, T.E. Wang, C.H. Chu, S.C. Shih, Y.J. Chen, Caffeic acid phenethyl ester induces apoptosis of human pancreatic cancer cells involving caspase and mitochondrial dysfunction, Pancreatology. 8 (2008) 566-576.

[22] D.L. Garner, C.A. Thomas, Organelle-specific probe JC-1 identifies membrane potential differences in the mitochondrial function of bovine sperm, Molecular Reproduction and Development. 53 (1999) 222-229.

[23] H.K Erdemli, S. Akyol, F. Armutcu, M.A. Gulec, M. Canbal, O. Akyol, Melatonin and caffeic acid phenethyl ester in the regulation of mitochondrial function and apoptosis: The basis for future medical approaches. Life Sciences. 148 (2016) 305-312.

[24] H.F. Liao, Y.Y. Chen, J.J. Liu, M.L. Hsu, H.J. Shieh, H.J. Liao, C.J. Shieh, M.S. Shiao, Y.J. Chen, Inhibitory Effect of Caffeic Acid Phenethyl Ester on Angiogenesis, Tumor Invasion, and Metastasis, Journal of Agricultural and Food Chemistry. 51 (2003) 7907-7912.

[25] K. Siewiera, M. Łabieniec-Watała, Rola polifenoli roślinnych w łagodzeniu niekorzystnego wpływu cukrzycy na homeostazę funkcjonowania mitochondriów (The role of plant polyphenols in alleviating the adverse effects of diabetes on mitochondrial homeostasis), Postępy Fitoterapii. 1 (2013) 36-41.

[26] W. Li, N. He, L. Tian, X. Shi, X. Yang, Inhibitory effects of polyphenol-enriched extract from Ziyang tea against human breast cancer MCF-7 cells through reactive oxygen species - dependent mitochondria molecular mechanism, Journal of Food and Drug Analysis. 2 (2015) 101-112.

Olga Polyakova
Research Centre for Industrial Problems of Development of the NAS of Ukraine
1a Inzhenernyi Ln., Kharkiv, 61166, Ukraine, polya_o@ukr.net

Viktoriia Shlykova
Research Centre for Industrial Problems of Development of the NAS of Ukraine
1a Inzhenernyi Ln., Kharkiv, 61166, Ukraine, v.shlykova@ukr.net

INNOVATION FACTORS IN THE CYCLICAL DEVELOPMENT OF UKRAINIAN INDUSTRIES

Abstract
This article deals with the determination of the stages of development of Ukrainian industries with regard to the factors driving innovation. Based on an analysis of literary sources carried out, the most common indicators of the stages of development of industries have been identified, and it is proposed to classify them into structural, volumetric, dynamic, and innovation ones, given the specificity of the relevant statistical data regarding Ukraine. Calculations have shown that most industries are in a declining phase in terms of the majority of volumetric and innovation criteria. In some industries there are positive trends to intensify the innovation activity of businesses, while the chemical and engineering industries, which have the highest level of technological development, are in a decline phase.

Key words: industries, cyclical development, stages of development, innovation factors

Introduction
The global financial crisis has shown that the real economy, as opposed to the financial sector, is more stable and that it creates most of the products and jobs in developed countries.

The process of deindustrialization of the Ukrainian economy has been going on for more than two decades. In the period 2001-2016, the share of industry in GDP declined by 10 percentage points. Only low- and medium-technology production – the manufacture of food, the manufacture of basic metals, and mining — demonstrated the highest rate of development and relative stability. At the same time, a continuous reduction in the volumes of production, investment, and employment has been observed in the engineering industry, which belongs to high-tech industries. The European Commission called on the governments and societies of EU member states to restore industry as the main driving force of economic and social development. As highlighted in the relevant communiqué, a strong manufacturing base will be the key to restoring Europe's economy and competitiveness in the coming years, because industry provides the largest multiplier effect in the economy of countries as a whole, creating the largest volumes of added value. That is why, in EU countries, there are widely used various forms of government support for the development of a new type of industry, which are intended to restore and maintain the EU leadership in global industrial production in the long term.

The deepening crisis in Ukraine's industry does not allow the execution of simultaneous reconstruction in all directions, therefore, when providing support the government should take into account the state the stage of development, and potential of each specific industry in the economy.

The need to determine the stages of the development of industry in order to form an effective industrial policy is noted both by national [1] and foreign [2] researchers.

Thus, the purpose of the study is to determine the stages of development of Ukrainian industries with regard to the factors driving innovation.

Literature review
In modern literature, from 3 to 6-9 stages of development of industry are distinguished. The traditional life cycle model is associated with the development of M. Porter and includes four stages of development:

introduction, growth, maturity, and decline (crisis). Many researchers follow this approach. A detailed analysis of the characteristics of the four stages of industry development is presented in [3, 4]. Unlike Porter's approach, the Moore model is based on consumer requirements for products in an industry, and it comprises three phases: functionality, reliability, and convenience, which correspond to the improvement of technologies in order to satisfy consumer needs.

Given the possibility of different scenarios of industrial development when technologies become obsolete, the decline phase can end in the complete disappearance of an industry, or its transition to a new state of equilibrium (with a much smaller production volume) with the old technology being preserved.

Existing approaches to defining the concept of a life cycle and the correlation of stages, mostly for characterising the development of an enterprise, are studied in detail in the work of O. Matiushenko [5].

In general, approaches to determining the stage of development of an industry can be divided, depending on the preferential use of individual indicators, into the following groups:
- quantitative approaches, which primarily consider the volumes of factors involved and the results of production;
- innovative approaches, which are based on the assumption of the leading role of innovations in the development of an industry;
- complex approaches, which use a wide range of indicators to assess an industry's stage of development;
- individual approaches, which have a limited scope of use due to the specificity of an industry.

With a quantitative approach, the most applicable are indicators of production, sales, investments, employment, resources, etc.

S. Smirnova [6] considers the development of industrial clusters and proposes the use of methods of multivariate analysis to determine the stage of their life cycle. The feature space to characterise enterprises and clusters includes the following indicators: the current state of the market; the forecast state of the market; the intensity of competition; the availability of raw materials; and the availability of labour resources.

Based on the concept suggested by M. Porter, N. Rychyhina determines the development stages of the manufacture of textiles [7] and engineering [8] using the following main criteria: the number of enterprises; the production volume in physical and monetary terms; the number of employed; the number of equipment upgrades; the introduction of advanced technologies; the number of newly developed products (in the most recent period); and financial results.

The reasons for skipping one of the stages of the life cycle ("closing up", decline) by industries with a high degree of vertical integration, which do not experience any exit from the market, are analyzed in [9] using the example of the manufacturing of jet engines for civil aviation. The high degree of vertical integration of the network of engine and aircraft manufacturers prevents mass entry into and exit from the industry and provides a certain degree of stability. A life cycle analysis is based on the number of manufacturers and their production links. It should be noted that, at the stage of introduction of this industry, the main role was played by the experience of industry producers for the purpose of military aviation, which created large entry barriers for other potential participants. The features of such industries should be taken into account when analyzing the stages of their life cycle.

Innovative approaches to assessing the stage of development of an industry (known as the Abernathy-Utterback model), based on the leading role of innovation in economic development and the change of technological modes, focus on expenditure on R & D, and innovation, the volume of new and innovative products, the R & D intensity of an industry, etc., the degree of specialization / unification of equipment and products [10]. The peculiarity of each stage in terms of the origin of innovations is shown in [11], which points to the introduction of innovations at the early stages of development from other technologically related industries, in contrast to the later stages, where innovations have an endogenous origin.

An original approach to assessing the level of innovation development of an industry is proposed in [12], where authors distinguish between innovation potential and innovation activity, with innovation potential being adjusted in accordance with the level of innovative risk that reduces the potential. The authors use a uniform

scale to identify the level of innovation activity in different situations. Thus, the main criterion for determining the stage of development of an industry is the level of its innovational activity. The disadvantage of this approach is that among the singled out situations (stages), namely: "introduction", "formation", "smooth implementation" and "stability", there is no general crisis stage (decline). Thus, the indicators of innovational activity are not enough to determine the stage of development of an industry if they are not analysed in long-term dynamics.

Innovative processes are considered by S. Kuznetsov as the key factor in altering the stage of an industry's life cycle [13]. The main idea of defining the cycles of an industry is based on the hypothesis of the exhaustion of innovations, i.e., the decrease in efficiency of the available technologies, which leads to the decline of the industry. However, a higher innovational activity in industries related to the selected one (in the author's research — the forestry industry) can extend the maturity and efficiency of the industry.

Within the framework of an innovative approach, some researchers suggest using the idea of the existence of two types of threats of obsolescence – the threat to core activities and the threat to core assets — to define an industry's life cycle [10]. Obsolescence of core activities refers to the key factors that ensured the industry's profitability in the past, the obsolescence of core assets (competitiveness) is associated with knowledge, brands, patents, etc., which ensure the uniqueness of the organization in the market.

Comprehensive assessments include a variety of indicators that are usually combined into an integral indicator.

To assess the level of technological development of industries, L. Strelkova and S. Kabanov [14] propose the use of 20 indicators, which are grouped as follows: the efficiency of using fixed assets; innovative products and new technologies; organizations that implement technological innovations and their co-operation; use of human resources in the field of R & D; the operating costs associated with technological innovation; and intellectual property. The methodology involves the construction of an integral indicator of the level of an industry's technological development as a weighted sum of sub-indices.

Based on an analysis of 21 manufacturing industries in six European countries, the authors [15] investigated the innovational activity of new and existing firms at different stages of their life cycle. The initial assumption was the endogenous nature of economic growth associated with investing in R & D to create innovation. The authors distinguished two types of innovations (aimed at increasing t efficiency and qualitative characteristics) and determined the conditions of using one or another type at different stages of a firm's life cycle by the method of stochastic boundary estimation. Determining the stages of an industries' life cycle is based on panel data on production volume, value added, investment, labour costs and expenditure on R & D. The interpretation of quadratic models of panel data on countries' sales volumes (presented as logarithms) allows the determination of the stages of growth and maturity of an industry. The first derivative of these models makes it possible to determine the degree of maturity: industries with the highest degree of maturity are oil refinery, textile production and shipbuilding; with the lowest degree of maturity — production of computer equipment, communication equipment, pharmaceuticals and the precision instruments industry.

Some researchers have suggested identifying the stages of the life cycle of industries in terms of the quadrants of the BCG matrix. The transitions between the stages correspond to the transitions between quadrants [16], which allows consideration of regression processes in industries.

Regional features of the life cycle stages of the mining industry are associated with the exploration, use and exhaustion of stocks, as well as the availability of innovative technologies, as described in [17]. The difference in the life cycle stages of the industry in different regions affects the duration of the life cycle stages of the entire industry. The main criterion for determining the stages of the life cycle is the average annual increase in the volume of production, which is the largest in the stage of growth, and approaches zero in the maturity phase.

It is proposed to use economic and mathematical modeling for distinguishing the stages of growth — slow and rapid. Based on the data on gross revenue, capitalization, the number of employees, current liquidity, financial leverage, and taking into account the industry affiliation of a company, in [18] a probit-model of the transition of a company to the stage of rapid growth was constructed. In the paper it is shown that a decrease in the likelihood of transition to the stage of rapid growth is typical for industrial enterprises, which is mainly due to

the growth of debts hindering rapid growth. A detailed analysis of empirical methods to identify the stages of the life cycle of industries or products is given in [19].

Grebel et al. [20] focus on the peculiarities of the life cycle stages of the knowledge-oriented industries that arose in the late 20th century. The authors note that the concept of a life cycle, which was developed during the 20th century, has a very limited application in relation to new industries. A peculiarity of the development of such sectors is the simultaneous existence of large, highly differentiated firms, those oriented towards new technologies, which interact with state research institutes within a single innovation space. Due to this, the diffusion of knowledge and innovation is moving at a faster rate. The dynamics of the life cycle for knowledge-oriented industries is determined by the processes of transferring knowledge and technologies. Thus, the main criteria for determining the stage of the life cycle are the emergence and degree of implementation of new technologies, the specialization of new and reorientation of existing firms, as well as the growth rate of new knowledge. A quantitative measure may be the number of new patents (growth index), and the degree of concentration in the industry.

M. van Dijk [21] presents an empirical examination of differences between the dynamic and structural characteristics of industries that are in different stages of development, using the example of the Dutch economy. The formulated hypotheses are based on the Klepper innovative model of the life cycle of an industry, which implies a dynamic increase in the return on technological changes and takes into account the innovative opportunities and scale of the firm. The survey covered a period of 15 years and considered more than 10 thousand firms, of which 2.8 thousand existed throughout the period and provided more than half of the jobs and volume of sales. The list of indicators that were investigated for each firm comprised: the number of hired workers, sales volume (including re-exports), gross output, gross intermediate consumption, gross value added, indirect taxes, labour costs (including deductions to social funds), and gross profit.

To determine what stage of the lifecycle an industry is in, M. van Dijk [21] uses only two indicators: the growth rate of the total number of firms, and the growth rate of gross sales during the period under study. To assess an industry's stage of development by rate of growth/decline, we used the scale to estimate the significance of the deviation from zero "significantly smaller than zero", "zero", "significantly greater than zero", which was tested using the Student's criterion. At present, the approach is not applicable to determine the stages of development of Ukrainian industries, as it involves a large sample of data on the primary elements of industries — businesses — over a long period of time.

Thus, the list of indicators used to determine the stage of development of different economic sectors (including manufacturing ones) is wide enough (Tab. 1).

Table 1. Indicators of the stages of development of industries used in global practice

Industry structure	Production activity	Innovation activity
Number of enterprises	Volume of production (sales)	Innovation activity of enterprises (including large and small ones)
Rate of change in the number of enterprises	Rate of change in volumes of production	Expenditure on innovation activity
Degree of concentration in the industry	Financial results	Expenditure on R & D
Share of the industry in the domestic market	Export volumes	Number of implemented innovative technologies
Risk level	Depreciation of fixed assets	Number of patents received
Share of small enterprises	Volume of capital investments	Volume of sales of innovative products
Level of competition	Product turnover	
	Volume of orders	
	Dynamics of prices for products	
	Profitability	
	Structure of capital	
	Number of employees	

Source: Author's

The first set of indicators reflects an approach in which the main emphasis is placed on the rate of growth (decrease) in the number of firms over a certain period, the time when the number of firms is the greatest and the number of years when the growth (decrease) in the number of firms is observed. It should be noted that different methods allow the definition of a different number of stages of development of the industry — from two (growth — fall) to five.

The second group corresponds to Porter's quantitative approach. Therefore, the main focus is on volumes of resources, the efficiency of use, results, and the number of employed used as an additional criterion.

The formation of the third group of indicators is based on the suggestion that the innovational activity is high at the initial stages and is low at the stage of stability and decline. Moreover, the phase of introduction and the phase of decline of innovation is predominantly inherent in small businesses. For identification, direct indicators (the volume of sales of innovative products) and indirect ones (including the number of patents, expenditure on R & D) are applied. To use them, a targeted survey of business entities is necessary [19]. It is the activity in obtaining patents that is considered as a sign of the stage of technological development of an industry [22].

The possibilities of using certain indicators to determine the stages of development of Ukrainian industries are limited by the availability of relevant information for a long period of time. Therefore, in the case of Ukraine, the criteria shown in Figure 1 will be used.
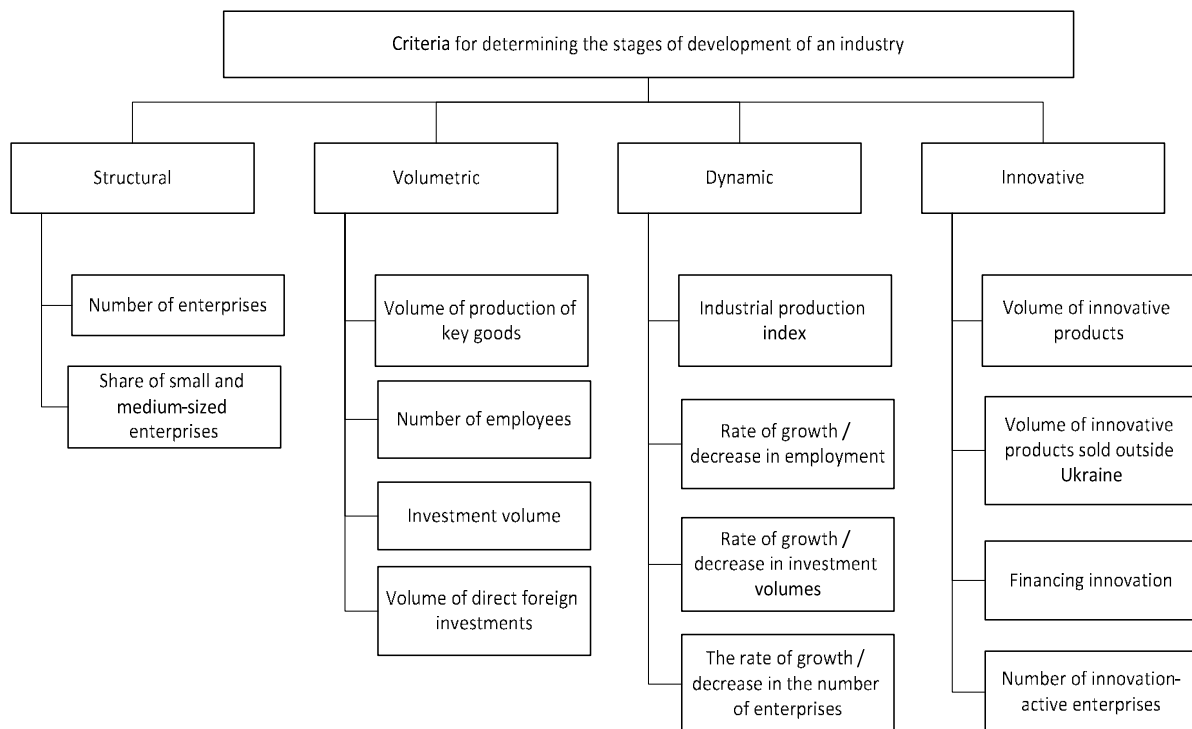
Fig. 1. Classification of criteria for identifying the stages of the life cycle of Ukrainian industries
Source: Author's

The structural and volumetric criteria for determining the stages of development of industries are used to carry out a preliminary analysis and calculate dynamic indicators. Dynamic indicators are calculated in the form of a chain and basic rates of growth (increase) are used for the formal definition of the development stage. Innovation criteria are used to assess the technological level and potential of development of an industry at the current stage. In view of the significant influence of inflationary processes, preference should be given to physical indicators or to those that are assigned in the same comparative base.

Thus, assessing the stage of development of Ukrainian industries according to the proposed criteria will make it possible to simultaneously reveal the main problems of the development of industries, with regard to their place in the country's economy, social impact, and the degree of technological development.

Assessing the stages of development of Ukrainian industries

To determine the features of the stages of development of Ukrainian industries based on the criteria presented in Figure 1, the data of the State Statistics Service of Ukraine for 2001-2015 [23, 24, 25, 26, 27] were used.

To determine the stage of development of Ukrainian industries an approach described in [21] was used, which is based on estimating the rates of growth / decline in the quantitative characteristics of businesses. According to this approach, to provide an absolute quantitative characteristic, the rate of growth/decline for a certain period of time is determined and then the hypothesis regarding the significance (non-significance) of the deviation of the rate of change from zero using Student's criterion is tested as follows:

Table 2. Deviation of the rate of change from zero using Student's criterion where τ is the rate of change of the quantitative indicator; t is the calculated value of the Student's t-criterion, t=1.75 – the critical value of the Student's criterion at a level of confidence probability of 0.05.

Rate of change (τ)	Student's criterion
significantly smaller than zero ($\tau \ll 0$)	$t < -1.75$
approximately equal to zero ($\tau \approx 0$)	$-1.75 \leq t \leq 1.75$
significantly greater than zero ($\tau \gg 0$)	$t > 1.75$

Source: Author's

The calculations were carried out for the types of industrial activity the data on the development of which is available for at least 10 years. Due to the change in the classification of types of economic activity and the limited list of industrial activities, the assessment of the development stage was carried out by aggregate types of activity.

Figure 2 presents the dynamics of the number of mining enterprises, which demonstrates that during the period 2001-2007 there was an increase in their number due to the expansion of non-energy mineral extraction.
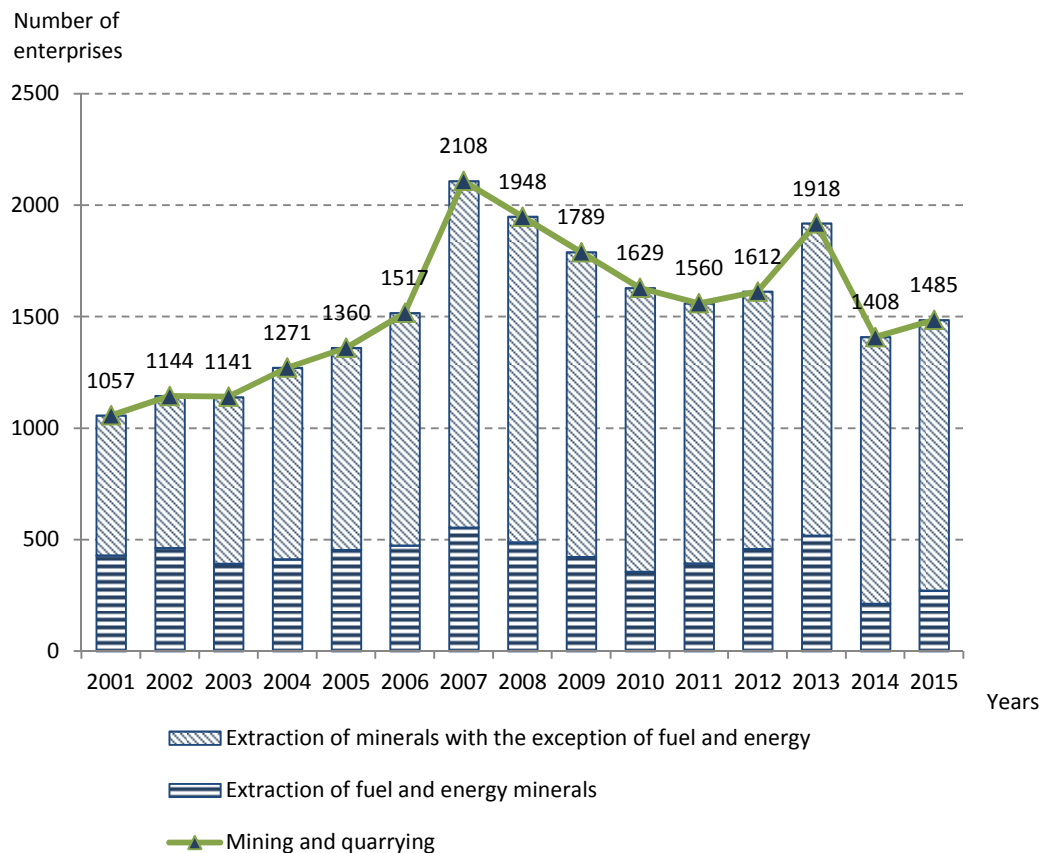

Fig. 2. Dynamics of the number of mining enterprises
Source: Author's

Since 2008 , a general decrease in the number of enterprises involved in this type of activity has been observed, mainly due to the fall in the number of enterprises specialising in the mining of hard coal and lignite (from 280 to 157).

The dynamics of the number of enterprises in some types of manufacturing industries is shown in Figure 3. In general, manufacturing also experienced a decrease in the number of enterprises, including the largest types of industrial activity.
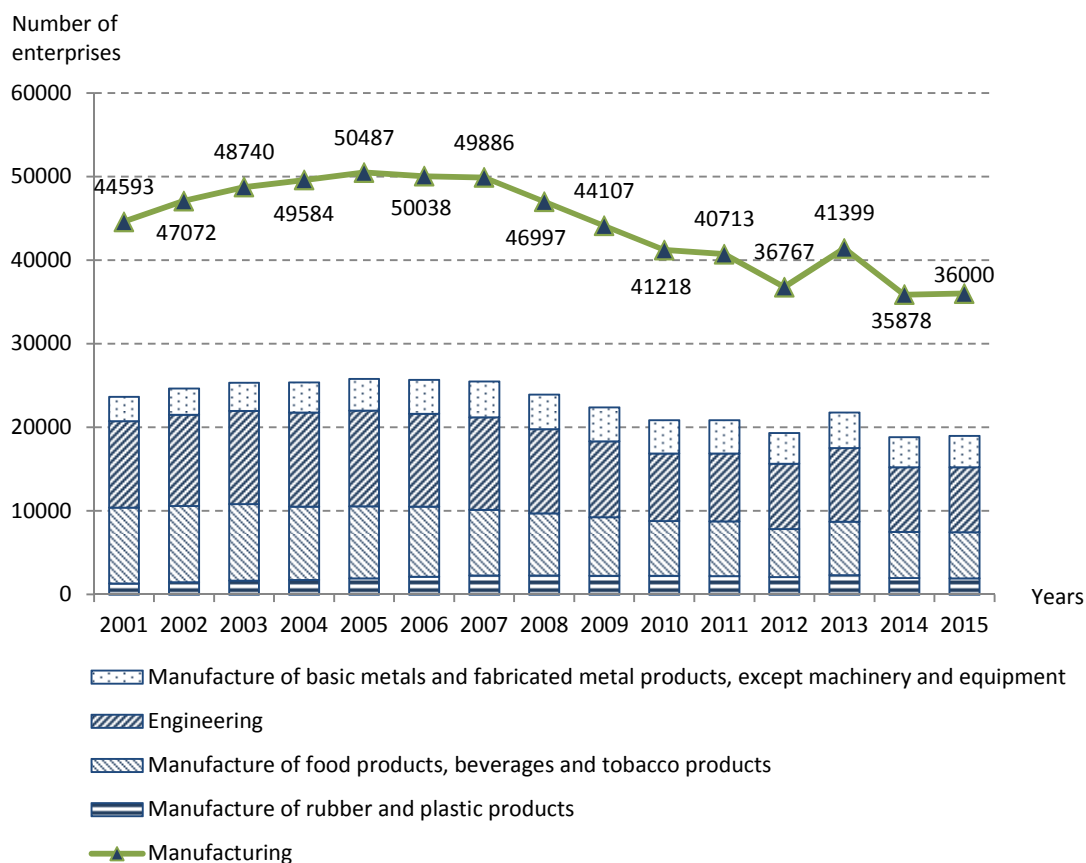

Fig. 3. Dynamics of the number of enterprises in the manufacturing industry by the largest types of industrial activity
Source: Author's

The results of calculating the rate of change in the number of businesses by selected industrial activities showed that two periods can be distinguished in the dynamics of the number of enterprises in almost all types of industrial activities. The first period — from 2001 to 2007 (for some industries, the period from 2001 to 2005) — is characterized by an increase in business activity and, in most cases, positive rates of increase in the number of businesses. The second period — from 2008 to 2015 (or from 2006 to 2015) — is characterized by a decline in business activity, a decrease in the number of enterprises, and negative rates of change in almost all industries. The largest decrease was recorded in 2014, which is partly due to excluding the data on the Autonomous Republic of Crimea from the calculation. However, the total number of enterprises of various industries in the AR of Crimea did not exceed 3 % of the total number of enterprises in the country, while the fall reached 9-14 %, i.e., it was significantly higher than the objectively conditioned.

The analysis of the calculated values of the Student's criterion confirms the significant fluctuations in the number of businesses during the two periods under consideration. To determine the current stage of the development of the industries, the rates of change in relation to the reference year of 2001 were used. The results of the calculations showed that only three industries (non-energy mineral extraction, production of rubber and plastic products, and manufacture of basic metals) are in the growth stage by the number of businesses. At the same time, Ukrainian industry, as a whole, is in the maturity phase (although it displays negative dynamics) while the manufacturing industry, in particular high-tech engineering, is in the decline

phase. Thus, it once again confirmed the need to take measures for the reconstruction and revival of national industry.

It should be noted that since at the beginning of the second period in the industries whose phase was identified as "maturity", a decrease in the number of businesses was observed, this phase is closer to "overmaturity", i.e., it results from negative dynamics.

The preliminary analysis of the dynamics of employment in the industries based on the data on the number of staff in 2001-2015 showed a steady decline in employment rates in all types of industrial activities in favor of service industries, as shown in Figure 4.
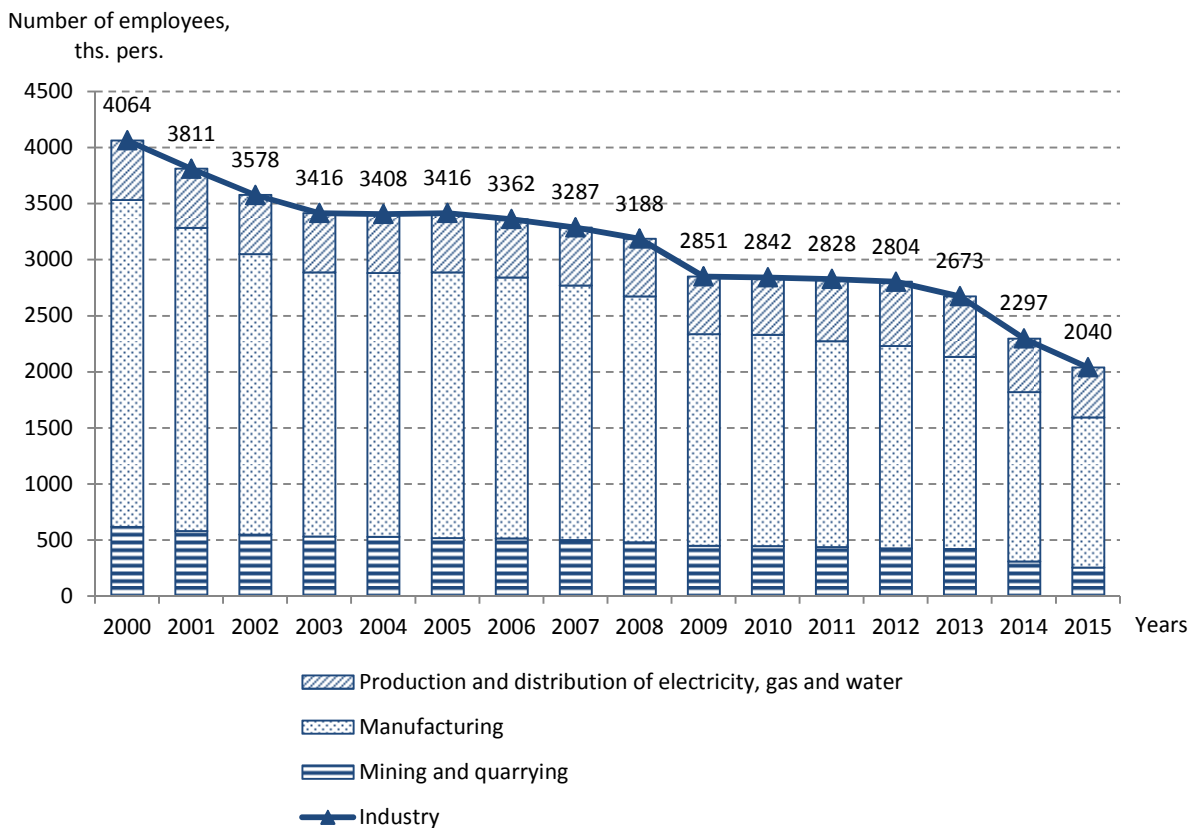
Fig. 4. Dynamics of the average number of staff in Ukrainian industry
Source: Author's

The analysis performed of the chain rates of change in the number of employees by industry showed that the total trend in all sectors of the economy is determined by the negative rate of change in employment, while no rate that is significantly greater than zero was observed throughout the period under study. The only exception is wood processing; the pulp and paper industry, and publishing; the manufacture of rubber and plastic products and the manufacture of basic metals in the periods from 2003 to 2007 and from 2010 to 2011.

The results of the assessment of the rate of change in relation to the reference year of 2001 make it possible to state that all industries are in the phase of decline.

To analyse the stage of development of industries by volume of production, data was used regarding the production volumes of certain key homogeneous types of industrial products in physical terms for 2003-2006. A preliminary analysis of the data concerning such groups of products as finished steel, mineral fertilizers, sugar, etc., starting from1990, showed that in almost all industries there was a sharp decline in production in the period 1990-1996, even the production of oil decreased by 40 % over the 5 years. Thus, it should be noted that since 1995-1996, the manufacturing of most products has reached a new equilibrium level after the crisis and a new, shorter, life cycle has begun. In the cycle, there is no period of introduction, and the growth rate was not high. To determine the current stage of development of industries, the data regarding the period from 2003 to 2016 were used.

Chain rates of change in the volume of production suggest the presence of different stable and unstable trends in the development of industries. The most positive changes were observed in 2011, which is due to a gradual decrease in the impact of the global financial crisis of 2008-2009. Only one of the considered positions — the manufacture of synthetic dyes — demonstrated a positive growth rate throughout the whole period. A decline in the production volume of oil and sugar was also observed in 2013 and 2015. As evidenced by the data obtained as a result of calculating the Student's criterion, the growth rate was significantly greater than zero for most product positions. At the same time, in 2013-2014, the situation changed to the opposite, and the rate of change was significantly smaller than zero.

The basic rates of change in the production volumes in 2016 as compared to 2003 were used to assess the stage of development of the industries. The aggregation of the rate of change was carried out using the weighted average for all product positions that relate to a particular type of industrial activity:

$$\tau_i^a = \sum_{j \in J_i} w_{ji} \tau_j ,$$

where τ_i^a is the aggregate rate of change for industry i;
   j is the product position,
   J_i is the set of product positions that are relevant to industry i;
   w_{ji} is the weight coefficient, which is equal to the normalised value of the correlation coefficient of the rate of change in the production volume of product of type j and the index of industrial production in industry i;
   τ_j is the rate of change in the production volume of product j.

The results of calculating the aggregate rates of change in the production volume of industries and the assessment of the stage of the industries' development showed that national industry in general and mining and manufacturing in particular are in the stage of maturity. This is due to the aggregation and mutual compensation in the rate of change in various types of industrial activity.

Only two industries — the manufacture of food products, beverages and tobacco products, and the manufacture of wood products and paper — are in the growth stage. Among mining industries, extraction of energy minerals is in the decline phase, primarily due to the loss of capacity in some districts of the Donetsk and Luhansk regions. The manufacture of coke and refined petroleum products, of chemicals, and engineering are in the decline phase as well. The significant decrease in the production volume in most positions of the engineering industry has had a considerable negative impact, since it is a high-tech one and should be among the industries of the real sector in the post- and neo-industrial economy. The positive trend is that the manufacture of electrical, electronic and optical equipment is in the stage of maturity, mainly due to a significant increase in the production volume of measuring equipment in recent years, mainly for the needs of housing and communal services. However, in most product positions of this type of engineering, there are also negative trends towards decline.

Investments in fixed assets, as a rule, differ considerably from the stages of the life cycle of an industry. For the analysis of investment processes, indices of investment in fixed assets were used, which made it possible to eliminate inflationary effects.

The calculations based on the Student's criterion show that in 2007 and from 2011 to 2012 investments significantly increased, while in 2014-2015, to the contrary, a significant decrease in the volume of investments in all industries was observed. At the same time, the growth of investments for the whole of the period under study was also significant.

It has been determined that a vast majority of industries are in the growth stage, with the exception of the manufacture of coke and refined petroleum products, whose stage of development is identified as decline. The data on the degree of depreciation of fixed assets contradict this conclusion, since throughout the period under study, the degree of depreciation was constantly increasing, or remained unchanged in all industries. The only exception is the metallurgical industry and the mining of metal ores. However, this is the result of the exclusion from the calculations of a part of the businesses which use considerably obsolete technologies that are located in the Donetsk and Luhansk regions. This indicates the ineffectiveness of investment in fixed assets, which is carried out only to replace the retired or completely operationally unserviceable assets. Thus, the application

of this criterion to determine the stages of development of the Ukrainian industries is currently inexpedient, since it does not make it possible to make an objective assessment.

The analysis of the innovation component of Ukrainian industries was carried out in terms of the number of enterprises engaging innovation activity, the volumes of innovation products sold, incl. outside Ukraine, and expenditure on innovation activity. Since, starting from 2015, the data on their innovational activity include only the results of businesses with the number of employees totaling not less than 50 persons, direct comparison with the previous years is incorrect. Therefore, to identify the trends, the data for 2005-2014 were used.

In general, during 2005-2014, the number of industrial enterprises engaging innovation activity had a weak growth trend (Fig. 5), but in the high-tech chemical industry, there was a slowdown in the innovational activity of businesses. A sharp decline (from 38 % to 28.6 %) occurred in the manufacture of coke and refined petroleum products.
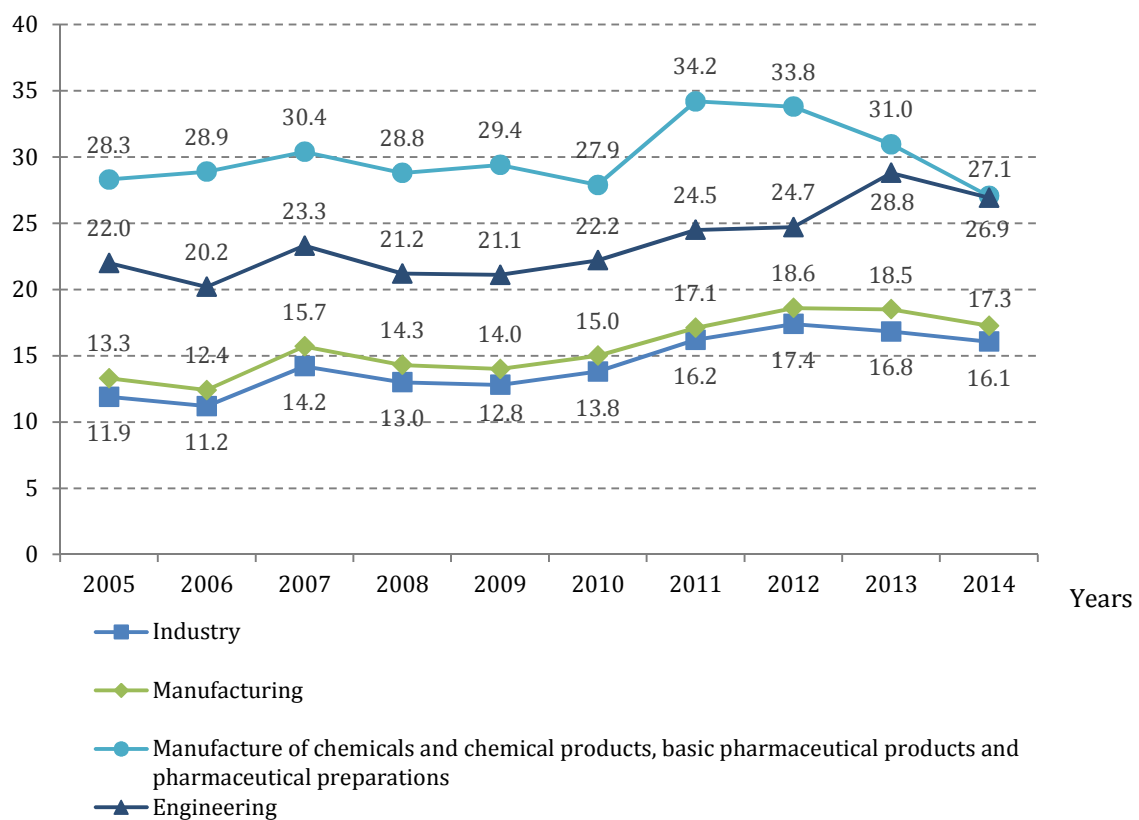
Fig. 5. Dynamics of the share of businesses engaging in innovational activity by separate types of industrial activity
Source: Author's

A positive trend is the increase in innovational activity of engineering enterprises from 22 % in 2005 to 26.9 % in 2014.

The analysis of the correlation interactions showed a close connection between the innovational activity of engineering enterprises and businesses in the chemical industry (0.81), the manufacture of plastics (0.74) and the manufacture of food products (0.86). The interaction among the rest of the industries is medium, with the exception of the manufacture of furniture and other products, the correlation with which is absent (0.08). Thus, we can assume that intensification of innovational activity in one industry can contribute to an increase in the share of innovational activity of businesses in other industries.

In general, in terms of the number of innovation-active businesses, the vast majority of industries are in the maturity phase, with the exception of the manufacture of coke and refined petroleum products, which is in decline.

In order to identify the trends and significance of changes in the innovational activity of enterprises in various industries, an estimation of the difference in the average values for the two sub-periods using the Student's criterion was carried out.

In terms of the share of volumes of realised innovative products in the total volume of sales, both for Ukrainian industry as a whole and for most of its individual industries, a significant decrease was observed. Critical changes in the dynamics of the volumes of innovative products took place in 2008-2010. In this case, the indicator decreased almost 2 times across the industries, except the manufacture of chemical and pharmaceutical products, where the volume decreased 5 times.

Similarly, the share of innovative products sold abroad in the production volume of most industries declined considerably. The period 2013-2014 appeared to be critical, which is largely due to the loss of traditional product markets in Russia and the CIS countries.

Testing the hypotheses about change in the stages of development showed that a change in the stage from maturity to decline took place in the mining industry and most manufacturing industries. Only in several industries, such as the manufacture of textiles, the manufacture of coke and refined petroleum products, and non-specific engineering, such changes were not observed, which allows the determination of their stage of development as maturity. But the dynamics of the volume of innovative products is very volatile in these industries, which creates the risk of transition to the phase of decline.

The financing of innovational activity also had some unstable dynamics during 2005-2014. To carry out the analysis and exclude inflationary effects, the data on the amount of financing were deflated using producer price indices. The dynamics of the expenditure on innovational activity is shown in Figure 6.
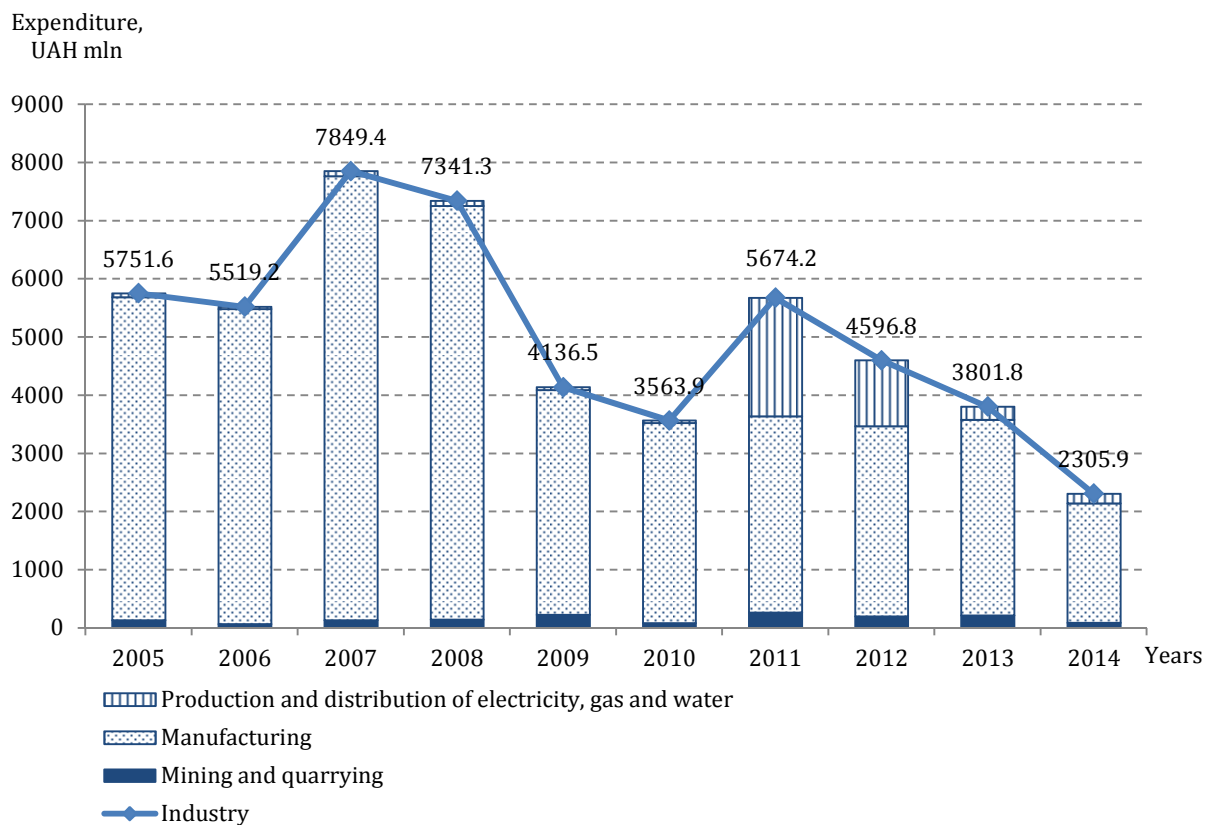

Fig. 6. Dynamics of the expenditure on innovational activity in Ukrainian industry
Source: Author's

As can be seen, manufacturing industry faced a reduction in expenditure on innovational activity. A burst of financing was observed only in the supply of electricity, gas, water, etc. in 2011-2012.

A detailed analysis of the rate of change in expenditure on innovational activity shows that the stage of development of the national industry in general and the manufacturing industry in particular is characterised as decline. The mining and quarrying industry, the manufacture of food, and the manufacture of textiles are in the stage of maturity. Two manufacturing industries — the manufacture of wood and the products of wood, and manufacture of furniture are in the stage of growth, as the expenditure on innovational activity has increased significantly.

The generalised results of the identification of the stage of the industries' development by all the applied criteria are shown in Table 3.

Table 3. Identification of the stages of the industries' development based on the system of criteria

Type of industrial activities	Criteria						Generalised stage
	Number of businesses	Number of employees	Volume of production of key products	Innovation-active enterprises	Volume of sales of innovative products	Financing of innovation activity	
1	2	3	4	6	7	8	9
Industry	maturity	*decline*	maturity	maturity	maturity	*decline*	risk of decline
Mining and manufacturing	maturity	*decline*	maturity	maturity	maturity	maturity	risk of decline
Mining and quarrying	**growth**	*decline*	*decline*	maturity	maturity	maturity	risk of decline
Extraction of fuel and energy minerals	*decline*	*decline*	*decline*	maturity	maturity	maturity	risk of decline
Extraction of minerals, except fuel and energy	**growth**	*decline*	maturity	maturity	maturity	maturity	risk of decline
Manufacturing	*decline*	*decline*	maturity	maturity	maturity	*decline*	decline
Manufacture of food products, beverages and tobacco products	*decline*	*decline*	**growth**	maturity	*decline*	maturity	risk of decline
Manufacture of textiles, wearing apparel, leather, leather products and other materials	*decline*	*decline*	maturity	maturity	maturity	maturity	risk of decline
Manufacture of leather, leather products and other materials	*decline*	*decline*	**growth**	maturity	maturity	maturity	risk of decline
Manufacture of wood and of products of wood and cork, except furniture	*decline*	*decline*	*decline*	maturity	*decline*	**growth**	decline
Pulp and paper production, publishing activities	*decline*	*decline*	maturity	maturity	*decline*	**growth**	risk of decline
Manufacture of coke and refined petroleum products	*decline*	*decline*	maturity	*decline*	maturity	*decline*	decline
Manufacture of chemicals and chemical products	*maturity*	*decline*	*decline*	maturity	*decline*	*decline*	decline
Manufacture of rubber and plastic products	**growth**	*decline*	maturity	maturity	*decline*	*decline*	risk of decline

Type of industrial	Criteria						Generalised
1	2	3	4	6	7	8	9
Manufacture of other non-metallic mineral products	maturity	*decline*	—	maturity	maturity	**growth**	risk of decline
Manufacture of basic metals, fabricated metal products, except machinery and equipment	**growth**	*decline*	maturity	maturity	*decline*	*decline*	risk of decline
Engineering	*decline*	*decline*	*decline*	maturity	*decline*	*decline*	decline
Manufacture of computer, electronic and optical products	*decline*	*decline*	*decline*	maturity	*decline*	*decline*	decline
Manufacture of machinery and equipment not elsewhere classified	*decline*	*decline*	maturity	**growth**	maturity	*decline*	risk of decline
Manufacture of vehicles	*decline*	*decline*	*decline*	maturity	*decline*	*decline*	decline
Supply of electricity, gas, steam and air conditioning	maturity	*decline*	*decline*	**growth**	maturity	**growth**	risk of decline

Note. * The investment component is excluded from the final calculation due to the inadequacy of identifying the development stages of the industries.

Source: Author's

Summary and conclusions

The results of the assessment of the development stages demonstrate that almost all industries have passed the maturity phase and are on the verge of maturity and decline, or are already in the phase of decline, both by the majority of volumetric criteria and by innovation criteria.

The presence of a certain potential for innovational development is confirmed by the fact that in terms of the innovational criteria the industries that specialise in the manufacturing of wood and the products of wood are in the phase of growth. In some engineering industries (the manufacture of machinery and equipment not elsewhere classified), there are positive growth trends in the innovational activity of businesses. In general, the chemical and engineering industries, which have the highest level of technological development, are in the decline phase.

Thus, the trends revealed in the development of the national industry as a whole and the identification of the stages of development of individual industries makes it possible to draw a conclusion on the low level of efficiency of the Ukrainian economy, which is the result of long de-industrialization and the transition of most industries to the phase of decline. The reconstruction of industry should be aimed at technological upgrading, the activation of innovational activity, the stimulation of employment by attracting investment to create high-tech industries and fundamentally upgrade the existing ones.

References

[1] V.Ye. Khaustova, Industrial policy in Ukraine: formation and forecasting: monograph, Kharkiv, 2015.
[2] K. Warwick, Beyond Industrial Policy: Emerging Issues and New Trends // OECD Science, Technology and Industry Policy Papers, 2, OECD Publishing, Paris, 2013, 57. http://dx.doi.org/10.1787/5k4869clw0xp-en [01.12.2017]
[3] A.V. Novickaya, Strategic alternatives of the organization development on the view of the stage of the life cycle of the market, Vestnik Universiteta, State University of Management, 11 (2012) 126-131.
[4] O. Y. Lotysh, Features strategic analysis of sector, Efficient economy: Electronic scientific professional edition, 2016, 11: http://www.economy.nayka.com.ua/?op=1&z=5258 [12.12.2017]
[5] O.I. Matiushenko, Enterprise Life Cycle: Essence, Models, Estimation, The Problems of Economy, 4 (2010) 82-91.

[6] S.M. Smirnova, Assessment of the stage of industrial cluster development: modeling approaches, Materials of the scientific-practical conference "The role of business in the transformation of Russian society. Economic and Applied Problems of System Management: Current Trends", 2014, pp. 214-218.

[7] N.S. Rychihina, Analysis of stages of «life cycle» of development textile branch of the Ivanovo region (Russia), Economics and banks 2 (2013) 88-96.

[8] N.S. Rychihina, The analysis of life cycle and processes of spontaneous restructuring of machine-building industry in the region, Regional economics: theory and practice 365 (2014) 10-21.

[9] A. Bonaccorsi, P. Giuru, Industry life cycle and the evolution of an industry network, Laboratory of Economic and Management Sant'Anna School of Advanced Studies, Working Paper Series, 2000, 4, 46 http://www.lem.sssup.it/WPLem/files/2000-04.pdf [20.12.2017]

[10] A. Sabol, M. Šander, D. Fučkan, The concept of industry life cycle and development of business strategies, International conference "Active Citizenship by Management, Knowledge Management & Innovation Knowledge and Learning", Zadar, 2013, pp. 635-642.

[11] J. Krafft, J.-L. Ravix, The firm and its governance along the industry life cycle, In: B. Laperche, D. Uzunidis (Eds.), Powerful Finance and Innovation Trends in High-Risk Economy, Palgrave MacMillan, London, 2008. pp. 131-148. https://hal.archives-ouvertes.fr/hal-00211206 [20.12.2017]

[12] L.S. Valinurova, N.A. Kuz'minyh, Assessment of the level of innovative development of industries, Innovations 104 (2007) 42-47.

[13] S.G. Kuznetsov, Allocation of Industry Cycles in the Forest Sector of Russia Using the Principle of Innovation Exhaustion, Science prospects 68 (2015) 93-96.

[14] L.V. Strelkova, S.S. Kabanov, Technological development of industry branches: assessment and prospects, Vestnik of Lobachevsky State University of Nizhni Novgorod 2 (2012) 247-251.

[15] M. Sanders, J. Bos, C. Economidou, R&D over the life cycle, Tjalling C. Koopmans Research Institute Discussion Paper Series, 26 (2007) 07-18. http://www.koopmansinstitute.uu.nl [04.01.2018]

[16] O. Skotarenko, L. Babkina, Choice of strategies for changing the stages of the life cycle of points of economic growth in the regions of the Russian Federation, Risk: Resources, Information, Supply, Competition 3 (2013) 124-128.

[17] O.S. Kozlova, The impact of the regional phases of the oil extraction life cycle on the duration of the sector's life cycle, Bulletin of Baikal State University 27 (2017) 27-31.

[18] E.V. Krasil'nikova, Economic-mathematical modeling of transition to a stage of rapid growth and evaluation of micro and mezo-factors, Electronic scientific and practical journal "Synergy" 6 (2016) 54-60.

[19] S. Tavassoli, Innovation Determinants over Industry Life Cycle. Department of Industrial Economics, Blekinge Institute of Technology, Center for Strategic Innovation Research Electronic Working paper Series, Karlskrona, Sweden 11 (2012) 34.

[20] T. Grebel, L. Krafft, P.P. Saviotti, On the life cycle of knowledge intensive sectors, Revue de l'OFCE, Presses de Sciences Po, special issue (2006) 63-85. https://hal.archives-ouvertes.fr/hal-00203585 [04.01.2018]

[21] M. van Dijk, Industry life cycle in Dutch manufacturing, Working paper, UNU-MERIT Research Memoranda, Maastricht 14 (1998) 34. http://citeseerx.ist.psu.edu/viewdoc/download?doi=10.1.1.199.5305&rep=rep1&type=pdf [04.01.2018]

[22] M.D. Madvar, H. Khosropour, A. Khosravanian, M. Mirafshar et. al. Patent-based technology life cycle analysis: the case of the petroleum industry, Foresight and STI governance 10 (2016) 72-79. DOI: 10.17323/1995-459X.2016.4.72.79

[23] State Statistics Service of Ukraine. Official Site: www.ukrstat.gov.ua [20.02.2018]

[24] Industry of Ukraine in 2007-2010. Statistical Publication. State Statistics Service of Ukraine, Kyiv, 2011.

[25] Industry of Ukraine in 2011-2015. Statistical Publication. State Statistics Service of Ukraine, Kyiv, 2016.

[26] Statistical Yearbook 2007. Statistical Publication. State Statistics Service of Ukraine, Kyiv, 2008.

[27] Statistical Yearbook 2010. Statistical Publication. State Statistics Service of Ukraine, Kyiv, 2011.

Katarzyna Król, Alicja Ponder, Magdalena Gantner
Faculty of Human Nutrition and Consumer Sciences, Department of Functional Food, Ecological Food and Commodities, Warsaw University Life of Sciences
ul. Nowoursynowska 159c, 02-776 Warsaw, Poland, katarzyna_krol@sggw.pl

THE EFFECT OF SUGAR SUBSTITUTES ON SELECTED CHARACTERISTICS OF SHORTCRUST PASTRY

Abstract
The aim of this study was to evaluate the possibility of substituting sugar in crust pastry with natural substitutes, such as stevia, xylitol, coconut sugar as well as dried banana. Furthermore, a comparison of physicochemical properties was carried out. The crust pastry obtained was analyzed in terms of color by CIEL*a*b*, textures, water activity, bake loss, semi-consumer assessments and the nutritional value was calculated. There was a clear impact caused by the sugar substitute on the physicochemical properties and their sensory assessment. The cakes with xylitol had the closest color, smell and taste to the control sample (with sucrose). The cakes with dried banana had a significantly reduced hardness compared to the control sample. The lowest bake loss was observed in the case of pastry with dried banana, while the highest was in the case of xylitol. In sensory analysis, the "Just-about-right" method was used, and pastries with a sweeter taste were more desirable (xylitol) and pastry with the stevia substitute showed the lowest desirability. The lowest energy value per 100 g was obtained for stevia (392 kcal/ 100g), while for xylitol energy, the value was reduced by 6%.

Key words
Xylitol, stevia, dried banana, coconut sugar, crust pastry

Introduction
Sugar, which is currently consumed by society in increasing quantities, is a substance that causes many diseases, known as civilization diseases, such as obesity, diabetes, hypertension and coronary heart disease [1]. However, Sucrose in bakery products makes a major contribution to providing sweetness, controlling moisture retention, influencing air incorporation, stabilizing air bubbles, and limiting the swelling of starch during baking, all of which help to create a finer texture [2].

The baking industry is currently witnessing a situation in which the labeling claims of products, like sugar free, reduced calorie, gluten-free and fibre rich, are attracting health-conscious consumers. Consumers are becoming more and more aware of this, and out of concern for their own health, often choose healthier products. Due to this, the food industry, over the last several years, has been investigating ways to reduce the levels of free sugars within their products to comply with guidelines and regulations, such as those of the World Health Organization, which has made a strong recommendation to reduce the level of sugar in the diet to less than 10%, and preferably as low as 5% [3, 4]. It is important to find alternative sugar replacers for traditional sugars in order to improve the quality of low-sugar pastry products. The energy content of sweet bakery products may be appropriately reduced by substituting sucrose with non-nutritive, naturally occurring (further denoted as natural) or artificial high-intensity sweeteners. Sweeteners can be classified according to the following criteria:
- Origin (natural or artificial),
- Consistency (powders/syrups),
- Energy value (nutritive or non-nutritive),
- Technological function (bulking agent or sweeteners).

Stevia is a glycoside isolated from the plant *Stevia Rebaudiana Bertoni* [5]. Stevioside can be isolated from dried leaves and is approximately 300-400 times sweeter than sucrose, however the bitterness that presents as an aftertaste affects the sensory quality of the final product [6]. Some studies have suggested that stevia increases insulin sensitivity and glucose tolerance in human cells and safety issues concerning stevia showed no negative side effects. Furthermore, stevia glycosides were recently approved for use as a sweetener by the

Joint Food and Agriculture Organization/World Organization Expert Committee on Food Additives and ADI is 4 mg/kg day [7].

Xylitol is a sugar alcohol obtained by replacing an aldehyde group with a hydroxyl group. Xylitol is the sweetest of the polyols, being equivalent to sucrose in sweetness, but with fewer calories, and lower glycemic index [8, 9]. The most common application of xylitol is in chewing gum, because it is very convenient due to its sensory properties. It is also used in candies, gelatins, chocolate, yogurt, and a wide range of confectionery products. Furthermore, xylitol dissolves in the mouth to give a pleasant sensation of cooling and freshness after consumption [10].

Coconut sugar has been used as a traditional sweetener in Asia and is now gaining popularity because of its natural and minimal processes. A recent work has stated that the GI of coconut sap sugar was reported to be in the low category (35-45) [11]. The main component of coconut sugar is sucrose (about 70-80%) combined with glucose (3-9%) and fructose (3-9%). Palm sugar is produced from filtered juice, which is heated for several hours at a temperature of about 100°C until concentration and a typical aroma is obtained. The Maillard reaction and caramelization occur during the processing of palm sugar [12].

Dried bananas can be used as substitute for sugar, because of its sweet taste. Mostly, dried banana consists of simple sugars as well as dietary fibre (starch) (6.4g / 100g). Dried bananas contain about 4 times more potassium, calcium, phosphorus and magnesium and other minerals than the fresh ones. Their energy value is 97kcal / 100g [13].

However, the decrease in the sucrose content is accompanied by significant changes in texture, volume, colour, taste, hardness, surface finish and shelf life of the product. These changes may negatively influence product acceptability and also affect processing properties of doughs or batters. Furthermore, sugar substitutes have high sweetness intensity but it does not support texture characteristics [14]. Non-caloric sweeteners does not participate in Maillard reaction or caramelization resulting in lighter color after baking. Furthermore, sugar alcohol have lower humectancy and do not retain a moistness compared to sugar [15].There are many published studies that show reduced sucrose products to be less acceptable than their full-sucrose counterparts [15, 16, 17, 18].

The objective aim of this study was to investigate the possibility of replacing sugar with different natural sweeteners in making short crust pasty. For this purpose, four different substitutes were used (stevia, xylitol, coconut sugar, dried bananas). Then, the physical and sensory properties of cakes were evaluated.

Materials and methods

The material was short crust pastry. As the basic ingredients 200 g flour (type 450), 30 g egg yolk, 120 g butter (83% of fat) and 2 g salt were used for every type of cake. In the cake with xylitol and coconut sugar formulation, 60 g was used, with stevia 0,2 g, with dried banana 70 g. The control sample was made using saccharose (60g) as a sweetener. Then, all ingredients were mixed in mixer (Kenwood Major Classic) for a 5 min and then covered in plastic wrap and refrigerate the dough for 30 min. After that was baked in a convection oven (Kuppersbusch 10xGN1/1/) 180˚C for 30 min. Each of the prepared samples weighed 170 g and were baked in silicone mold with 20 cm diameter and were prepared in 8 replications. The samples were cooled at room temperature for 10 minutes, covered by cellophane and finally kept at an ambient temperature, in a dry and dark place, until they were analyzed. For sensory evaluation the samples were prepared one day before of each trial.

Water activity (a_w) was measured at 20 ± 2°C on 2 replicates for each sample with a dew point hygrometer Aqualab® series 3 TEV (Decagon Devices Inc., Pullman, WA., U.S.A. The bake loss of pastry was calculated by weighing one piece before and after baking. The difference in weight was averaged and reported as a percentage bake loss.

The instrumental measurement of the colour of the pastry was performed in the L*a*b* color system, where L* – lightness, a* – the colour axis ranging from greenness (-a*) to redness (+a*), b* – colour axis ranging from blueness (-b*) to yellowness (+b*). The colour was measured by a Minolta chromameter (CR-400, Konica Minolta Inc., Tokyo, Japan). The chromameter was calibrated using a white standard plate

($L* = 98.45$, $a* = −0.10$, $b* = −0.13$). A measuring head with a diameter of 8mm and a D65 illuminant was used. The determination of colour parameters was performed by randomly measuring 10 different places on each surface. The total colour change (ΔE) is a measure of the difference between the control sample and a tested sample and was calculated using the following equation: ($\Delta E* = [(L_1*-L_2*)^2 + (a_1*-a_2*)^2 + (b_1*-b_2*)^2]^{1/2}$).

For measuring the textural properties of cakes, an Instron universal testing machine (Model 5965, Instron, Canton, MA, USA) with Bluehill®2 software was used, which included a compression test. The compression test was carried out using a flat probe. A sample deformation was limited to 50% for all the determined parameters. This deformation percentage was found to be sufficient to break a crusty pastry. The test was conducted 6 times, where one speed test (10 mm/min) was applied. The force curve (N) versus distance (mm) allows the hardness to be calculated. The hardness of the short crust pastry was designated as the maximum compression force (N). Ten replicates of each formulation were conducted.

In the sensory evaluation of the pastry, the "Just About Right" (JAR) method was used and 39 (28 female, 11 male) participants were invited to semi-consumer analysis. For each sample, participants were asked to rate their overall liking and attribute intensity. The attributes assessed included: hardness, colour, odour, crispness, sweet flavour and metallic aftertaste. "Just-about-right" (JAR) scales were designed as continuous line scales (-4 to 4) with three descriptive anchors, low intensity ("Much Too Weak") on the left end, ("Just About Right") at the centre, and high intensity ("Much Too Strong") on the right end. Samples were served in a sequential order, with a minimum two-minute mandatory break between each sample. Participants rinsed with filtered water between samples to reduce potential carry-over effects.

The caloric value of pastry was calculated on the basis of the information on the packaging (fat 9 kcal/1 g, protein, carbohydrate, saccharose, dried banana, coconut sugar 4 kcal/1g, stevia 0,2 kcal/1 g). At the beginning, the energy value of the whole product was obtained, and then it was converted into 100g of product and per portion of product, which was taken as 30g.

Statistical analysis: all experiments were carried out in triplicate and average values with standard deviation were calculated. The statistical differences were checked using the one-way ANOVA method and Tukey's post-hoc test (at a significance level α=0.05). P-values lower than 0.05 were considered statistically significant and homogenous groups were noted with the same letters in tables. Analyses were conducted using Statistica Software version 12.0 (StatStoft, Tulsa, USA).

Results and discussion
The physical properties (water activity, bake loss, colour parameters and hardness) of four types of pastry are shown in Table 1. Results showed that there was significant difference ($p < 0.05$) between each sample in terms of a_w, bake loss, L*, a *, b*, ΔE* and hardness.

Water activity is an important indicator for product design, shelf-life and food safety. If a product is kept below a certain water activity, then it is possible to inhibit the growth of fungi/bacteria/mold, thus the shelf-life is longer. In the case of the a_w sample with xylitol (0.67), it was characterized by a lower level and other samples were in a homogeneous group and varied from 0.70 to 0.76. Water activity in the range 0.55-0.9 is considered as medium water activity, and bacteria usually require at least 0.91 and fungi at least 0.71. All of our samples are in this group and the growth of bacteria is inhibited. Furthermore, xylitol is more hygroscopic than sucrose, therefore, it seems reasonable that partial or complete elimination of sucrose led to a reduction in the water activity of dietetic pastry [14]. However in our study polyols showed a lower water activity than sample with saccharose, what is not in consistent with studied conducted by Majeed et al. (2018) [22], but is in close agreement with study conducted by Nourmohammadi and Peighambardoust (2016) [15]. Investigated by Winkelhausen et al. (2007) [19], xylitol improved microbial stability and shelf-life of cakes as it provided lower water activity at the same concentration with sucrose, which was confirmed with obtained results In our study.

Table 1. Physical properties of short crust pastry obtained from different sweeteners (coconut sugar, dried banana, xylitol, stevia and saccharose).

	Coconut sugar	Dried banana	Xylitol	Stevia	Control sample
a_w	0.73	0.70	0.67	0.71	0.76
Bake loss (%)	17.01 ± 0.34[b]	16.21 ± 0.21[b]	20.21± 0.11[c]	20.23 ± 0.20[c]	14.21 ± 0.12[a]
L*	42.43 ± 0.20[a]	46.23 ± 0.04[a]	68.24 ± 0.14[bc]	70.54 ± 0.11[c]	63.03 ± 0.26[b]
a*	12.5 ± 0.12[c]	8.62 ± 0.12[b]	10.22 ± 0.16[c]	4.92 ± 0.03[a]	11.04 ± 0.03[c]
b*	25.70 ± 0.08[a]	35.82 ± 0.22[b]	37.26 ± 0.03[b]	34.80 ± 0.07[b]	35.54 ± 0.24[b]
ΔE*	20.72 ± 1.21[b]	3.54 ± 0.18[a]	3.32 ± 0.19[a]	3.01 ± 0.03[a]	-
Hardness (N)	15.02 ± 1.32[b]	6.69 ± 0.95[a]	25.04 ± 0.46[c]	6.94 ± 0.54[a]	13.52 ± 0.59[b]

Values are expressed with the standard deviation. Lowercase letters in rows (a-c) show between which samples were statistical differences ($p < 0.05$).

Source: Author's

The bake loss of pastry was the smallest and similar for the control sample, coconut sugar and dried banana, while the highest was for xylitol and stevia. Dried banana have a higher water holding capacity compared to sweeteners, due to its higher protein content [13]. Proteins would increase water holding capacity, thus enhancing the swelling ability, an important function of protein in preparation of viscous foods such as soups, dough and baked products [24]. Similar results was obtained by Akesowan (2009) [25] bake loss was increased compared to control sample with saccharose.

The colour values measured by a colorimeter showed that L* was the smallest for coconut sugar and the highest for stevia. The lightness (L*) of short crust pastry displayed an increasing trend along with the increasing substitution level of sugar (stevia and xylitol). For a* coordinate (redness) the highest was coconut and the control sample, the smallest for samples with sweeteners. For b* coordinate (yellowness) only the sample with coconut sugar showed a lower value of b*, other samples are in a homogeneous group. The darker colour of pastry from coconut sugar and dried banana is correlated with the initial darker colour of the product. Furthermore, some authors have suggested that the darker color of the pastry is related to higher protein as well as sugar content, and thus a more intense Maillard reaction (browning and caramelization of sugar is considered to produce brown pigments during baking) [13]. Furthermore, it is believed that sugar alcohols (xylitol) and stevia are not able to participate (thermal stability) in the Maillard reaction due to the lack of functional groups [14]. This is in keeping with the findings of Martínez-Cervera et al. (2011) [25], which showed the addition of erythritol in muffins appeared not to influence the crust color. Furthermore, Gao et al. (2017) [21] also reported increase of L* value in muffins with stevia as a sweetener, what is in close agreement with obtained results.

The results of the hardness showed that pastry made with dried banana and stevia decreased significantly at the 55-56% level compared to the control sample and increase in the case of the sample made with coconut sugar and xylitol at 10%-84% level. According to Nourmohammadi and Peighambardoust [13] the investigated correlation between water activity and hardness (the higher the water activity, the higher the crumb firmness) was also obtained from this study. Other studies showed that replacing sugar with polyoils may effect on decrease of hardness and firmness of cakes compare to control samples with saccharose [27].

Table 2. Evaluation of the nutritional composition of the short crust pastry obtained

	Coconut sugar	Dried banana	Xylitol	Stevia	Control sample
Energy (kcal)	448	450	427	392	452
Protein [g]	6.5	7.1	6.5	6.5	6.5
Carbohydrates [g]	50	52	49	36	51
Sugar [g]	13.5	0	0	0	15
Fat [g]	24	24	24	24	24
Fibre [g]	1.2	2.2	1.2	1.2	1.2

Source: Author's

The results of nutritional composition are shown in Table 2. The proximate values of sugar decreased with the increased level of sugar substitutes. The high energy values were the results of high fat content (24g/sample) which provide 9kcal/1 gram. The proximate values of energy and sugar were highest in the control sample, while the lowest was in the stevia sample, where the energy was reduced by 13% and carbohydrates by 30%.
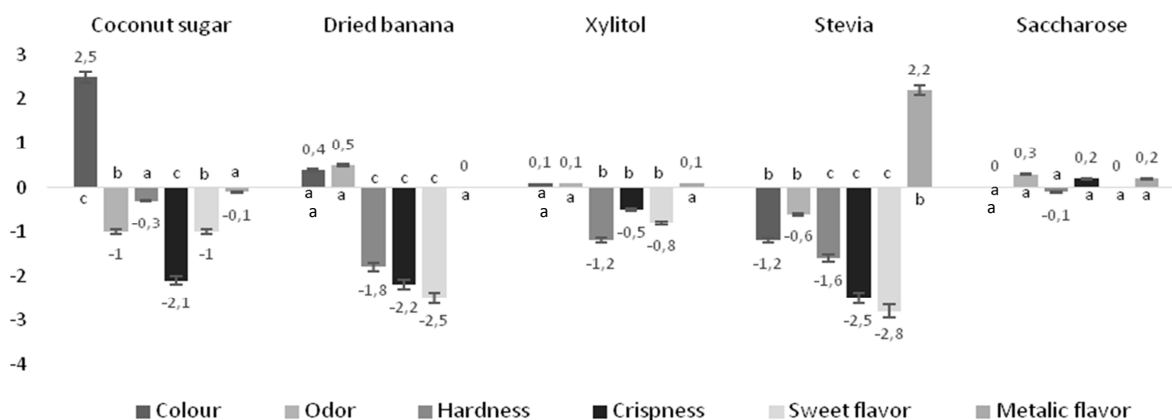

Fig. 1. The effect of the replacement of sugar with coconut sugar, dried banana, xylitol and stevia on the sensory characteristics of short crust pastry. Lowercase letters on figure (a-c) show between which samples were statistical differences (p <0.05).
Source: Author's

In the sample with dried banana, an increase of protein and fibre content was observed in the range between 8.5% and 90%, respectively. The lower content of sugar in the sample with coconut sugar is the result of minimal processing and a higher content of dietary fibre, especially inulin. These could play an important role in lowering the GI values of palm sugars when compared to refined sugarcane which contains almost 100% of sucrose [9, 15].

The sensory scores of short crust pastry with sugar substitutes are presented in Figure 1. The JAR scale was selected as it is designed to find the optimum/most appropriate level of a specific attribute and is easy for panelists to understand. According to the presented results, there was a significant difference between all investigates samples ($p < 0.05$). The largest deviations from the control sample were recorded for the sample with stevia, where colour, odour, hardness, crispness sweet flavor were "too weak"/"much too weak", while a metallic aftertaste was determined as "too strong". According to the sensory evaluation, stevia as a substitution in cakes resulted in the occurrence of a little bitterness which is attributed to the inherent bitterness of steviol glycosides [28]. Mean JAR rating for the colour of samples with dried banana and xylitol was similar to the control sample, while for coconut sugar the colour was "too strong". The smallest deviations from the standard were recorded for the xylitol sample, which revealed that short crust pastry with xylitol reformulation was found to be most acceptable by the panelist. To the best of our knowledge, this is the first work presenting JAR sensory analysis of short crust pastry, however, other studies with sugar replacements showed that, in sensory evaluation, samples with xylitol were the best substitute for the sugar contained in cakes [17, 19] and results are in close agreement with results obtained by Winkelhausen et al. [19].

Summary and conclusions

Sweeteners cannot solely replace sugar and the food industry, however it is important to find alternative sugar replacers for traditional sugars in order to improve the quality of low-sugar cakes. To summarise, sweeteners influenced the physicochemical (a_w, colour, hardness and bake loss) properties of short crust pastry. The caloric content of pastry with coconut sugar, dried banana, xylitol, stevia and sucralose are 448, 450, 427, 392, 452 kcal/100g, respectively (estimated by the raw materials used for each cake). Sugar alcohol such as xylitol, among the four tested substances, was found to be the best substitute and in the sensory evaluation score was similar to sugar-containing short crust pastry and physical properties (a_w, color coordinates) were comparable to control sample However, for wider acceptance of products with xylitol, consumers should be educated and learn more about the benefits of xylitol itself. However, further optimizing is required to obtain muffins with satisfactory textural properties and mouthfeel and an appealing appearance that would satisfy consumer preference.

References

[1] D. Włodarek, E. Lange, L. Kozłowska, D. Głąbska, Dietoterapia. Wydawnictwo Lekarskie PZWL, Warszawa 2014, 188, 252-253, 257, 259, 274, 282.

[2] Y.-H. Hui, W.-K. Nip, Sweeteners, In: W. Zhou, Y. H. Hui (Eds.), Bakery Products: Science and Technology, Wiley-Blackwell, Oxford, UK, 2006, pp. 137–160.

[3] World Health Organization (WHO) Guideline, Sugars Intake for Adults and Children, WHO, Geneva, 2015.

[4] D. Martyn, M. Darch, A. Roberts, H. Youl Lee, T. Tian, N. Kaburagi, P. Belmar, Low-/No-Calorie Sweeteners: A Review of Global Intakes. Nutrients 10 (2018) 357.

[5] A. Sclafani, M. Bahrani, S. Zukerman, K. Achroff. Stevia and saccharin preferences in rats and mice. Chem Senses 35 (2010) 433-443.

[6] US Food & Drugs Administration, Code of federal regulations title 21. Chapter I, Subchapter B, Washington, DC, 2012.

[7] S.D. Anton, C.K. Martin, H. Han, S. Coulon, W.T. Cefalu, P. Geiselman. Effects of stevia, aspartame, and sucrose on food intake, satiety, and postprandial glucose and insulin levels. Appetite 55 (2010) 37-43.

[8] T. Varzakas, A. Labropoulos, S. Anestis (Eds.), Sweeteners: Nutritional Aspects, Applications, and Production Technology, CRC Press, Boca Raton, 2012.

[9] R. Pulicharla, L. Lonappan, S.K. Brar, M. Verma, Production of renewable C5 platform chemicals and potential application, in: S.K. Brar S.J. Sarma, K. Pakshirajan (Eds.), Platform Chemical Biorefinery, Elsevier, Amsterdam, 2017, pp. 201-216.

[10] Y. Arcano, O. Garcia, D. Mandelli, W. Carvalho, L. Pontes, Xylitol: A review on the progress and challenges of its production by chemical route, Catalysis Today 8 (2018) DOI: 10.1016/j.cattod.2018.07.060.

[11] T.P. Trinidad, A.C. Mallillin, R.S. Sagum, R.R. Encabo, Glycemic index of commonly consumed carbohydrate foods in the Philippines, Journal of Functional Foods 2 (2010) 271-274.

[12] K. Srikaeo, R. Thongta, Effects of sugarcane, palm sugar, coconut sugar and sorbitol on starch digestibility and physicochemical properties of wheat-based foods, International Food Research Journal 22 (2015) 923-929.

[13] P.P. Subedi, K.B. Walsh, Assessments of sugar and starch in intact banana and mango fruit by SWNIR spectroscopy, Postharvest Biology and Technology 62 (2011) 238-245.

[14] A.M. Abdel-Salam, A.S. Ammar, W.K. Galal, Evaluation and properties of formulated low calories functional yoghurt cake, Journal of Food, Agriculture & Environment 2 (2009) 218–221.

[15] E. Nourmohammadi, S. Peighambardoust, New Concept in Reduced-Calorie Sponge Cake Production by Xylitol and Oligofructose, Journal of Food Quality 39 (2016) 6.

[16] L. Laguna, P. Varela, A. Salvador, T. Sanz, S.M. Fiszman, Balancing texture and other sensory features in reduced fat short-dough biscuits, Journal of Texture Studies 43 (2011) 235–245.

[17] A., Chauhan, D.C. Saxena, S. Singh, Physical, textural, and sensory characteristics of wheat and amaranth flour blend cookies, Food Science & Technology 2 (2016) 1125773.

[18] P.K. Vayalil. Date fruits (Phoenix dactylifera Linn): An emerging medicinal food, Critical Reviews in Food Science and Nutrition 52 (2010) 249-271.

[19] E. Winkelhausen, R. Jovanovska-Malinovska, E. Velickova, S. Kuzmanova, Sensory and Microbiological quality of a baked product containing xylitol as an alternative sweetener, International Journal of food properties 10 (2010) 639 – 649.

[20] S. Struck, D. Jaros, C.S. Brennan, H. Rohm, Sugar replacement in sweetened bakery goods, International Journal of Food Science and Technology 49 (2014) 1963–1976.

[21] J. Gao, M.A. Brennan, S.L. Mason, C.S. Brennan, Effects of Sugar Substitution with "Stevianna" on the Sensory Characteristics of Muffins, Journal of Food Quality 2 (2017) 1-11.

[22] M. Majeed, M. Mohmod, M.U. Khan. M. Fazel. M. Shariati, I. Pigorev, Effect of sorbitol on dough rheology and quality of sugar replaced cookies, Potravinarstvo Slovak Journal of Food Sciences 1 (2018) 50-56.

[23] S.M. Savita, K. Sheela, S. Sunanda, A. G. Shankar, P. Ramakrishna, Stevia rebaudiana—A Functional Component for Food Industry, Journal of Human Ecology, 4 (2004) 261-264.

[24] A. Akesowan, Quality of Reduced-Fat Chiffon Cakes Prepared with Erythritol-Sucralose as Replacement for Sugar, Pakistan Journal of Nutrition 8 (2009) 1383-1386.

[25] S. Martínez-Cervera, A. Salvador, B. Muguerza, L. Moulay, S. M. Fiszman, Cocoa fibre and its application as a fat replacer in chocolate muffins, LWT—Food Science and Technology 3 (2011) 729–736.

[26] V. Psimouli, V. Oreopoulou, The effect of alternative sweeteners on batter rheology and cake properties. J. Food Sci. Agric. 92 (2012) 99–105.

[27] M.C. Carakostas, L.L. Curry, A.C. Boileau, D.J. Brusick, Overview: the history, technical function and safety of rebaudioside A, a naturally occurring steviol glycoside, for use in food and beverages, Food and Chemical Toxicology, 7 (2008) S1–S10.

[28] E. Gallagher, C. O'Brien, A. Scannell, E. Arendt, Evaluation of sugar replacers in short dough biscuit production. Journal of food engineering 56 (2003) 261-263.

Monika Janas, Alicja Zawadzka
Faculty of Process and Environmental Engineering, Lodz University of Technology,
90-924 Lodz, Wolczanska 213, monika.janas@edu.p.lodz.pl

DEGRADATION OF PENTACHLOROPHENOL BY HIGH TEMPERATURE HYDROLYSIS

Abstract
The long-term use of plant protection products in agriculture, including pentachlorophenol (PCP), has contributed to their widespread distribution in the natural environment. So far, no cheap and effective techniques for removing chlorophenols by physicochemical or biological methods have been developed. Therefore, alternative methods of neutralizing them are currently being sought. The aim of the study was to investigate the possibility of pentachlorophenol decomposition by high temperature thermohydrolysis. The decomposition process was carried out at a constant pressure of 25 MPa, in the temperature range of 20°C to 500°C and at various volumetric flows of PCP through the reactor. Detailed analysis of the results showed that the process and degree of pentachlorophenol reduction depended on residence time in the reactor and the process temperature. The obtained results indicate that thermohydrolysis in supercritical water is not an effective method to neutralize pentachlorophenol. The high costs of conducting this process together with an average degree of PCP conversion (the conversion of pentachlorophenol at the lowest volumetric flow rate through the reactor reached about 45%) cause that thermohydrolysis at high temperature is not a cost-effective method of neutralizing pentachlorophenol.

Keywords
pentachlorophenol, thermohydrolysis, supercritical water, neutralization

Introduction
Civilization progress is inextricably linked to the increase in the amount of generated pollutants. The physicochemical and biological methods used so far in wastewater treatment cease to be effective against many new, biologically active and ecotoxic pollutants contained in wastewater [1-3]. Chlorophenols, especially pentachlorophenol (2,3,4,5,6-pentachlorophenol), are particularly toxic and dangerous to the environment.
PCP is a synthetic organic substance that does not occur naturally in the environment. Pure pentachlorophenol is in the form of colorless or white crystals, poorly soluble in water and very well in organic solvents. PCP is a stable compound and its stability is due to the presence of five chlorine atoms attached to the aromatic ring. Pentachlorophenol was first introduced in 1936 by the chemical companies Dow and Monsanto as a wood preservative. The long-term use of pentachlorophenol has contributed to its widespread distribution in the environment, which leads to a steady increase of PCP concentration in the ecosystem [4-5]. The main source of environmental pollution with pentachlorophenol was the use of preparations containing PCP, which as a result of various transformations got into the water, air and soil. Pentachlorophenol was commonly used as a wood preservative, herbicide, fungicide, bactericide, algaecide, molluscicide, insecticide, biocide and defoliant. Large amounts of pentachlorophenol got into the environment as a result of wood treatment with PCP-containing preparations and as a consequence of mass spraying of arable fields with biocides. As a result of surface runoffs, pentachlorophenol used in agriculture was transported together with other pollutants to surface and underground water. Additionally, PCP was used in soaps and detergents applied in medicine and as an additive to adhesives, latex paints and paper. Pentachlorophenol was used in sealing substances being in contact with food and in plastic reusable containers for storage of loose food products. Pentachlorophenol was also used in the photographic and tanning industry as well as in paper and cellulose plants [5-7].

Pentachlorophenol is highly toxic to both microorganisms and humans, and its toxicity increases with concentration. PCP is absorbed through the respiratory tract, digestive system and skin [8-9]. Pentachlorophenol can cause many different symptoms of poisoning in humans depending on how it enters the body and the time of exposure. PCP can cause fever, breathing problems, hyperhidrosis, tachycardia and metabolic acidosis, and can bring about liver damage and problems with the immune system. People exposed to prolonged contact with pentachlorophenol during the production of PCP, woodworking and impregnation may suffer from acute poisoning manifested by high fever, headaches, irritation of the mucous membranes,

skin redness, rash, vomiting, increased thirst, as well as accelerated heartbeat and breathing. Both in offices and in the home environment people are exposed to pentachlorophenol which is released into the environment from wooden elements impregnated with a PCP-containing agent. In chronically exposed workers (during PCP production, impregnation and woodworking) there may occur heavy poisoning with pentachlorophenol, which can result in high fever, headaches, irritation of the mucous membranes, redness of the skin, rash, vomiting, increased thirst, and accelerated heartbeat and breath. When relatively high doses of PCP are regularly introduced into the body, this compound is present throughout the body and accumulates in the liver, kidneys, brain, spleen and adipose tissue, which leads to enlargement and dysfunction of individual organs and weakens the immune system [10-12].

In 1999, the Environmental Protection Agency (EPA) classified pentachlorophenol as a moderately toxic xenobiotic and set standards for its maximum concentration in various environments. According to the standards, the maximum level of soil contamination with pentachlorophenol is 1 mg/kg, and the maximum permissible concentration of pentachlorophenol in drinking water is 0.022 mg/dm^3. Occupational Safety and Health Administration (OSHA) has introduced standards for the maximum concentration of pentachlorophenol that workers may be exposed to during a 40-hour working week. The highest permissible concentration of pentachlorophenol in the air at workplaces in production plants was set at 0.5 mg/m^3 [13-16].

Despite legal regulations regarding the restriction of the use of pentachlorophenol introduced at the beginning of the 21st century, its amount in the natural environment, due to its low biodegradability potential, has not significantly decreased [15]. The durability of PCP in the environment varies and ranges from several hours to many years. The rate of pentachlorophenol decomposition largely depends on PCP concentration, the presence of microorganisms capable of transforming pentachlorophenol, access of light radiation or the pH of the environment [17]. Due to its resistance to microbial degradation and high toxicity, numerous studies are carried out to develop a relatively cheap and efficient method of removing this xenobiotic from the environment [18-21].

Promising methods of neutralizing such toxic pollutants are the so-called hydrothermal technologies, in particular thermohydrolysis in supercritical water, occurring at high temperature and water pressure (above critical temperature T_{cr} = 374°C and critical pressure P_{cr}=22.1 MPa). Under supercritical water conditions, a reaction environment with very favorable application properties is obtained [22-26]. High diffusivity and heat capacity of water intensify heat and mass transfer processes. Features such as good miscibility with gases and the ability to manipulate thermodynamic properties such as polarity, solution, acid-base properties, etc. have made it possible to widely use thermohydrolysis to decompose various chemical compounds [27-29]. Despite numerous studies on this process, knowledge about the mechanisms governing it is still insufficient.

Aim of the work
The aim of the work was to investigate the possibility of decomposition of pentachlorophenol and to check the possibility of using the high-temperature thermohydrolysis process for its decomposition. The tests were carried out at a constant pressure of 25 MPa, in the temperature range from 20°C to 500°C and at four different volumetric flow rates of PCP through the reactor.

Experimental
The possibility of using a high-temperature thermohydrolysis process to decompose pentachlorophenol was investigated in the study. The experiments were carried out in a laboratory scale on a setup consisting of the following elements:
- HPLC high-pressure plug pump (Jasco, Japan) to supply solutions of the tested compounds at 25 MPa,
- electrically heated and 6.0 m long flow reactor made of SS216 stainless steel with external diameter of 6.0 mm and inner diameter of 2.5 mm,
- pressure and temperature meter,
- tube-in-tube heat exchanger serving as a cooler and allowing the reaction mixture leaving the reactor to cool down,
- temperature controller allowing a determined temperature to be kept in the system,
- Back Pressure Regulator (TESCOM, France) to maintain a set pressure in the system.

The setup for conducting thermohydrolysis in supercritical conditions is shown in Figure 1.
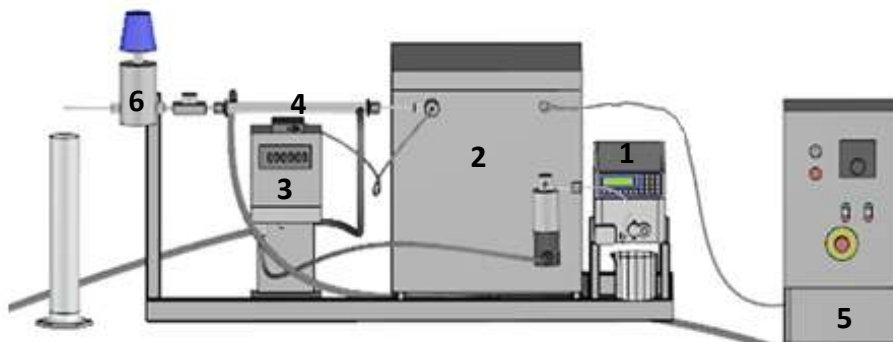

Fig. 1. Diagram of the installation for investigating the process of pentachlorophenol thermohydrolysis
1 – HPLC pump, 2 – electrically heated flow reactor, 3 – pressure and temperature measuring system, 4 – cooler,
5 – temperature regulator, 6 – pressure regulator
Source: Author's

Thermohydrolysis was carried out on model solutions of pentachlorophenol with initial concentration equal to 15 mg/dm^3, at temperature ranging from 20°C to 500°C, constant pressure 25.0 MPa and for four different volumetric flow rates through the reactor equal to 2.5 cm^3/min, 5 cm^3/min, 7.5 cm^3/min and 10 cm^3/min. After 30 minutes from the moment when the set temperature and pressure in the reactor were established, three 15 cm^3 samples of the reaction mixture were withdrawn at 20-minute intervals. The concentration of pentachlorophenol was determined by Reverse Phase High Performance Liquid Chromatography (RP HPLC). Before analysis, the samples were filtered through Whatman membrane filters of cellulose nitrate (porosity 0.2 μm). The measurement was carried out using a Perkin Elmer liquid chromatograph equipped with a Hypresil GOLD capillary column (250 × 4.6 mm) and a Hypresil GOLD pre-column, 5 μm 10 x 4 mm. The HPLC system used in the tests consisted of a pump and DAD type UV/VIS detector. The conditions for conducting analyses were selected in accordance with the principles of chromatographic separation of mixtures based on affinity to the substance for filling the column. The eluent was acetonitrile and acetate buffer, the proportions of which were 60 and 40%, respectively. The flow rate of the eluent through the column was 1 ml/min, while the retention time of pentachlorophenol was about 7.25 min. The injection volume of the sample per column was 2 μl. Detection was carried out at a wavelength of 252 nm, which roughly corresponded to the absorption maximum of pentachlorophenol. PCP concentration in the samples was determined using standard curves prepared using the Turbo Chrom program and developed for pentachlorophenol at concentrations ranging from 0 to 15 mg/l.

Results
The paper presents results of research on the process of pentachlorophenol thermohydrolysis under supercritical conditions. Figure 2 shows changes in the concentration of pentachlorophenol depending on the residence time in the reactor. In addition, the temperature corresponding to the critical point is marked with a dashed line in each chart of Fig. 2. From a chemical point of view, it is very important, because in its vicinity all water properties are changing rapidly.
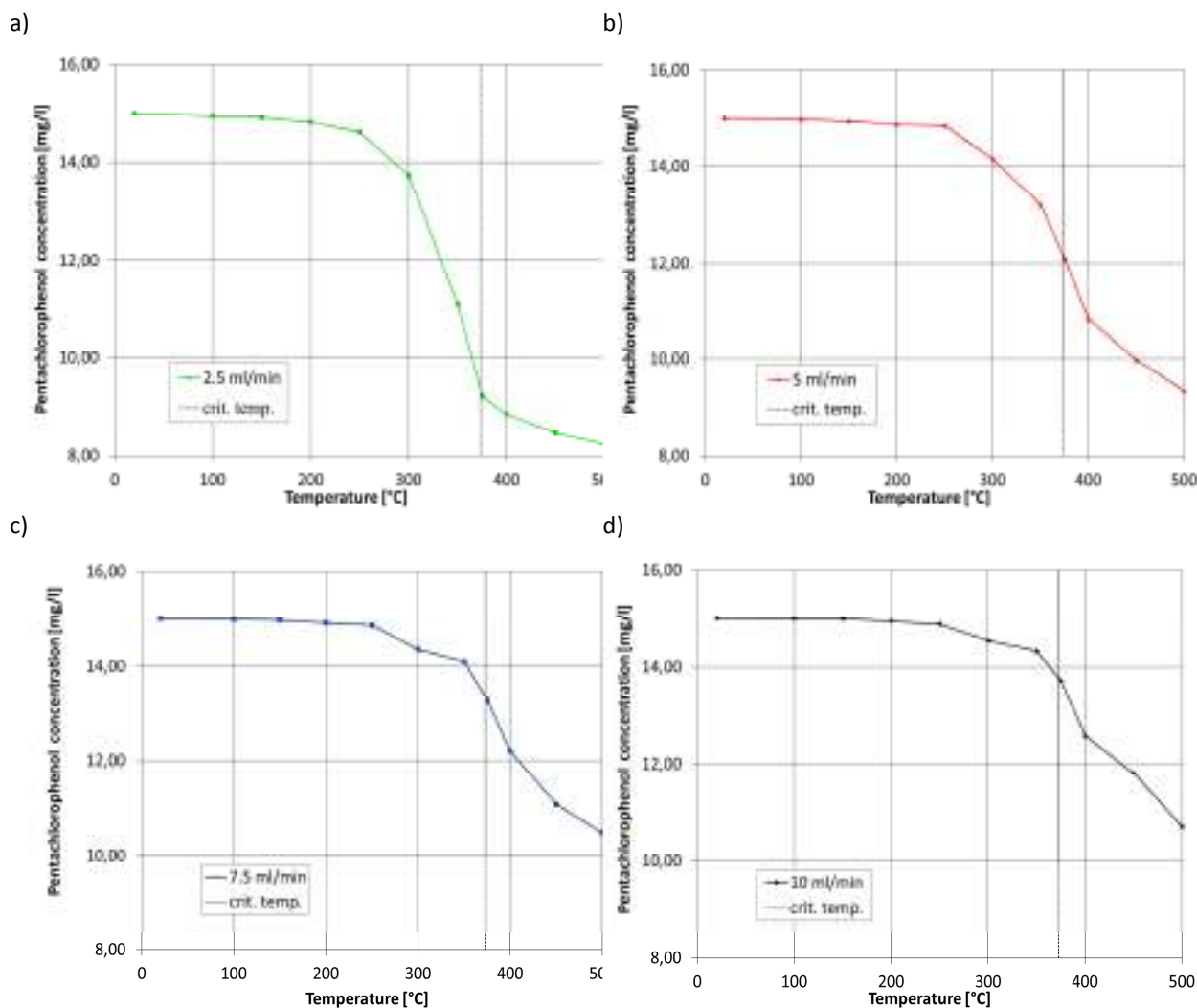
Fig. 2. Changes in the concentration of pentachlorophenol depending on the volumetric flow rate through the reactor: a) 2.5 cm^3/min, b) 5 cm^3/min, c) 7.5 cm^3/min, d) 10 cm^3/min

Source: Author's

When analyzing the curves that characterize the temperature dependence of initial concentration of pentachlorophenol fed to the reactor, it was observed that at low temperatures PCP concentration was virtually unchanged, and only above 300°C it dropped sharply. Based on the performed studies, it was found that the concentration of pentachlorophenol measured at the end of the process depended on temperature. For all analyzed flow rates of the solution through the reactor, a reduction in PCP concentration was observed with increasing temperature. In particular, these changes can be observed near the pseudocritical point. At the same time, it should be noted that as the volumetric flow rate through the final reactor increases, the PCP concentration grows. At the volumetric flow rate of the reaction mass equal to 2.5 cm^3/min and temperature 500°C, the decrease in PCP concentration was almost twice as high, falling from 15 mg/dm^3 to 8 mg/dm^3, while for the same conditions but at a volumetric flow through the reactor equal to 10 cm^3/min, the initial concentration was reduced by approximately 30%.

Figure 3 shows the dependence of the degree of conversion of the tested compound on the volumetric flow rate of PCP through the reactor for 2.5 cm^3/min, 5 cm^3/min, 7.5 cm^3/min and 10 cm^3/min at constant pressure of 25MPa.
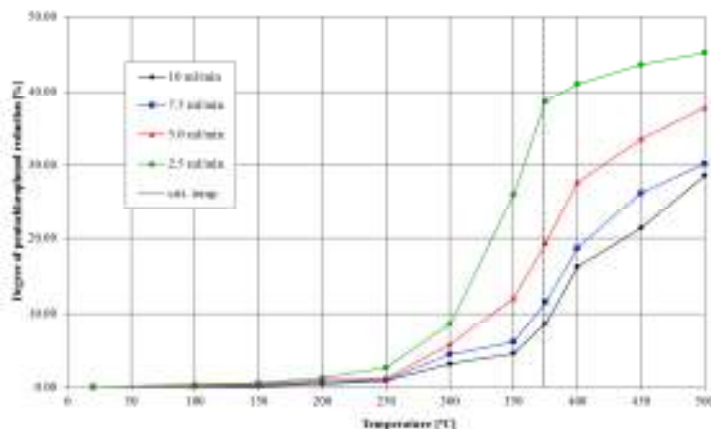
Fig. 3. Dependence of the degree of pentachlorophenol reduction as a function of temperature for different volumetric flow rates of liquid through the reactor equal to 2.5 cm^3/min, 5 cm^3/min, 7.5 cm^3/min and 10 cm^3/min at pressure 25 MPa.
Source: Author's

A detailed analysis of the temperature-dependent pentachlorophenol reduction curves allows us to conclude that the percentage of its conversion depends on the volumetric flow through the reactor. The longer the residence time of pentachlorophenol in the reactor, the greater the reduction of PCP. At low temperatures the degree of pentachlorophenol conversion is virtually zero. A gradual but slight increase in PCP conversion is observed only at 300°C. Approximately 45% PCP conversion was obtained for the lowest flow rate of 2.5 ml/min at 500°C. This level of conversion, considering the high costs of running the process, is not satisfactory and indicates that the high-temperature thermohydrolysis cannot be used as an effective method of pentachlorophenol decomposition.

In the literature there are many results of thermohydrolysis of organic compounds. However, there are no reports on this type of research in relation to pentachlorophenol. This is probably due to the fact that PCP dissolves very badly in water. The high-temperature hydrolysis process is tested for compounds with much better solubility. Nevertheless, the properties of this compound, its toxicity and use in many preparations cause that an effective method of PCP degradation is sought. Actually the best PCP degradation results are achieved by biological methods, which are characterized by low costs of the process.

Summary
Over fifty years of the use of chlorophenols, including PCP, has contributed to their widespread distribution in the natural environment and living organisms. People who come into contact with products containing PCP are particularly vulnerable to its toxic effects, which carry an increased risk of cancer, fetal defects, mutations, blood composition disorders and changes in the nervous system.

The paper presents the results of studies on high-temperature hydrolysis of pentachlorophenol. The tests were carried out at a constant pressure of 25 MPa in the temperature range of 20°C to 500°C and at four different volumetric flows of PCP through the reactor equal to 2.5 ml/min, 5 ml/min, 7.5 ml/min and 10 ml/min.

In studies on high-temperature thermohydrolysis of pentachlorophenol, an unsatisfactory degree of reduction of this compound was obtained. The PCP conversion increased with increasing process temperature. The highest degree of pentachlorophenol reduction amounting to about 45% was achieved for the lowest volumetric flow rate through the reactor equal to 2.5 ml/min at 500°C. This level indicates the average efficiency of the high-temperature hydrolysis process, which, combined with the high cost of the process, causes the process to be unprofitable for pentachlorophenol removal. This does not preclude the use of thermohydrolysis in supercritical water as an effective way to treat wastewater containing PCP. Therefore, it is necessary and justified to continue research on the process of high-temperature thermohydrolysis.

References
[1] P. Fernández, J.O. Grimalt, On the global distribution of persistent organic pollutants, Chimia, 57(9) (2003) 514-521

[2] M. Farré, S. Pérez, C. Gonçalves, M.F. Alpendurada, D. Barceló, Green analytical chemistry in the determination of organic pollutants in the aquatic environment, TrAC Trends in Analytical Chemistry, 29 (11) (2010) 1347-1362

[3] J. Jacob, J. Cherian, Review of environmental and human exposure to persistent organic pollutants, Asian Social Science, 9 (2012) 107-120

[4] W. Zheng, X. Wang, H. Yu, X. Tao, Y. Zhou, W. Qu, Global trends and diversity in pentachlorophenol levels in the environment and in humans: a meta-analysis, Environmental Science and Technology, 45(11) (2011) 4668-4675

[5] J. Gunschera, F. Fuhrmann, T. Salthammer, A. Schulze, E. Uhde, Formation and emission of chloroanisoles as indoor pollutants, Environmental Science and Pollutant Research International, 11(3) (2004) 147-51

[6] B. Fisher, Pentachlorophenol, Toxicology and Environmental Fate, Journal of Pesticide Reform, 11(1) (1991) 2-5

[7] M. Czaplicka, Sources and transformations of chlorophenols in the natural environment, Science of the Total Environment, 322 (2004), 21-39

[8] J.K. Piotrowski, Podstawy toksykologii, WTN, Warszawa, 2006

[9] K.R. Rao, Pentachlorophenol: Chemistry, Pharmacology and Environmental Toxicology, Plenum, New York, 1987.

[10] H. Choudhury, J. Coleman, C.T. De Rosa, J.F. Stara, Pentachlorophenol: health and environmental effects profile, Toxicology and Industrial Health, 2 (1986) 483–596

[11] S. Yang, X. Han, C. Wei, J. Chen, D. Yi, The toxic effects of pentachlorophenol on rat Sertoli cells in vitro, Environmental Toxicology and Pharmacology, 20 (1) (2005) 182-187

[12] K. Wahl, A. Kotz, J. Hädrich, R. Malisch, M. Anastassiades, I. Sigalova, The guar gum case: contamination with PCP and dioxins and analytical problems. In: Organohalogen Compounds, 70 (2008)

[13] US EPA -U.S. Environmental Protection Agency: Integrated risk information system on pentachlorophenol. National Centre for Environmental Assessment, Office of Research and Development, Washington, DC, 1999

[14] ATSDR/US Public Health Service, Agency for Toxic Substances and Disease Registry, Toxicological profile for pentachlorophenol, Atlanta, GA, 1994.

[15]Agency for Toxic Substances and Disease Registry, Hazardous Substances Database, Atlanta, GA, 1998.

[16] Ordinance of the Minister of Family, Labor and Social Policy of June 12, 2018 on the highest permissible concentrations and intensities of agents harmful to health in the work environment (Journal of Laws 2018, item 1286)

[17] S.O. Agbo, E. Küster, A. Georgi, J. Akkanen, M.T. Leppänen, J.V.K. Kukkonen, Photostability and toxicity of pentachlorophenol and phenanthrene, Journal of Hazardous Materials, 189 (1-2) (2011) 235-240

[18] S.K. Bhattacharya, Q. Yuan, P. Jin, Removal of pentachlorophenol from wastewater by combined anaerobic-aerobic treatment, Journal of Hazardous Materials, 49 (1996) 143-154

[19] A.D. Mosca, M.C. Tomei, Pentachlorophenol aerobic removal in a sequential reactor: start-up procedure and kinetic study, Environmental Technology, 36(3) (2015) 327-335

[20] B. Antizar-Ladisaro, N.I. Galil, Biosorption of phenol and chlorophenols by acclimated residential biomass under bioremediation conditions in a sandy aquifer, Water Research, 38 (2004) 267-276

[21] J.A. Zimbron, K.F. Reardon, Fenton's oxidation of pentachlorophenol, Water Research, 43 (2009) 1831-1840

[22] M.J. Cocero, Supercritical water processes: Future prospects, The Journal of Supercritical Fluids. 134 (2018) 124-132

[23] N. Akiya, P.E. Savage, Roles of water for chemical reactions in high-temperature water, Chemical Reviews, 102 (2002)

[24] W. He, G. Li, L. Kong, H. Wang, J. Huang, J. Xu, Application of hydrothermal reaction in resource recovery of organic wastes, Resources Conservation Recycling, 52 (2008) 691-699

[25] A. Martin, M. D. Bermejo, M. J. Cocero, Recent developments of supercritical water oxidation: a patents review, Recent Patents on Chemical Engineering, 4 (2011) 219-230

[26] H. Weingartner, E.U. Franck, Supercritical water as a solvent, Angewandte Chemie International Edition, 44 (2005) 2672-2692.

[27] W. Wagner, A. Pruss, The IAPWS Formulation 1995 for the Thermodynamic Properties of Ordinary Water Substance for General and Scientific Use, Journal of Physical and Chemical Reference Data, 31 (2) (2002) 387-535

[28] D.A. Palmer, R. Fernandez-Prini, A.H. Harvey, Aqueous systems at elevated temperatures and pressures, Elsevier Academic Press (2004)

[29] G. Brunner, Hydrothermal and supercritical water processes, 1st Edition, Supercritical Fluid Science and Technology Series 5, Kiran E. (ed.), Elsevier, Oxford (2014)

Andrzej Klimek
Research and Innovation Centre Pro-Akademia
ul. Innowacyjna 9/11, 95-050 Konstantynów Łódzki, Poland, andrzejrklimek@gmail.com

Isidoros Ziogou, Apostolos Michopoulos, Theodoros Zachariadis
Energy and Environmental Economics and Policy Group (3EP), Department of Environmental Science and Technology, Cyprus University of Technology
Athinon and Anexartisias Corner, P.O. Box 50329, 3603 Lemesos, Cyprus, michopoulos.apostolos@ucy.ac.cy

Sadiq Gulma
Green Habitat Initiative
Abuja, Nigeria, sagulma101@gmail.com

Dina Suhanova
Faculty of Architecture and Design, „RISEBA" University of Business, Arts and Technology
Durbes iela 4, Riga, Latvia, dina.suhanova@riseba.lv

Mure Agbonlahor
Agricultural Economics & Farm Management Department, Federal University of Agriculture,
PMB 2240, Abeokuta, Ogun State, Nigeria, agbonlahormu@funaab.edu.ng

Sabine Jung-Waclik
Brimatech Services GmbH
Lothringerstraße 14/3, A–1030 Vienna, Austria, sjw@brimatech.at

GREEN ROOFS DISSEMINATION REGARDING THEIR POTENTIAL CONTRIBUTION IN ADDRESSING THE UHI EFFECT

Abstract
The article aims at summarising the state of the art in the efforts of researchers and innovators to find viable solutions to mitigate the urban heat island (UHI) effect. This effect is loosely connected with the greenhouse effect, however, it certainly creates a severe negative synergy together with it. As green roofs are a well-known answer how to address the UHI effect, the ways how to make their massive and global deployment convenient are discussed. Initially, the differences and similarities between urbanisation in developed and developing countries are described. Then the paper depicts solutions, especially synergic ones, for making the dissemination of green roofs viable, such as rainwater and energy harvesting or urban agriculture. Then the authors conclude that retrofitting the existing roofs is the only method for reaching the desired scale and discuss available business models necessary for introducing the prosumer approach to the retrofitting.

Key words
green roofs, Urban Heat Islands, urban regeneration, prosumer model, efficiency of FWE resources

Introduction
As the world's population approaches the 8 billion mark, a characteristic feature of the demographics, across countries, is the increasing rate of urbanization. The growth in the population of urban settlers cuts across countries and continents. Economic and social factors present strong pull factors that attract people, especially the youth and people within the economic age brackets, to urban areas. A cursory look at the growth trend over the last 3 decades suggests a sustained and rapid increase. It is estimated that over 65% of the world's population will be residing in urban areas by 2025. [1] In 2005 half of the global population lived in urban agglomeration areas. Worldwide, 457 large cities (with a population of 1,000,000 or more), 1,063 medium cities (with a population between 500,000 and 1,000,000) and 2,896 smaller cities (population of more than 150,000) exist. [2]

In 1810, so even before the global warming began, it was observed that the temperature of urban environment is higher than in the surrounding areas, nowadays for approximately 3°C. [3] Then the reason of this phenomenon has been found in modifying the urban land surface (e.g. paving the roads or building houses), together with waste heating streams, and it has been called an urban heat island (UHI) effect. Its major consequence are the increasing: air conditioning demand, air pollution, greenhouse gas emissions, as well as the number of heat-related illnesses, including fatal ones. [4] It has also a negative impact on water quality. [3] Disturbed air circulation causes breezes at its perimeter while the centre remains still, which leads to an intensified steam condensation. This in turn results in more frequent rains. [5] In most of contemporary cities the rainwater is perceived as a problem rather than a resource. Furthermore, as rainwater passes by "concrete deserts", it is so hot that it can be dangerous for ecosystems of the surface water. [6] Additionally, all these phenomena cause a rain shadow effect at peri-urban areas, which should negatively affect the surrounding agriculture. [5] Furthermore, the hot air forms many kilometres-high stacks called urban thermal plumes. Their impact at higher latitudes, namely above 40°N and 40°S, is much greater as net cooling in the Earth-atmosphere system occurs there due to radiation. [7] It concerns especially highly urbanised areas of Northern Hemisphere. Nghiem et al. [8] claim that the plumes perturb the wind directions even in macroscale and the northern polar jet stream deviation leads to melting of the Arctic ice cap even more than the global warming. UHI effect reduction is a contribution not only to sustainability, but also to comfort of living in a given city. Summer heatwaves are fault of increased mortality of elderly people as within the United States alone, an average of 1,000 people die each year due to this reason, even though they affect only citizens living in temperate climate. [4] The number as well as the intensity of urban heat days (days with a maximum temperature over 30°C) will dramatically increase in upcoming years (9.6 heat days average occurred yearly in Vienna between 1961 and 1990, while between 1981 and 2010 it raised to 15.2 heat days per annum mean). [9]

It is estimated that the heat accumulation in roofs is responsible in 40% of the average entire UHI effect impact. [10] The rise of the greenhouse gases emissions has been leading to warming the mean global temperature for 0.85°C between years 1880 and 2012 [11] and the ecological footprint is 1.6 times bigger than Earth's surface, which means that the global nature resources are depleted 1.6 times faster than they are renewed. [12] Therefore, lowering the accumulation and addressing the accompanying phenomena are an important challenge for the cities of the future. Without any adaptive urban design, the temperature greenhouse gas-induced increase until 2100 in California was calculated to be as high as 1.31 degrees Celsius, but a 100% deployment of "cool roofs" – meaning either green roofs, either traditional roofs diffusing much of solar radiation received, due to their bright colour – would result in a temperature drop of 1.47 degrees Celsius — more than the increase. [13]

The green roofs are the most common solution which has a potential of mitigating UHIs nowadays and improving the sustainability of the cities, even if such a single structure has only very limited impact on the environment and although in many cases they are not designed with such intention and they address the discussed problem only as a side effect of their presence. Firstly, the reflection coefficient for a green roof is hard to be measured, even though it is estimated that absorption of such a roof is 2 to 9 times lower than for an ordinary, dark roof structure. Secondly, green roofs have good thermal insulation properties, decreasing power demands for air-conditioning and space heating. Thirdly, their biological activity contributes to absorption of carbon dioxide and other greenhouse gases. Fourthly, they increase the water retention, mitigating this way a risk of a sudden local flooding, which rising frequency is another consequence of climate change. Last but not least, they provide heavily trafficked city centres with a green cover, which directly decreases the air pollution in those areas, most vulnerable to this phenomenon. All of these facts make the issues of green roofs dissemination and sustainable urbanisation strongly intertwined. The problems and challenges related to green roof construction and maintenance have been expanded in upcoming sections.

If we assume that tackling the UHIs by means of a mass-scale green roof introduction is a question of utmost importance, we remain failing to know who should take the responsibility of that. The developed countries are wealthy and globally indebted in terms of carbon emissions, while the developing countries are very populous, which means that potentially even a moderate increase of consumption level there, which seems to be inevitable eventually, would result in a big raise of carbon emissions.

Green roofs and urbanization in developed countries

As previously stated by Georgescu et al., massive deployment of "cool roofs" would result in a significant temperature drop. [13] Still, this research was not related to the influence of green roofs, which would apparently have a greater positive environmental impact. Developed countries tend to be conscious of the climate change threats and opportunities to tackle them, like one mentioned above, meanwhile having powerful tools to introduce adequate policies. On balance, their responsibility for the climate change mitigation should be bigger, because biocapacity deficit of such countries as USA (-4.8 global hectares per person) [14] or Japan (-4.1 gha/person) [14] significantly contributes to making the whole world the ecologically indebted.

Therefore, developed countries are making research and implementation activities concerning the dissemination of green roofs and the former show it will be profitable. The simulations, assuming coverage of 50% of existing Southern California rooftops with green roofs or cool roofs, were made and demonstrated that it would give 1,625 GWh of direct energy savings per year, which would let save more than $200 million and avoid producing 465 thousand tons of CO_2 *per annum*. [15]

Planning regulations in many developed countries strongly encourage using green roofs, but predominantly in relation to new constructions. In Toronto, they are mandatory for the roofs with gross floor area of 2,000 m^2 or higher. [16] The same in Copenhagen, where since 2010 they have been mandated in most new local plans. [17] Financial incentives have also been put into practice. The city of Vienna started a programme of financial incentives for constructions of new green roofs. The amount of funding depends on the substrate height (cm) of the green roof system. It can range between 8 and 25 € per square meter, with an upper limit of 2,200 Euro per project. [18] Other European cities with subsidies for green roofs are Linz, Groningen, Rotterdam, Amsterdam and The Hague. [19]

Despite such an amount of evidence advocating green roofs dissemination and in spite of existing regulations discouraging from creating "dark roofs" on new buildings, the occurrence of green ones is still far from having a significant impact on climate, to any extent. Two main reasons for this are following: they are virtually absent in buildings from 20th century or older, which still compose vast majority of the world's building stock, and even now they are still up to two times more expensive than regular structures, therefore the give no clear benefits for the investors [20, 21].

Urbanization in developing countries

Urbanization in developing countries is different from that of developed countries. [22] In the former, it is more associated with increase in natural population (excess birth rate over death rate), while in developed countries, it is more towards increased infrastructural and economic development with less increase in population.

In 2010, human population in developing and developed countries are estimated around 2.6 billion and 960 million with urbanization level of about 46% and 78% respectively. And this trend is expected to continue with over 90% of the population growth expected to take place in urban areas of developing countries. [22] Urbanization level of developing countries forecasted for the year 2050 is at 64.11% and the corresponding average annual rate of change of the percentage for urban areas between 2010 to 2050 is 1.70%. The rate is more alarming when compared to that of developed countries for the same period which is 0.41%. [22]

Another important factor accelerating urbanization in developing countries is migration from rural to urban areas, due to perceived better urban life and economic opportunities in cities. That is why Cobbinnah et al. described urbanization in Africa as premature often associated with unsustainable land development and huge urban poverty. [22] It is rapid, unplanned and unsustainable.

According to World Urbanization Prospects 2018, up to 68% of the population in urban areas are projected to be living in slum conditions by the year 2050. [23] These shanty town conditions have been defined by UN HABITAT to be any of inadequate access to both sufficient water and sanitation, proper shelter to protect from adverse weather conditions, living in a room of not more than 3 people and prevention from forced eviction. [24]

Cohen further identified other key challenges like socioeconomic fragmentation amongst cities (middle and high income areas enjoy better urban basic services than low income areas in the same city): water, waste management, land development planning and congestion. [25]

Green roof dissemination in developing countries
Much has not been recorded on direct green roof dissemination in majority of developing countries. Dissemination is mostly carried out through a general concept of promoting green building technologies (GBTs) or through the enforcement of green building regulations and rating systems. Using green roof dissemination largely limits substantive information to be found on the topic. However, using GBTs which encompasses green roofs may improve the situation on available data.

Some developing countries have green building rating systems they have adopted as a regulation. African countries continue to be the most interesting as part of those in developing world. Kenya and South Africa have set green building standards to follow as building regulations. They have adapted the Australian Green Start rating system to suit their local climate and needs. In Nigeria's capital city Abuja, developers are being asked to incorporate green building concepts when applying for building permits. However, these concepts are less specific about green roofs. A few countries though have considered possibilities of its usage through surveying building professionals.

Darko & Chan reported on strategies needed to promote the adoption of GBTs and identified 5 top major things to do, as agreed by the responses of 43 construction professionals in Ghana to be statistically significant: increased publicity of GBTs in the media, related educational and training programs for professionals, making available institutional framework for effective implementation, strengthened R&D (Research & Development) and financial and further market based incentives for GBT adoption [26]. In comparison to US (a developed country) the strategies to promote dissemination and adoption differ, often because of economic status.

Chan et al. investigated the dissemination of green building technologies in Ghana, a developing country. The most critical barriers identified in their usage starts from the belief of high cost of employing GBTs, lack of government incentives, lack of financing schemes (e.g. Bank loans), unavailability of GBTs suppliers and lack of institutes and facilities for R&D of GBTs, arranged in order of agreement by the respondents of the survey. [27]

Using a factor analysis of the 20 critical barriers identified from a literature survey, five groups emerged that categorized these barriers; government related, human related, information related, market related and cost and risk-related. The critical of them in Ghana is government related; lack of green building rating systems and labelling, lack of green building codes and regulations, lack of green building technological training for professionals, lack of GBTs promotion by government, lack of demonstration of projects, lack of local institutes and facilities for R&D of GBTs and lack of government incentives. [27]

However, in Nigeria, a few of the government-related barriers are being reduced with the intervention of GIZ (Die Deutsche Gesellschaft für Internationale Zusammenarbeit GmbH – English: *German Corporation for International Cooperation Ltd.*) who works together with the Federal Ministry of Works. They have been able to develop an energy efficiency building code and put in place a training program for interested professionals.

Lotfi studied the green roof development in Iran [28] and reported similar results to Chan et al. [27] Cost of installing a green roof in Iran seems to be the biggest barrier to its adoption, followed by lack of managerial and policy aspects that failed to establish the critical role of green roofs in sustainably urban development.

Awareness on green roofs is not common to both among building owners and designers. Such concepts are more used by international clients who get contracts to build within the continent. Small and local contractors have little knowledge of green roofs promoted by the general lack of sufficient knowledge and research on the concept.

For green roofs to thrive, plants native to the areas must be known. Research on plants suitable to be used as green roofs is less with only a few reporting on the types of plant they used and success.

Energy & water efficiency of green roofs

Green roofs offer many positive services, among which are urban heat island (UHI) mitigation, increased thermal comfort for building occupants and important energy savings. [29] More specifically, heat fluxes from building roofs can decrease by roughly 80% in summer, while reduction in energy consumption during the same period can reach almost 17% compared with conventional roofs. A noteworthy temperature difference of the order of 4°C between traditional and vegetated roofs can also be spotted in winter. [30]

Various experimental approaches have been employed so far attempting to evaluate the thermal and energy performance of green roofs. Bevilacqua et al. found that under common Mediterranean climatic conditions and in comparison, with conventional roofing options, thermal energy entering from the building's green roof can be eliminated during summer, while the corresponding energy flowing outwards in winter can be reduced up to 37%. [31] In Shanghai, a coastal city with hot and humid summers, the cooling effect of green roofs is more pronounced on sunny days, with the largest difference in heat flows through the roof reaching 15 W/m^2. [32] In cold climates, like the one prevailing in West Lafayette, Indiana, the examined retrofit option was found to cut down the heat loss of the inner roof area by almost 18% during the whole heating period. [33] Green roofs also present higher air temperature above their surface compared to white gravel roofs in regions with temperate climates, where heating is more important than cooling. [34]

Recent studies have confirmed that the main factors influencing the energy efficiency of a green roof are the height of the selected vegetation, the leaf area index (LAI), the minimum stomatal resistance, and the growing medium's depth [35–37]. Berardi found that the examined building energy consumption is more strongly affected by soil height than by the LAI of the green roof, while the magnitude of LAI is proportional to the cooling effect on the local microclimate of urban areas. [38] This is of great importance, keeping in mind that the UHI effect is directly linked with energy consumption in cities – for example, the effect of the summer UHI alone has reportedly raised the air-conditioning load up to 12% in Manchester, UK. [39] Green roofs coupled with vegetation at pedestrian level positively affect the urban microclimate [40], with urban planning conditions, design configuration and prevailing local climatic characteristics being the major factors in their overall performance [41].

Apart from their contribution to energy conservation, green roofs are also beneficial for the management of storm water run-off in cities, where their implementation at a large scale can ultimately reduce urban flood events. [42–44] Percentage-wise, the water retention levels can range from 35.5% to 100%, with a mean retention of 77.2% according to Zhang et al. [45] Moreover, a total average retention of 66% of a full-scale extensive green roof has been found by Nawaz et al. [46] In absolute terms and for optimal conditions, storm water storage capacities can vary from 25 mm to 40-50 mm. [47]

In an effort to investigate the parameters affecting the water retention efficiency of green roofs, a stochastic weather generator coupled with a conceptual hydrological model have recently been used. [48] The results of this study indicated that the water retentiveness is proportional to the roof's soil depth, with humid subtropical climates being in favour of a green roof's retention performance and in contrast with Mediterranean ones. Following also a simulation approach, Szota et al. used a water balance model and found that the rainfall detention capacity can increase with the appropriate combination of irrigation regimes and drought tackling strategies. [49] Other parameters that play a determining role in the hydrological performance of green roofs are the vegetation characteristics and the physical properties of the layers' components. [50, 51]

The remaining water that escapes green roofs during intensive precipitation events can lead to leakage of nutrients and metals and thus may adversely affect the quality of downstream water bodies, especially in the case of recently applied constructions. [52] This can be mainly attributed to the high organic matter content of the green roof's soil substrate, which leads to a more brownish colour, dissolved salts and higher nutrient concentrations like phosphorous in the removed water. [53, 54] According to Wang et al., adding an absorption layer comprising a mixture of active charcoal and/or pumice with perlite and vermiculite below the growing medium is sufficient to achieve the desirable balance between water runoff attenuation, pollution amelioration and optimal service lifetime of a green roof. [55]

Urban Agriculture and green roofs food production

As it is estimated that over 65% of the world's population will be residing in urban areas by 2025, this projection brings to fore issues of the sustainability of the system, because as cities expand, so do the food needs of urban families. [56] With increasing urbanisation, issue of sustainability of the food supply system have become more vexed with reference to social, economic, food production and environmental concerns. While alimentary and financial breakdowns are painful both for rural and urban dwellers, the urban poor have been suffering arguably the hardest considering food access, due to their low resilience. Consumers in the cities are almost exclusively dependent on buying food and changes in food prices and income have a direct translation into decreasing purchasing power and rising rates of food insecurity, thus affecting dietary quantity and quality this way. [57]

Meeting the food needs of the urban population in a sustainable manner is a major development challenge. Urban agriculture provides food, employment and incomes for urban dwellers [58–60]. The products are either consumed by the producers, or sold in urban markets, such as the increasingly popular weekend farmers' markets and organic kiosks found in many cities. The sustainability aspect of the production is emphasized because the locally produced food requires less transportation (pollution and cost) and refrigeration (packaging and storage), it can supply nearby markets with fresher produce.

Growth and expansion of urban agriculture over the years have been a result of high urban pull (both available and affordable) for food. The urban lifestyle and food demand regime are markedly different from those of rural societies. The difference in types of food demand can be attributed to the, characteristically, mobile and non-sedentary nature of urban employments, short family food preparation/consumption time, and increase in mass produced fast foods and highly variable income status. These characteristics orient the food needs to ready-to-eat or quickly prepared food items such as poultry, chips, fruits and vegetables. The need to supply these items not only cheaply but also freshly had encouraged urban and peri-urban agriculture. With increasing urbanization, the concern of how to furnish adequate amount of cheap, safe and nutritious food to the urban population has led to a reawakening of interest in urban agriculture.

Urban agriculture is a form of localising production (growing, processing, distribution and consumption) of food within the urban space. [61] Apart from the food security gains which entail the supply of cheap and fresh foods to the urban inhabitants, urban agriculture also adds environmental benefits and aesthetic appeal to urban environment. However, over time, the land space which was traditionally used for agriculture within the urban space has decreased or even ceased to exist due to increase in residential, commercial structures and facilities networks. In urban areas, due to the high demand of land for development and residential purposes, the opportunity cost of using land space for agricultural production is very high. Rooftop agricultural production or use of living roofs for food production had offered a new frontier in urban agriculture. While urban farming includes the production of crops and livestock, green roof or rooftop agriculture is most often associated with crop production. Osmundson succinctly set forth what typifies green roof agriculture, as the cultivation of crops in open space that is separated from the ground by a building or other raised structure. [62]

Rooftop agriculture is most exclusively used with crop production and the crops cultivated are usually annuals or short duration crops (fruits and vegetables). They are above-ground-level food production systems, involving use of raised platforms (spaces on top of human-made structures), referred to as green roofs or living roofs. Since they are above ground and usually on raised platforms, they present a separate set of operational challenges that have economic, architectural and biological implications. Some of the associated challenges that have been identified includes: high establishment and architectural re-engineering costs, limited space and load limits, accessibility, selection/choice of crops to be planted, as well as issues of pollution of roof runoff. However, some of the associated benefits from adopting green roof urban agriculture, apart from those mentioned before, include:

- Production of socially and economically cheap and fresh foods
- Retention (detain and slow runoff) of storm water which is a form of rain water harvesting technology. This has significant cost savings advantage in water cost reduction as well as in the design and management of infrastructure.
- Economically, they provide a durability effect on the roofing materials and insulate from sound and trap dusts. The green layer protects the roof membrane from harsh climatic effects, puncture, and UV damage.

- ▪ The roof has full solar exposure with no risk of construction blocking the sun isolation. (minor risk of overshadowing by the neighbouring buildings)
- ▪ Aesthetic appeal associated with greening effects and the ability of the green roofs to attract and butterflies and birds to urban environments.

Asserting to the increasing popularity of green roof, Engelhard reported that green roofs are gaining popularity as a tool to mitigate many of the negative environmental effects caused by urbanisation. [63] He further highlighted that green roofs have been proven to reduce the UHI effect, absorb storm water, decrease energy used for heating and cooling, improve air quality, and sequester and store carbon and other greenhouse gases contributing to global climate change.

A study conducted by Ableman found that with good management conditions crops performance in green roofs approximate that under normal field condition as rooftop growing conditions are not substantially different from those on the ground. [64] Considering the fast urbanising rate of our cities and the concomitant demand for cheap, fresh and healthy foods, and with the identified economic, social and environmental benefits of using living roof for food production, it is envisaged that the future is bright for green roofs use in food production. In another study Engelhard made a study on the different types of design of living roofs. [65] While observing that rooftop agricultural projects are responding to poor environmental, social and economic conditions in cities, he highlighted global climate change, hunger and economic recession as among the issues shaping current urban gardens. He however concluded that though there are many encouraging signs for the growth of rooftop agriculture, issues of land tenure, natural resources, zoning, funding and development trends continue to affect their success.

Optimizing food production efficiency from green roofs
Efficiency in food production is attained when the output generated from the system exceeds the value of the technical inputs used. System efficiency is a precondition for sustainability. As an efficient food production system will support basic ingredients for a sustainable system, green roofs use in urban agriculture generates output that are cheaper in the long run. The availability of a ready and high-value consumer market in the urban area (farmers' markets, restaurants and organic kiosks) means that the products are exchanged for better prices and payment is usually direct to the producer. Also, there is usually little or no facilitating and logistic costs associated with transportation, storage and packaging. While limited space and the peculiarities of rooftop technology may limit the quantity and types of crops that can be produced from this system, the production system is highly efficient and factors productivity are high. Green roofs technology offers huge benefits to make modern food production cheaper and environmentally friendlier. [66]

Sustainable production system is a key element of the sustainable development goal (SDGs) of the United Nations. A sustainable system is one that incorporate the 3 pillars of profit, planet and people. It is a production system that yields a non-declining output over time while at the same time ensuring the natural resource base is not compromised. A sustainable urban food production system must therefore address issues of profitability and environmental sustainability. It will include the application of natural principles to grow enough food for people without depleting the natural resources that sustains it or polluting its environment and ensuring economic viability. According to Earles, variants of a sustainable agricultural system include organic, biodynamic, alternative and bio-intensive farming. [67] Sustainable agriculture is the product of a self-sustaining production intensification regime. It is an attempt to reduce over-exploitation of the natural resources base through the minimizing the depletion of native resources and use of external inputs in production. Sustainable agriculture was a response to green revolution that was characterized by industrial production models that emphasized high productivity at the expense of water, soil, biodiversity. [68] Soil, water, nutrients and biodiversity health are fundamental ingredients for a sustainable biological system. Sustainability is achievable by establishing cultivation practices that encourage the health of these elements. Key access benefits of rooftop gardens is their nearness and absence of competition from lack of tenure. An individual or business cultivating their roof space does not have to make the trip to and from an allotment or community garden. Also, one of the great insecurities of urban agriculture centres on tenure. Community gardens, allotments, and temporary garden plots are often displaced by what are viewed as more productive/developmental uses of the land. Lack of tenure has a profound effect on the activities undertaken in an agricultural enterprise. Most urban gardeners will be reluctant to invest the time and energy required if

they cannot be assured continued use of the land. However, rooftop gardens are not likely to face competition with other uses of the space and can therefore offer greater security of tenure than other spaces. [69, 70]

Retrofitting

The world-famous Swiss-French modernist architect Le Corbusier advocated the use of the green roofs already in his architecture manifesto "Five points of Architecture" publicly announced in 1923. [71] Referring to him with the ongoing, still rising and above explained environmental concerns, nowadays it would be safe to say that use of the green roofs in the building construction is also a sustainably justified choice. The term "green roof", also called eco-roofs, living roofs, planted roofs or vegetated roofs, alludes to the roofs of the buildings that are partially or fully covered up with the living flora consisting of the strata of a waterproofing membrane, growing medium and the vegetation as a top layer. The roof can rightfully be called the fifth façade of the building, thus it is important to consider also such factors as the aesthetical look, the acquirements for its functional use and environmentally friendly performance, e.g. reduction of UHI effect, management and infiltration of the rainwater, air purification, improvement of the environment, reduction of CO_2 emissions.

The application of the green roofs for new constructions nowadays is widespread globally. Although it may seem a contemporary trend with manifestation of roof gardens stretching back to modernist architecture, the history of the emergence of green roofs already dates back to the ancient times. The world's most famous green roof was one of the seven wonders of the ancient world – the hanging gardens of Babylon, constructed around 8th–6th century BCE. The green roof construction is also a tradition of hundreds of years in Scandinavia, especially Norway. For the vernacular building construction in Nordic countries the turf roofs soaked in the birch tar were used helping to cool the house in the summer and keep it warm in the winter. Scandinavian countries in general can be glorified for their experience and history in the use of green roofs.

The previous studies suggest that the use of green roofs is highly recommended in the refurbishment of already existing buildings. [15, 30, 38, 43, 65] Widely adopting the green roofs for building retrofitting may result in a number of local advantages, the increase of the building performance indicators as crucial one, essentially leading to the more global impacts described before. The building stock ages inevitably and the older buildings consume more energy comparing to the newly built, thus retrofitting by means of energy-efficient technologies can leave significant impact. Typical flat roofs may be perceived also as aesthetically unattractive so speaking of the quality of urban life the green roof installed on the building can transform a lackluster rooftop into an aesthetically pleasing and attractive extra amenities for the occupants and humanize the built environment in the dense metropolis. As targeted in this research the green roofs can also serve for yielding crops and harvesting the food production. However, retrofit of the buildings with green roofs also comes with the certain challenges, namely structural restrains and additional loads, needs for the waterproofing and proper installation technology, access and maintenance.

There are two types of green roofs distinguished – extensive with the soil thickness between 5 and 15 cm, where such plants as mosses, sedum, graminaceous and succulent are used, and intensive that is more similar to conventional roof garden with the growing variety of plants, shrubs, small trees and the soil thickness of more than 20 cm. The difficulty of the retrofitting the buildings with green roofs lays in the fact that this kind of roof appends additional load on the existing roof structure. Taking into considerations the load-bearing capacity and weight considerations, the more suitable green roofs used for building retrofitting are the extensive ones – in Germany 80% of green roofs is extensive. [72] The reason for that is the comparably low added load, as the profile of the roof construction is lighter, thinner and may not require the additional support of the existing construction. Since the expected weight for extensive green roof is 50 to 200 kg/m^2, extensive and semi-intensive green roofs are more appropriate for retrofitting. The expected weight of typical turf roof is as much as 300 – 400 kg/m^2. [72] Choosing the plant species like stonecrop with lower requirements for the substrate, the weigh load of the roof can be diminished. As added weight may turn into expensive structural upgrade, it is crucial to keep the weight of the green roof lower, to consult with the structural engineer and use certain weight-saving strategies. The green roof can be applicable both to flat and steep constructions. If the steepness exceeds 20°, the substrate layer must be secured for the rinsing rainwater. [73] The steepness more than 40° is not recommendable for the installation of the green roofs. As for the designers the following aspects should be also considered: the layout of the heaviest planted elements, drainage, safety measures for the maintenance and use, watering system for vegetation and the conditions of the site in general. The technical solution for the roof design may also differ in various climate zones.

For the extensive green roofs popular in Europe, the layering consists of a coarse, mineral based growing medium, planted with sedum or other plants able to survive tough conditions. The typical composition of extensive green roofs are as follows: load-bearing slab or roof deck, vapor control barrier, insulation layer, waterproof membrane, root barrier (geo-textile), drainage layer, filter layer, growing substrate or porous soil and vegetation layer. Aforementioned small plants used for the top layer are selected so that they grow mostly horizontally ensuring dense coverage. The substrate is a rather thin layer of porous soil – mixture of sand, clay, mineral aggregates and organic substances. The thickness of the soil can be from 3 to 15 cm. However the layer of soil for intensive green roofs to grow larger crops and trees may reach 60 cm, the shrubs can be planted with 40 cm of soil, thus the weight of the green roof layering can reach 800 – 1000 kg/m^2. [73] In many cases the load-bearing capacity and the condition of the existing roofing system can limit the application of the green roof.

Building reconstruction and retrofitting to adjust the energy parameters of the building performance is widely performed but the studies confirm that the use of green roofs in building retrofit can be beneficial in several aspects: the prolongation of the life-cycle of the original roof construction, improving the building's energy efficiency, acoustic comfort, more natural look and feel, biodiversity, accessible public and private green area, urban gardening. However, still educating different actors, including designers and contractors and professionals specializing in green roof construction design is necessary. Admittedly, it's not always possible to convince developers to the application of green roofs, because there are still few examples in Northern latitudes and more conservative investors are not familiar with the technological advancements.

If we talk about a green roof, then, objectively, its construction is more expensive than a traditional, "dark" roof. Green roof solution will be more interesting for developers and owners with the concerns about sustainability and energy efficiency of a building. Independent researchers have shown that the green roof is a forward-looking and well-founded investment for both the private developer and the cities. This is also evidenced by the fact that more and more cities and countries are prohibiting flat roofs from new buildings and the installation of green roofs in many places is a mandatory requirement for them.

Business models

Nature-based solutions (NBS) are a form of eco-innovations. They promote nature as a means for e.g. providing solutions to climate change, low air quality, loss of biodiversity etc. and consist of different ecological domains, where buildings, facades and roofs are one of them. NBS can help overcoming urban sustainability challenges by providing services, creating benefits and holding value for different urban actors. The concept of business model innovation is a potential enabler of nature-based solutions and sustainability. Sustainable business model literature assesses the ability of certain business models to contribute to sustainability development and links environmental, social and economic performance of businesses to their technological, organizational and social innovation activities. [74] Bocken et al. propose 8 sustainable business model archetypes: [75]
- Maximize material and energy efficiency
- Create value from waste
- Substitute the use of finite resources with renewable and natural processes
- Deliver functionality rather than ownership
- Adopt a stewardship role
- Encourage sufficiency
- Re-purpose the business for society and environment
- Develop scale-up solutions
- NBS in the ecological domain of roofs are related to several sustainable business model archetypes:
- Maximizing material and energy efficiency: green roofs provide isolation and protection of buildings and their roofs
- Creating value from waste: building-integrated agriculture uses the water, heat and organic waste of the building which can be reused as input for delivering agricultural produce
- Substitute with renewable and natural processes: contribution to decreasing rain- and stormwater run-off, improving air quality through natural processes. [74]

These ecosystem benefits are of public nature, which leads to difficulties in finding private investments. For NBS related to a building, the investment decision takes place primarily at a decentralized level, with the building owner or the entrepreneur implementing the green roofs. [74] Khare et al. suggest a tripartite model,

according to which initiatives must be financially beneficial to all stakeholders. [76] Collaboration between local government, local businesses and residents is a necessary condition and success depends on creating a balanced win–win situation for all stakeholders.

Conclusions/Summary

The contribution of the heat accumulated by the roofs to the urban heat island phenomenon is so vast that in theory the termination of this accumulation would be enough to reverse the entire phenomenon [13]. Even though, even in such environmentally conscious countries as the members of EU, the mass-scale introduction of green roofs is not easy and encounters many obstacles. One of the reasons is the fact that relatively much of urban tissue covering European cities is at least 50 years old, which means that it comes from the ages when environmental issues were hardly recognised and methods of retrofitting the existing green roofs have not been very developed yet. In the meantime, the cities in the developing countries are growing really fast, but this rise is uncontrolled and unsustainable. [22]

Further comparison between conditions in developed and developing countries did not give clear answer to a dilemma which of them should become a focus area for a green roof mass-scale introduction. In terms of the water retentiveness the green roofs in humid subtropical climates are better than in Mediterranean ones [48] and we can assume that the former ones represent the developing world, while the latter – the developed one. On the other hand, green roof retrofitting makes significant savings on heating, which is redundant in subtropical climates. [31, 34] It means that none of the areas of the globe is a natural leader which could be responsible for mass-scale introduction of such roofs.

Assuming that tackling the UHIs is priceless in terms of a climate change, a way to disseminate green roofs must be found, as otherwise there is no major chance that they become in widespread use unless they are simply profitable and in a foreseeable future no financial support from public authorities can be expected in the developing countries. Such incentives for green roof constructions can be found in some of the developed countries, but green roof conversions are more necessary instead, even though they are more expensive. To alleviate this discrepancy, extensive green roofs are recommended.

All of this means that the world needs solutions that would make new green roof constructions in developing countries and of green roof retrofitting in developed countries profitable and the prosumer model is a good prospect for such an option. It is based on an assumption that is a cornerstone for the dispersed renewable energy production idea, which implies that energy, in a form of electricity, heat or gas, but also other consumable utility goods, like water or food, can be not only consumed, but also produced almost effortlessly by the users of a building, in this specific case covered by green roof.

Especially merging the idea of urban farming with green roofs looks promising, as the urban growing conditions they have many economic advantages that have been mentioned while not being substantially different from those on the ground. It is also a little contribution to the sustainability, as agricultural land use, among natural ones, is one of the least carbon footprint reducing. Still, in terms of economic costs, the extensive green roofs seem to be better than intensive ones.

References

[1] United Nations, Department of Economic and Social Affairs, Population Division,
World Urbanization Prospects: The 2014 Revision, Highlights (ST/ESA/SER.A/352). https://esa.un.org/unpd/wup/publications/files/wup2014-report.pdf Retrieved 06. 07. 2018

[2] A. Mazlan, Between Vision and Reality of Becoming a Smart City, 3rd Smart Cities Conference, Kuala Lumpur 2017 http://www.smartcitiesasia.com/smart-city-vision/ Retrieved 06. 07. 2018

[3] Heat Island Effect, Environmental Protection Agency, https://www.epa.gov/heat-islands Retrieved 06. 07. 2018

[4] S.A. Changnon Jr., K.E. Kunkel, B.C. Reinke, Impacts and responses to the 1995 heat wave: A call to action, Bulletin of the American Meteorological Society. 77 (1996), 1497–1506. doi:10.1175/1520-0477(1996)077<1497:IARTTH>2.0.CO;2

[5] C.C. van Heerwaarden, J. Vilà-Guerau de Arellano, Relative humidity as an indicator for cloud formation over heterogeneous land surfaces", Journal of the Atmospheric Sciences. 65 (2008), 3263–3277.

[6] E. Shochat, P.S. Warren, S.H. Faeth, N.E. McIntyre, D. Hope, From Patterns to Emerging Processes in Mechanistic Urban Ecology, Trends in Ecology & Evolution. 21 (2006) 3. doi:10.1016/j.tree.2005.11.019.

[7] J.E. Walsh, W.L. Chapman, V. Romanovsky, J.H. Christensen, M. Stendel, Global Climate Model Performance over Alaska and Greenland, J. Climate. 21 (23) (2008), 6156–74. doi:10.1175/2008JCLI2163.1.

[8] S.V. Nghiem, I.G. Rigor, D.K. Perovich, P. Clemente-Colón, J.W. Weatherly, G. Neumann, Rapid reduction of Arctic perennial sea ice, Geophysical Research Letters. 34 (2007) L19504

[9] L. Wiesboeck et al., Heat Vulnerability, Poverty and Health Inequalities in Urban Migrant Communities: A Pilot Study from Vienna, in: W. Leal Filho, U.M. Azeiteiro, F. Alves (Eds.), Climate Change and Health: Improving Resilience and Reducing Risks, Springer, Berlin, 2016, p. 392.

[10] R.A.W. Albers, P.R. Bosch, B. Blocken, A.A.J.F. Van Den Dobbelsteen, L.W.A. Van Hove, T.J.M. Spit et al., Overview of challenges and achievements in the Climate Adaptation of Cities and in the Climate Proof Cities program, Building and environment. 83 (2015) 1-10.

[11] Climate Change 2013: The Physical Science Basis, IPCC Fifth Assessment Report, WGI AR5 (2013) 5.

[12] Global Footprint Network, Data Sources, http://data.footprintnetwork.org/ Retrieved 06. 07. 2018

[13] M. Georgescu, P.E. Morefield, B.G. Bierwagen, C.P. Weaver, Urban Adaptation Can Roll Back Warming of Emerging Megapolitan Regions, Proceedings of the National Academy of Sciences of the United States of America. 111 (2014) 2909–2914. doi:10.1073/pnas.1322280111

[14] National Footprint Accounts edition (Data Year 2014); building on World Development Indicators, The World Bank (2016); U.N. Food and Agriculture Organization, Rome, 2018.

[15] N. Garrison, C. Horowitz, C.A. Lunghino, How Green Roofs and Cool Roofs Can Reduce Energy Use, Address Climate Change, and Protect Water Resources in Southern California, Natural Resources Defense Council & Emmett Center on Climate Change and the Environment at UCLA School of Law, Report 12-06-B, Los Angeles, 2012.

[16] City of Toronto, Green Roof Bylaw https://www.toronto.ca/city-government/planning-development/official-plan-guidelines/green-roofs/green-roof-bylaw/ Retrieved 06. 07. 2018

[17] Green Roofs Copenhagen, http://www.klimatilpasning.dk/media/631048/green_roofs_copenhagen.pdf Retrieved 06. 07. 2018

[18] International Green Roof City Network. Case Study Vienna, Austria, http://www.igra-world.com/images/city_network/IGRN-Case-Study-Vienna-IGRA.pdf Retrieved 06. 07. 2018

[19] G. Prokop, H. Jobstmann, A. Schonbauer, Overview of best practices for limiting soil sealing or mitigating its effects in EU-27, European Commission, Final report, Brussels, 2011.

[20] T. Carter, A. Keeler, Life-cycle cost–benefit analysis of extensive vegetated roof systems, Journal of environmental management. 87.3 (2008) 350-363.

[21] I. Ziogou, A. Michopoulos, V. Voulgari, Th. Zachariadis, Energy, environmental and economic assessment of electricity savings from the operation of green roofs in urban office buildings of a warm Mediterranean region, Journal of Cleaner Production. 168 (2017) 346-356.

[22] P.B. Cobbinah, M.O. Erdiaw-Kwasie, P. Amoateng, Africa's urbanization: implications for sustainable development, Cities. 47 (2015) 62-67.

[23] United Nations Department of Economic and Social Affairs (UN DESA). 2018 Revision of World Urbanization Prospects. https://www.un.org/development/desa/publications/2018-revision-of-world-urbanization-prospects.html, Retrieved 06. 07. 2018

[24] UN HABITAT. State of the World's Cities 2006/07. http://mirror.unhabitat.org/documents/media_centre/sowcr2006/SOWCR%205.pdf Retrieved 06. 07. 2018

[25] B. Cohen, Urbanization in developing countries: Current trends and future projections, and key challenges for sustainability, Technology in Society. 28 (2006) 63-80.

[26] A.P.C. Chan, A. Darko, Strategies to promote green building technologies adoption in developing countries: The case of Ghana. Building and Environment, 130 (2018) 74-84.

[27] A.P.C. Chan, A. Darko, A.O. Olanipekun, E.E. Ameyaw, Critical barriers to green building technologies adoption in developing countries: the case of Ghana. Journal of Cleaner Production, 172 (2018) 1067-1079.

[28] S. Lotfi, An investigation of urban green roof development in developing countries (a case study of Iran), Advances in Civil, Environmental, and Materials Research (ACEM' 12), http://www.i-asem.org/publication_conf/acem12/W4F-7.pdf, Retrieved 06. 07. 2018

[29] O. Saadatian, K. Sopian, E. Salleh, C.H. Lim, S. Riffat, E. Saadatian et al., A review of energy aspects of green roofs, Renew Sustain Energy Rev. 23 (2013) 155–168. doi:10.1016/j.rser.2013.02.022.

[30] A.B. Besir, E. Cuce, Green roofs and facades: A comprehensive review, Renew Sustain Energy Rev. 82 (2018) 915–939. doi:10.1016/j.rser.2017.09.106.

[31] P. Bevilacqua, D. Mazzeo, R. Bruno, N. Arcuri, Experimental investigation of the thermal performances of an extensive green roof in the Mediterranean area, Energy Build. 122 (2016) 63–69. doi:10.1016/j.enbuild.2016.03.062.

[32] Y. He, H. Yu, N. Dong, H. Ye, Thermal and energy performance assessment of extensive green roof in summer: A case study of a lightweight building in Shanghai, Energy Build. 127 (2016) 762–773. doi:10.1016/j.enbuild.2016.06.016.

[33] X. Tang, M. Qu, Phase change and thermal performance analysis for green roofs in cold climates, Energy Build. 121 (2016) 165–175. doi:10.1016/j.enbuild.2016.03.069.

[34] M. Taleghani, M. Tenpierik, A. van den Dobbelsteen, D.J. Sailor, Heat mitigation strategies in winter and summer: Field measurements in temperate climates, Build Environ. 81 (2014) 309–319. doi:10.1016/j.buildenv.2014.07.010.

[35] A.H. Refahi, H. Talkhabi, Investigating the effective factors on the reduction of energy consumption in residential buildings with green roofs, Renew Energy. 80 (2015) 595–603. doi:10.1016/j.renene.2015.02.030.

[36] C.M. Silva, M.G. Gomes, M. Silva, Green roofs energy performance in Mediterranean climate, Energy Build. 116 (2016) 318–325. doi:10.1016/j.enbuild.2016.01.012.

[37] V. Costanzo, G. Evola, L. Marletta, Energy savings in buildings or UHI mitigation? Comparison between green roofs and cool roofs, Energy Build. 114 (2016) 247–255. doi:10.1016/j.enbuild.2015.04.053.

[38] U. Berardi, The outdoor microclimate benefits and energy saving resulting from green roofs retrofits, Energy Build. 121 (2016) 217–229. doi:10.1016/j.enbuild.2016.03.021.

[39] C.P. Skelhorn, G. Levermore, S.J. Lindley, Impacts on cooling energy consumption due to the UHI and vegetation changes in Manchester, UK, Energy Build. 122 (2016) 150–159. doi:10.1016/j.enbuild.2016.01.035.

[40] S.S. Alcazar, F. Olivieri, J. Neila, Green roofs: Experimental and analytical study of its potential for urban microclimate regulation in Mediterranean–continental climates, Urban Clim. 17 (2016) 304–317. doi:10.1016/j.uclim.2016.02.004.

[41] T.E. Morakinyo, K.W.D. Kalani, C. Dahanayake, E. Ng, C.L. Chow, Temperature and cooling demand reduction by green-roof types in different climates and urban densities: A co-simulation parametric study, Energy Build. 145 (2017) 226–237. doi:10.1016/j.enbuild.2017.03.066.

[42] S.S.G. Hashemi, H. Bin Mahmud, M.A. Ashraf, Performance of green roofs with respect to water quality and reduction of energy consumption in tropics: A review, Renew Sustain Energy Rev. 52 (2015) 669–679. doi:10.1016/j.rser.2015.07.163.

[43] M. Karteris, I. Theodoridou, G. Mallinis, E. Tsiros, A. Karteris, Towards a green sustainable strategy for Mediterranean cities: Assessing the benefits of large-scale green roofs implementation in Thessaloniki, Northern Greece, using environmental modelling, GIS and very high spatial resolution remote sensing data, Renew Sustain Energy Rev. 58 (2016) 510–525. doi:10.1016/j.rser.2015.11.098.

[44] A. Volder, B. Dvorak, Event size, substrate water content and vegetation affect storm water retention efficiency of an un-irrigated extensive green roof system in Central Texas, Sustain Cities Soc. 10 (2014) 59–64. doi:10.1016/j.scs.2013.05.005.

[45] Q. Zhang, L. Miao, X. Wang, D. Liu, L. Zhu, B. Zhou et al., The capacity of greening roof to reduce stormwater runoff and pollution, Landsc Urban Plan. 144 (2015) 142–150. doi:10.1016/j.landurbplan.2015.08.017.

[46] R. Nawaz, A. McDonald, S. Postoyko, Hydrological performance of a full-scale extensive green roof located in a temperate climate, Ecol Eng. 82 (2015) 66–80. doi:10.1016/j.ecoleng.2014.11.061.

[47] B.G. Johannessen, H.M. Hanslin, T.M. Muthanna, Green roof performance potential in cold and wet regions. Ecol Eng. 106 (2017) 436–447. doi:10.1016/j.ecoleng.2017.06.011.

[48] F. Viola, M. Hellies, R. Deidda, Retention performance of green roofs in representative climates worldwide, J Hydrol. 553 (2017) 763–772. doi:10.1016/j.jhydrol.2017.08.033.

[49] C. Szota, C. Farrell, N.S.G. Williams, S.K. Arndt, T.D. Fletcher, Drought-avoiding plants with low water use can achieve high rainfall retention without jeopardising survival on green roofs, Sci Total Environ. 603–604: 2017;340–51. doi:10.1016/j.scitotenv.2017.06.061.

[50] S.S. Cipolla, M. Maglionico, I. Stojkov, A long-term hydrological modelling of an extensive green roof by means of SWMM, Ecol Eng. 95 (2016) 876–887. doi:10.1016/j.ecoleng.2016.07.009.

[51] C. Szota, T.D. Fletcher, C. Desbois, J.P. Rayner, N.S.G. Williams, C. Farrell, Laboratory tests of substrate physical properties may not represent the retention capacity of green roof substrates in situ, Water (Switzerland). 9 (2017) doi:10.3390/w9120920.

[52] I. Buffam, M.E. Mitchell, R.D. Durtsche, Environmental drivers of seasonal variation in green roof runoff water quality, Ecol Eng. 91 (2016) 506–514. doi:10.1016/j.ecoleng.2016.02.044.

[53] J. Hill, J. Drake, B. Sleep, Comparisons of extensive green roof media in Southern Ontario, Ecol Eng. 94 (2016) 418–426. doi:10.1016/j.ecoleng.2016.05.045.

[54] S. Beecham, M. Razzaghmanesh, Water quality and quantity investigation of green roofs in a dry climate, Water Res. 70 (2015) 370–384. doi:10.1016/j.watres.2014.12.015.

[55] X. Wang, Y .Tian, X. Zhao, The influence of dual-substrate-layer extensive green roofs on rainwater runoff quantity and quality, Sci Total Environ. 592 (2017) 465–476. doi:10.1016/j.scitotenv.2017.03.124.

[56] U.N. Food and Agriculture Organization in collaboration with U.N. Centre for Human Settlements (Habitat), Feeding the cities: The role of urban agriculture – factsheet, FAO, Rome, 1999.

[57] U.N. Food and Agriculture Organization, Fighting poverty and hunger: What role for Urban agriculture. http://www.fao.org/docrep/012/al377e/al377e00.pdf Retrieved 06. 07. 2018

[58] L.J.A. Mougeot, Growing better cities: Urban agriculture for sustainable development, International Development Research Centre, Ottawa, 2006.

[59] M. Hendrickson, M. Porth, Urban Agriculture—Best Practices and Possibilities, University of Missouri Extension, St. Louis, MO, 2012.

[60] C.G. Shabbir, J. Smit, A. Ratta, J. Nasr, Urban Agriculture: Food, Jobs and Sustainable Cities, United Nations Development Programme, New York, NY, 1996.

[61] M.U. Agbonlahor, S. Momoh, A.O. Dipeolu, Urban vegetable crop production and production efficiency, Int J Veg Sci. 13 (2007) 63–72. doi:10.1300/J512v13n02_06

[62] T. Osmundson, Roof gardens: history, design, and construction. Greenbacks from green roofs: forging a new industry in Canada, Canadian Mortgage and Housing Corporation, Ottawa, 1999.

[63] B. Engelhard, Rooftop to tabletop: Repurposing urban roofs for food production. An unpublished Master's Thesis in Landscape Architecture, University of Washington, Seattle, WA, 2010.

[64] M. Ableman, Agriculture's Next Frontier: How urban farms could feed the world, UTNE Reader. 102 (2000) 60–65.

[65] B. Engelhard, Green Roofs Will Flourish: Obstacles and Solutions in U.S. Green Roof Retrofits. Research paper for LARCH 561, University of Washington, Seattle, WA, 2008.

[66] L.L. Sheung, Rooftop Garden: Planting Seeds of Service, The Teacher's network, Boston, MA, 2001.

[67] R. Earles, Sustainable Agriculture: An Introduction, ATTRA: The National Sustainable Agriculture Information Service, Melbourne, Vic., 2005.

[68] G. Trauger, S. McFadden, Farms of Tomorrow Revisited: Community Supported Farms, Farm Supported Communities, Biodynamic Farming and Gardening Association, Kimberton, PA, 1997.

[69] J. S[t] Lawrence, Urban agriculture: the potential of rooftop gardening. An unpublished Master's Thesis in Environmental Studies, York University, Toronto, Ont., 1996.

[70] L.J. Pearson, L. Pearson, C.J. Pearson, Sustainable urban agriculture: Stocktake and opportunities, International Journal of Agricultural Sustainability. 8 (2010) 7-19.

[71] Le Corbusier, Five points of Architecture, in: Le Corbusier, Towards a New Architecture, J. Rodker, London, 1931. Reprint: Dover Publications, New York, 1985.

[72] E.C. Snodgrass, L. McIntyre, The Green Roof Manual: A Professional Guide to Design, Installation, and Maintenance, first ed., Timber Press, Portland, OR, 2010.

[73] V. Bokalders, M. Bloka, Ekoloģiskās būvniecības rokasgrāmata: kā projektēt veselīgas, racionālas un ilgtspējīgas ēkas, Domas spēks, Riga, 2013.

[74] H. Toxopeus, F. Polzin, Characterizing nature-based solutions from a business model and financing perspective. Deliverable 1.3 Part V of the H2020 project "Naturvation" https://naturvation.eu/sites/default/files/news/files/naturvation_characterizing_nature-based_solutions_from_a_business_model_and_financing_perspective.pdf Retrieved 06. 07. 2018

[75] N.M.P. Bocken, S.W. Short, P. Rana, S. Evans, A literature and practice review to develop sustainable business model archetypes, Journal of Cleaner Production. 65 (2014) 42-56. https://doi.org/10.1016/j.jclepro.2013.11.039

[76] A. Khare, Beckman, N. Crouse, Cities addressing climate change: Introducing a tripartite model for sustainable partnership. Sustainable Cities and Society. 1(4) (2011) 227-235. https://doi.org/10.1016/j.scs.2011.07.010

Justyna Czerwińska, Grzegorz Wielgosiński
Lodz University of Technology, Faculty of Process and Environmental Engineering
Wólczańska 213, 90-924 Łódź, Poland, justyna.czerwinska@edu.p.lodz.pl

CIGARETTE SMOKE OR EXHAUST GAS FROM WASTE INCINERATION – WHERE ARE MORE DIOXINS?

Abstract
In Poland, incineration is a relatively new method of waste treatment. Modern installations for waste incineration have two functions: they reduce the quantity (volume) of the waste and are a source of electricity and/or heat. During all combustion processes including waste incineration, polychlorinated dibenzo-p-dioxins (PCDDs) and polychlorinated dibenzofurans (PCD/Fs) (well known as dioxins) are formed. These compounds are considered to be extremely dangerous for living organisms including human beings.

Dioxins are formed in any process of combustion of solid and liquid fuels in the presence of chlorine, oxygen and organic matter at appropriate temperatures. Combustion processes also occur during cigarette smoking, which is also a source of dioxin emissions. Although smoking has been classified as a less important source of dioxins in the environment, it directly affects our health.

This work's aim is to determine and compare the degree of harmfulness caused by the amount of inhaled dioxins: cigarette smoking or living near a waste incineration plant.

Based on literature and experimental data, the concentration of dioxins in cigarette smoke and exhaust gases generated by municipal waste incineration plants as well as number of dioxins absorbed per day by the body will be presented.

Key words
polychlorinated dibenzo-p-dioxins, combustion, incineration plant, cigarettes

Introduction
Polychlorinated dibenzo-p-dioxins (PCDDs) and polychlorinated dibenzofurans (PCDFs), known in short as dioxins and furans, are widely regarded as one of the most dangerous environmental poisons.

The general name of dioxins usually covers the entire group of chemical compounds including 75 polychlorinated dibenzo-p-dioxins and 135 polychlorinated dibenzofurans, chemical compounds with the general formula shown in Figure 1. The dibenzo-p-dioxin molecule has two axes of symmetry, while the dibenzofuran molecule has one axis of symmetry, which explains significant differences in the number of congeners [1-3].
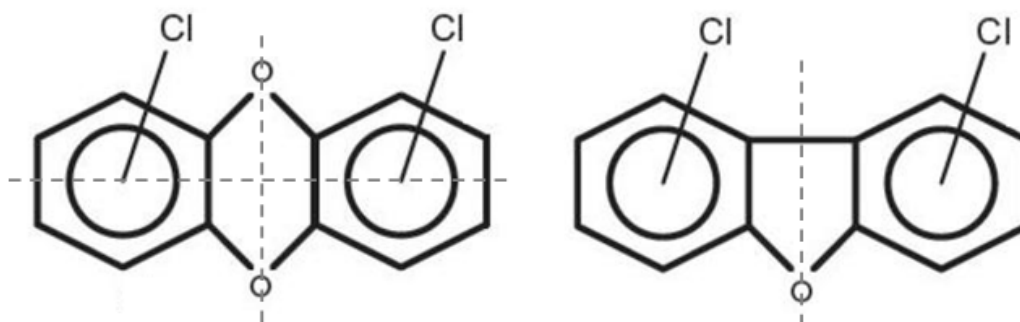

Fig. 1. Polychlorinated dibenzo-p-dioxins and polychlorinated dibenzofurans
Author's own source

A common feature of all dioxins and dioxin-like chemicals is their high melting point, low volatility and very good solubility in fats and hydrophobic solvents, with very low solubility in water [4-5].

Dioxins and furans are formed as an undesirable by-product in all combustion processes (including incineration of municipal, industrial and medical waste and sewage sludge as well as during the combustion of fossil fuels, in particular, hard coal, lignite and biomass) also in some industrial processes such as the production of pesticides, paper and cellulose, as well as in the iron and steel industry and in the production of non-ferrous metals.

The concentration of dioxins from municipal waste incineration plants in the flue gas stream is usually from 0.001 to 50 ng TEQ/m^3, depending on the exhaust gas treatment system [6-8]. Of course, the highest concentrations occur when there are no exhaust gas treatment systems. In the case of tests of dioxin emissions from industrial incinerators, results obtained were at a similar level as for municipal waste incineration plants [9-10]. For medical waste incineration plants, dioxin concentrations in the exhaust gases are slightly higher than for municipal waste incineration plants, which most probably results from simpler and less efficient exhaust gas treatment systems and high content of chlorine and chlorinated compounds in the incinerated waste [11-12].

Combustion of fuels in small domestic furnaces differs significantly from the combustion of the same fuels in large energy facilities. Usually, in small domestic furnaces, the oxygenation of the combustion zone is insufficient and, as a result, incomplete combustion occurs. This is manifested by increased emissions of carbon monoxide and organic micro-pollutants. The emission of dioxins from small furnaces may be low – concentrations in the emitter reaching 0.01-0.08 ng TEQ/m^3 [13], in other – slightly higher 0.03-1.2 ng TEQ/m^3 [14], and even 0.1-40 ng TEQ/m^3 [15], while in the case of fireplaces, concentrations exceeding even 20 ng TEQ/m^3 were observed [16].

The combustion processes during which dioxins and furans are formed also include cigarette smoking. Dioxin concentrations in the cigarette smoke can reach up to 2 ng TEQ/m^3, i.e. at least 20 times higher than the permissible concentrations of polychlorinated dibenzo-p-dioxins and polychlorinated dibenzofurans (PCDD/Fs) in exhaust gases from waste incineration plants [17]. Considering the large scale and widespread cigarette smoking, dioxin emissions from this source on the world scale can be significant.

Despite the very high toxicity of some dioxins and furans concerning certain animal organisms, it is difficult to compare them with other strong poisons present in the environment, because their action is not immediate at concentrations we encounter every day. The harmful effect of PCDD/Fs lies mainly in disturbing the endocrine function of the body, resulting in impaired fertility, problems with maintaining a pregnancy or even infertility [18]. This is primarily a disturbance of secretion of progesterone, a hormone necessary for the maintenance and proper course of pregnancy [19]. However, there is no scientific evidence that dioxins have carcinogenic properties [20-21]. Some health effects resulting from the long-lasting effects of low concentrations of PCCD/Fs include decreased immune system activity, disturbed psychomotor development of children, thyroid hormone dysfunction, decrease in the amount and quality of sperm and increased number of cases of ovarian cysts [22].

Research and results

Based on literature and mentioned above experimental data, it was decided to compare the concentrations of dioxins in cigarette smoke, exhaust gases produced during combustion of so-called refuse-derived fuel (RDF) and flue gas streams from domestic coal-fired boilers. The a number of dioxins absorbed per day in the body from the previously mentioned 3 sources was also compared.

The concentration of toxic substances in cigarette smoke is affected by the oxy-temperature conditions of the smoke produced. These conditions depend on the way of smoking a cigarette, i.e. on the so-called smoking topography. Based on the literature data [23-26], the following parameters of the topography of smoking were adopted (Table 1).

Table 1. Parameters of smoking topography

Parameter	Value
Puff volume	60 ml
Concentration of dioxins in cigarette smoke	2 ng/m^3
Time of smoking 1 cigarette	5 min
Number of puffs when smoking 1 cigarette	20
Number of cigarettes in one pack	20

Source: Author's

The calculations were made according to the following as Equations 1 and 2:
Amount of dioxins from smoking one cigarette:

$$E_{p1} = z \cdot V \cdot c_d \tag{1}$$

where: z - number of puffs when smoking 1 cigarette

V - puff volume

c_d - concentration of dioxins in cigarette smoke

Amount of dioxins from smoking one pack of cigarettes:

$$E_{p2} = E_{p1} \cdot n \tag{2}$$

where: n - number of cigarettes in one pack

When calculating the dioxin emissions from smoking from eq. (1) and (2) the dioxin emissions from smoking one cigarette (E_{p1}) is 0.0024 ng and from smoking one cigarette pack (E_{p2}) is 0.048 ng.

The amount of dioxin emissions and then the immission from waste incineration plants fired refuse derived fuel (RDF) was calculated for an example of a municipal waste incineration plant with a capacity of approx. 94,000 Mg/year. The concentration of dioxins in the flue gas stream taken for calculations was equal to 0.025 ng/m^3 [27-30]. This is the size typical for this incineration plant confirmed in several emission tests. For domestic coal-fired boilers, dioxin concentration of 9.2 ng/m^3 was adopted according to literature data [31-32]. Detailed data accepted for calculations are presented in Table 2.

Table 2. Input values used in the calculations

Parameter	Symbol	RDF incineration plant	Domestic coal-fired boiler
Fuel calorific value	w_D	7 000 kJ/kg	19 000 kJ/kg
Maximum fuel consumption	B_{max}	11 750 kg/h	50 kg/h
Excess air coefficient	λ	2.1	1.9
Dampness of flue gases	$[H_2O]$	10%	5%
Exhaust gas temperature	t	200°C	120°C
Concentration of dioxins in the smoke under conventional conditions	c_D	0.025 ng/m$_u^3$	9.2 ng/m$_u^3$
Concentration of sulfur dioxide in the exhaust gas	c_{SO2}	50 kg/h	2 000 kg/h
Concentration of nitrogen oxides in the exhaust gas	c_{NOx}	200 kg/h	600 kg/h
Emitter height	H	60 m	7 m
Emitter diameter	D	1.8 m	0.25 m
Gas flow rate in the emitter	u	12.3 m/s	4.2 m/s

Source: Author's

The scheme of emission calculation [33] and summary of results (Table 3) are presented below.
Theoretical air demand:

$$V_T = \frac{0.241 \cdot w_D}{1000} + 0{,}5$$

(3)

The amount of exhaust gases generated at complete combustion:

$$V_P = \frac{0.212 \cdot w_D}{1000} + 1{,}65$$

(4)

The indicator of the amount of generated flue gases:

$$V_C = V_P + (\lambda - 1) \cdot V_T$$

(5)

Flue gas stream under normal conditions:

$$V_N = B_{\max} \cdot V_C$$

(6)

Oxygen concentration in the exhaust gas:

$$C_{O_2} = \frac{(\lambda - 1) \cdot B \cdot V_T \cdot 21\%}{V_N}$$

(7)

Flue gas stream in real conditions:

$$V = V_N \cdot \frac{273 + t}{273}$$

(8)

Flue gas stream under conventional conditions:

$$V_u = V \cdot \frac{21 - [O_2]_{rzecz}}{21 - [O_2]_u} \cdot \frac{100 - [H_2O]}{100}$$

(9)

where: $[O_2]_{rzecz}$ - actual oxygen concentration in the exhaust gas

$[O_2]_u$ - oxygen concentration in conventional conditions (11% for waste incineration plant, 6% for coal combustion)

Maximum dioxin emission:

$$E_D = V_u \cdot c_D$$

(10)

Maximum emission of sulfur dioxide:

$$E_{SO2} = V_u \cdot c_{SO2}$$

(11)

Maximum emission of nitrogen oxides:

$$E_{NOx} = V_u \cdot c_{NOx}$$

(12)

Table 3. Results of emission calculations for RDF incinerators and domestic coal-fired boiler

Parameter	Symbol	RDF incinerator	Domestic coal-fired boiler
Theoretical air demand	V_T	2.187 m^3/kg	5.079 m^3/kg
Amount of exhaust gases generated at complete combustion	V_P	3.134 m^3/kg	5.678 m^3/kg
Indicator of the amount of generated flue gases	V_C	5.540 m^3/kg	10.249 m^3/kg
Flue gas stream under normal conditions	V_N	65 097 m$_N^3$/kg	512 m$_N^3$/kg
Oxygen concentration in the exhaust gas	C_{O_2}	9.12%	9.37%
Flue gas stream in real conditions	V	112 778 m^3/h	738 m^3/h
Flue gas stream under conventional conditions	V_u	19 450 m$_u^3$/h	160 m$_u^3$/h
Maximum emission of sulfur dioxide	E_{SO2}	0.972 kg/h	0.321 kg/h
Maximum emission of nitrogen oxides	E_{NOx}	3.890 kg/h	0.096 kg/h
Maximum emission of dioxins	E_D	0.486 µg/h	2.212 µg/h

Source: Author's

The presented data illustrate the number of dioxins in the flue gas stream. In the case of waste incineration plant, the introduction of exhaust gases into the environment takes place at a height of about 60 m above the earth's surface. For a domestic coal-fired boiler, the emitter is about 7 m above the earth's surface. When smoking cigarettes, the emitter (cigarette) is at the level of our lips, so there is a direct absorption of pollutants from cigarette smoke. Analyzing the phenomenon of spreading pollutants from the incineration plant and basing on calculations according to the Pasquill model made in the OPA03 program, it can be assumed that the concentrations of pollutants at the earth's surface are about 10^{11} times lower than the concentrations of pollutants in the exhaust gas stream in the RDF incinerator and around 10^{13} times smaller than in a domestic coal-fired boiler [34-36].

To determine the immission of dioxins during cigarette smoking, it was assumed that the volume of one breath is about 0.5 dm^3, the number of breaths per minute 16, and thus the volume of air inhaled per hour is 480 dm^3. The table below presents the values of dioxin immission inhaled by man from individual sources.

Table 4. The amount of dioxins inhaled by a human

Source	Value
Cigarette smoking	$4.8 \cdot 10^{-2}$ ng/pack
	$2.40 \cdot 10^{-3}$ ng/cigarette
Coal-fired boiler	$1.00 \cdot 10^{-4}$ ng/h
Waste incineration plant	$2.30 \cdot 10^{-3}$ ng/h

Source: Author's

For the RDF waste incineration plant and coal-fired boiler, the highest concentrations observed near the earth's surface at a distance of approx. 200-300 m from the emitter was assumed, which resulted from the calculations.

Summary and conclusions
Waste incineration is one of the best ways of its neutralization. Waste incineration plants practically do not have a negative impact on water and soil, which is a great advantage compared to a landfill. The volume of waste generated is also significantly reduced, and modern technologies make it possible to utilize combustion residues. However experience shows that such investments do not meet a positive reception in society. Each project of building a waste incineration plant instigates social protests. In general opinion waste incineration

plants cause very severe pollution of the environment. This is mainly due to the lack of information in society. Based on the analysis, it can be unequivocally stated that a man absorbs 0.0024 ng of dioxins while smoking one cigarette. During one working hour, the incinerator generates as many dioxins as it is produced during smoking of one cigarette. On the other hand, in the case of one-hour work of a domestic coal-fired boiler, one inhales as many dioxins as there are in 0.045 cigarette, in other words smoking 1 cigarette is equivalent to about 24 hours of exposure to the emission range from an old type coal-fired boiler. At the same time, it should be remembered that cigarette smoke contains significant quantities of highly toxic substances, including carcinogenic substances, such as benzo(a)pyrene, hence its harmfulness for the human body is many times higher [21].

References

[1] Y. Aoki, Polychlorinated Biphenyls, Polychlorinated Dibenzo-p-dioxins, and Polychlorinated Dibenzofurans as Endocrine Disrupters – What We Have Learned from Yusho Disease, Environ Res, 86 (2001) 2-11.

[2] A.J.J Mendes, The endocrine disrupters: a major medical challenge, Food Chem Toxicol, 40 (2002) 781-788.

[3] K. Steenland, J. Deddens, Dioxin: exposure-response analysis and risk assessment, Ind Health, 41 (2003) 175-180.

[4] S.P. Ryan, B.K. Gullett, D. Tabor, L. Oudejans, A. Touati, Determination of the vapor pressures of selected polychlorinated dibenzo-p-dioxins and dibenzofurans at 75-275°C, Chem Eng Sci, 60 (2005) 787-796.

[5] S. Oleszek-Kudlak, E. Shibata, T. Nakamura, Solubilities of selected PCDDs and PCDFs in water and various chloride solutions, J Chem Eng Data, 52 (2007) 1824-1829.

[6] J.H. Kao, K.S. Chen, G.P. Chang-Chein, I.Ch. Chou, Emissions of polychlorinated dibenzo-p-dioxins and dibenzofurans from various stationary sources, Aerosol Air Qual Res, 6 (2006) 170-179.

[7] L.F. Kin, W.J. Lee, G.P. Chang-Chien, Emissions of polychlorinated dibenzo-p-dioxins and dibenzofurans from various industrial sources, J Air Waste Manage, 56 (2006) 1707-1715.

[8] K.I. Choi, S.H. Lee, D.H. Lee, Emissions of PCDDs/DFs and dioxin like PCDs from small waste incinerations in Korea, Atmos Environ, 42 (2008) 940-948.

[9] A. Karademir, M. Bakoğlu, S. Ayberk, PCDD/F removal efficiencies of electrostatic precipitator and wet scrubbers in IZAYDAS hazardous waste incinerator, Fresenius Environ Bull, 12 (2003) 1228-1232.

[10] A. Karademir, M. Bakoğlu, F. Taspinar, S. Ayberk, Removal of PCDD/Fs from flue gas by a fixed-bed activated carbon filter in a hazardous waste incineration, Environ Sci Tech, 38 (2004) 1201-1207.

[11] S. Singh, V. Prakash, Toxic environmental release from medical waste incineration: a review, Environ Monit Assess, 132 (2007) 67-81.

[12] G. Mininni, A. Sbrilli, M. Bragugia, E. Guerriero, D. Marani, M. Rotatori, Dioxins, furans and polycyclic aromatic hydrocarbons emissions from a hospital and cemetery waste incinerator, Atmos Environ, 41 (2007) 8527-8536.

[13] F. Pfeiffer, M. Struschka, G. Baumbach, H. Hagenmeier, K.R.G. Hein, PCDD/PCDF emissions from small firing systems in households, Chemosphere, 40 (2000) 225-232.

[14] O. Schleicher, A. Jensen, T. Herrmann, O. Roots, A. Tordik, Dioxin emission from two oil shale fires power plants in Estonia, Organohalogen Compounds, 66 (2004) 1635-1641.

[15] G. Thanner, W. Moche, Emission von Dioxinen, PCBs und PAHs aus Kleinfeuerungen, Umweltbundesamt, Wien, Monographien, Band 153, 2002.

[16] B. Hedman, M. Naslund, S. Marklund, Emission of PCDD/F, PCB and HCB from combustion of firewood and pellets in residential stoves and boilers, Environ Sci Tech, 40 (2006) 4968-4975.

[17] T. Matsueda, Y. Kurokawa, M. Nakamura, Concentrations of PCDDs, PCDFs and coplanar PCBs in cigarettes from various countries, Organohalogen Compounds, 20 (1994) 331-334.

[18] E.L. Gregoraszczuk, Dioksyny – czynniki zaburzające funkcje endokrynne, VII Konferencja Naukowa "Dioksyny w Przemyśle i Środowisku", Kraków, 2005.

[19] M. Kogevinas, Human health effect of dioxins: cancer, reproductive and endocrine system effects, Hum Reprod Update, 7 (2001) 331-339.

[20] P. Cole, D. Trichopoulos, H. Pastides, T. Starr, J.S. Mandel, Dioxin and cancers: a critical review, Regul Toxicol Pharm, 38 (2003) 378-388.

[21] P. Boffeta, Human cancer from environmental pollutants: The epidemiological evidence, Mutat Res Gen Tox En, 608 (2006) 157-162.

[22] A. Schecter, L. Birnbaum, J.J. Ryan, J.D. Constable, Dioxins: an overview, Environ Res, 101 (2006) 419-428.

[23] T. Matsueda, Y. Kurokawa, M. Nakamura, S. Takada, K. Fukamachi, Concentrations of PCCDs, PCDFs and coplanar PCBs in cigarettes from various countries, Organohalogen Compounds, vol. 20 (1994) 331-334.

[24] D. Rubenstein, J. Jesty, D. Bluestein, Differences Between Mainstream and Sidestream Cigarette Smoke Extracts and Nicotine in the Activation of Platelets Under Static and Flow Conditions, Circulation, 109 (2004) 78-83.

[25] T. Aoyama, K. Ikeda, A. Takatori, T. Obal, Risk assessment of dioxins in cigarette smoke, Organohalogen Compounds, 65 (2003) 321-324.

[26] C.L. Wilson, J.A. Bodnar, B.G. Brown, W.T. Morgan, R.J. Potts, M.F. Borgerding, Assessment of dioxins and dioxin-like compounds in mainstream smoke from selected US cigarette brands and reference cigarettes, Food Chem Toxicol, 46 (2008) 1721-1733.

[27] H. Xiao, Y. Ru, Z. Peng, D. Yan, K.H. Karstensen, N. Wang, Q. Huang, Destruction and formation of polychlorinated dibenzo-p-dioxins and dibenzofurans during pretreatment and co-processing of municipal solid waste incineration fly ash in a cement kiln, Chemosphere, 210 (2018) 779-788.

[28] H. Zhuo, A. Meng, Y. Long, Q. Li, Y. Zhang, A review of dioxin-related substances during municipal solid waste incineration, Waste Manag, 36 (2015) 106-118.

[29] H. Cheng, Y. Hu, Curbing dioxin emissions from municipal solid waste incineration in China: Re-thinking about management policies and practices, Environ Pollut, 158 (2010) 2809-2814.

[30] H. Huang, A. Buekens, On the mechanisms of dioxin formation in combustion processes, Chemosphere, 31 (1995) 4099-4117.

[31] A. Grochowalski, J. Konieczyński, PCDDs/PCDFs, dl-PCBs and HCB in the flue gas from coal fired CFB boilers, Chemosphere, 73 (2008) 97-103.

[32] G. Wielgosiński, Emisja dioksyn z procesów termicznych i metody jej ograniczania, Polska Akademia Nauk Oddział w Łodzi, Komisja Ochrony Środowiska, 2009.

[33] H. Recknagel, E. Sprenger, W. Hönmann, E.R. Schramek, Taschenbuch für Heizung und Klimatechnik. R. Oldenburg Verlag, München, 1994.

[34] R. Zarzycki, G. Wielgosiński, Technologie i procesy ochrony powietrza, Wydawnictwo WNT, Warszawa, 2018.

[35] M.R. Beychok, Fundamentals of Stack Gas Dispersion, MR Beychok, New York, 2005.

[36] A. De Visscher, Air Dispersion Modeling: Foundations and Applications, Wiley, New York, 2013.